UNIVERSITY OF BIRMINGHAM

Nutritional and Hormonal Regulation of Skeletal Muscle Metabolism

By

Yasir Elhassan

A thesis submitted to the University of Birmingham for the degree of

DOCTOR OF PHILOSOPHY

Institute of Metabolism and Systems Research

College of Medical and Dental Sciences

University of Birmingham

July 2024

ABSTRACT

Nicotinamide Adenine Dinucleotide (NAD+) is a cofactor for enzymes serving cellular metabolic reactions and a consumed substrate for sirtuins and poly (adenosine diphosphate-ribose) polymerases (PARPs), enzymes that regulate protein deacetylation and DNA repair, and translate changes in energy and cell status into metabolic adaptations. Deranged NAD+ homeostasis and concurrent mitochondrial dysfunction are key features of ageing and age-related metabolic disease. Contemporary NAD+ precursors (vitamin B3 derivatives) showed promise as therapeutic nutraceuticals to restore target tissue NAD+ in at risk groups and have demonstrated improvements in mitochondrial function and sirtuin-dependent signalling in pre-clinical studies. We conducted the NADMet (**N**icotinamide **A**denine **D**inucleotide and Skeletal Muscle **Met**abolic Phenotype) clinical study to examine whether NAD+ can be increased in human tissues using oral nutraceutical approaches and assess for a potential role in combating metabolic disease and the unwanted effects of ageing. The results showed that the oral supplementation of the NAD+ precursor, nicotinamide riboside, in aged men was safe and well-tolerated leading to an increase in the skeletal muscle NAD+ metabolome and induced a specific transcriptomic signature without altering muscle specific or systemic metabolism.

NAD+ is also a parent molecule for NADPH which is a cofactor for the 11β-hydroxysteroid dehydrogenase type 1 (11β-HSD1) enzyme that regenerates glucocorticoids in the sarcoplasmic reticulum (SR) of skeletal muscle. The maintenance of the SR NADPH/NADP+ ratio is poorly understood. This work suggests a novel level of regulated glucocorticoid metabolism in skeletal muscle whereby 11β-HSD1 activity can be influenced by cellular redox status and NAD+ levels beyond the SR.

ACKNOWLEDGEMENTS

I would like to thank my supervisor, Professor Gareth Lavery, for his guidance and support, and, overall, friendship. I would also like to thank all members of the Lavery Group for holding my hand when I landed in the lab; Craig Doig, Rachel Fletcher, David Cartwright, and Lucy Oakey have taught me all the *in vitro* laboratory skills outlined in the thesis.

A special thanks to my parents who have sowed the seed that resulted in who I am today; I could not have asked for better parents.

I would like to dedicate this thesis to my wife Dalia and son Ahmed, who made their life with me wherever I went to support my career, and who have stood by me through the harder times, low moods, and sleepless nights. This would never have been possible without you.

TABLE OF CONTENTS

LIST OF FIGURES

ABBREVIATIONS

Acetyl CoA	Acetyl Coenzyme A
ACMS	Amino-3-carboxymuconate semialdehyde
ACS2	Acetyl-CoA synthetase 2
ACTH	Adrenocorticotrophin hormone
ADP	Adeonosine diphosphate
AMP	Adeonosine monophosphate
AMPK	Adenosine monophosphate-activated protein kinase
ATP	Adeonosine triphosphate
BSA	Bovine serum albumin
11β-HSD	11 β-hydroxysteroid dehydrogenases
CoA	Coenzyme A
CRH	Corticotrophin releasing hormone
DNA	Deoxyribonucleic acid
ER	Endoplasmic reticulum
ETC	Electron transport chain
FCCP	Carbonyl cyanide-4-(trifluoromethoxy) phenylhydrazone
FOXO1	Forkhead box protein O1
GR	Glucocorticoid receptor
G6P	Glucose 6-phosphate
HDACs	Histone deacetylases
HDL cholesterol	High-density lipoprotein cholesterol
HPA	Hypothalamic-pituitary-adrenal axis

H6PDH	Hexose-6-phosphate dehydrogenase
IDH2	Isocitrate dehydrogenase 2
LC-MS/MS	Liquid chromatography-mass spectrometry
LPL	Lipoprotein lipase
miRNA	MicroRNA
MR	Mineralocorticoid receptor
mtDNA	Mitochondrial DNA
NAAD	Nicotinic acid adenine dinucleotide
NAADP	Nicotinic acid adenine dinucleotide phosphate
NA	Nicotinic acid
NAD+	Nicotinamide adenine dinucleotide
NADH	Nicotinamide adenine dinucleotide + hydrogen
NADK	Nicotinic acid adenine dinucleotide kinase
NADP+	Nicotinamide adenine dinucleotide phosphate
NADPH	Nicotinamide adenine dinucleotide phosphate + hydrogen
NADS	NAD+ synthase
NAFLD	Non-alcoholic fatty liver disease
NAM	Nicotinamide
NAMN	Nicotinic acid mononucleotide
NAMPT	Nicotinamide phosphoribosyltransferase
NAPT	Nicotinic acid phosphoribosyltransferase
NAR	Nicotinic acid riboside
ND1	NADH dehydrogenase subunit 1
NEFA	Non-esterified fatty acids

NF-κB	Nuclear factor-KappaB
NMN	Nicotinamide mononucleotide
NMNAT	Nicotinamide mononucleotide adenylyltransferase
NQO2	Quinone oxidoreductase
NRF 1,2	Nuclear respiratory factor 1 and 2
NRH	Dihydronicotinamide riboside
NRK1/2	Nicotinamide riboside kinase 1/2
OGTT	Oral glucose tolerance test
OXPHOS	Oxidative phosphorylation
PGC-1α	Peroxisome proliferator-activated receptor-γ coactivator-1α
PRPP	5-phosphoribosyl-1-pyrophosphate
QPRT	Quinolinate phosphoribosyl-transferase
ROS	Reactive oxygen species
SDH	Succinate dehydrogenase
SOD2	Superoxide dismutase-2
TCA	Tricarboxylic acid cycle
PARPs	Poly-ADP robose polymerase
qPCR	Quantitative real time polymerase chain reaction
RNA	Ribonucleic acid
SR	Sarcoplasmic reticulum
T2DM	Type 2 diabetes mellitus
TFAM	Mitochondrial transcription factor A
TLC	Thin layer chromatography
UCP2	Uncoupling protein 2

Chapter 1: General Introduction

Parts of this chapter have been published as:

Targeting NAD+ in metabolic disease: new insights into an old molecule

Elhassan YS, Philp A, Lavery GG

Journal of the Endocrine Society, 2017 Jul 1; 1(7): 816–835

DOI: 10.1210/js.2017-00092

1.1. Role of Skeletal muscle

Skeletal muscle is the largest body organ accounting for nearly half of a healthy adult's total body mass, that is composed of myofibres and connective tissue and supported by neuronal and vascular networks (1). Skeletal muscle is vital to life, performing the mechanical work of locomotion and respiration and also central to whole body energy metabolism (2).

1.2. Skeletal Muscle Energy Metabolism

Skeletal muscle represents a key organ for maintaining an individual's energy homeostasis (3). It is the major site of storage of glycogen and therefore acts a reservoir to sustain body energy homeostasis enabling body systems to deal with metabolic stresses such as physical activity, nutrients intake, and fasting by balancing glucose uptake and glycogen degradation (4,5). To combat metabolic stress, skeletal muscle displays high plasticity by adapting, both as acute and chronic responses, to environmental challenges, cellular hormone signalling, and myokines (6,7). These muscle metabolic responses include, but not limited to, modulating mitochondrial biogenesis and function, mobilisation of glucose, and switch in energy substrate use (8,9).

The primary source of fuel used by skeletal muscle is dependent on the extent of muscle activity and energy demand; at rest, fat represents the primary source of energy (3). Creatine phosphate, which is stored in muscle, is metabolised to creatine with the concomitant donation of a phosphate group to adenosine diphosphate (ADP) to generate adenosine triphosphate (ATP) and represents a rapid short term source of energy (10). More sustained activity requires breakdown of muscle glycogen stores to generate glucose 6-phosphate (G6P) which is then further metabolised down the glycolysis pathway (11). During anaerobic glycolysis, a set of enzymatic reactions ensue to generate ATP from the degradation of glycose to pyruvate (12). Under aerobic conditions, such as during endurance activities when the demand for greater supply of energy is increased,

pyruvate enters the mitochondria and is metabolised to acetyl Coenzyme A (acetyl CoA) which is oxidised in the tricarboxylic acid cycle (TCA cycle) resulting in the reduction of NAD+ to NADH. NADH is a crucial reducing cofactor in oxidative phosphorylation resulting in larger quantities of ATP production (13).

Additionally, adipose-derived triglycerides can be metabolised to generate glycerol and free fatty acids. Free fatty acids are then mobilised to other cells where they are activated by reacting with Coenzyme A (CoA) to generate acyl CoA which enters the mitochondria and via β-oxidation converts to acetyl CoA which fuels the TCA cycle ultimately generating ATP (14).

Finally, when muscle energy stores are exhausted, such as during starvation, muscle is degraded to release amino acids (such as alanine and glutamine) for gluconeogenesis which predominantly takes place in the liver to then provide substrates for energy production (15). Clearly, the consumption of muscle-derived amino acids is not a sustainable source of energy as this can lead to muscle atrophy if protein synthesis is superseded by protein degradation (16).

1.3. Mitochondrial biogenesis and respiration

Mitochondria are dynamic double-membraned cell organelles, with their own circular genome, and are best known for their canonical role in the generation of energy by aerobic respiration through the consumption of metabolic fuels such as carbohydrates, fatty acids, or amino acids (13,17). Mitochondria consume 85-90% of cellular oxygen to allow oxidative phosphorylation (OXPHOS) which represents the primary metabolic pathway for ATP production from metabolic fuels (18). Mitochondrial biogenesis is the process of growth and division of existing mitochondria to maintain their function that is regulated by several factors including physical activity, oxidative stress, caloric restriction, cell regeneration and differentiation, age, and disease (19–21). For example, studies have suggested that during ageing there is disruption of mitochondrial

biogenesis, associated with disturbance of the activity of mitochondrial regulatory proteins such as AMP-activated protein kinase (AMPK), resulting in mitochondrial dysfunction (22). AMPK acts as an energy sensor within the cell to balance ATP generation and consumption. In low-energy states, AMPK is activated by the rise in ADP or AMP and in turns activates pathways that enhance energy production and limit consumption (23,24). AMPK can phosphorylate the transcriptional coactivator peroxisome proliferator-activated receptor-γ coactivator-1α (PGC-1α) which is the principal regulator of mitochondrial biogenesis. When PGC-1α is activated by deacetylation, it then activates sets of mitochondrial transcription factors, such as nuclear respiratory factor (NRF) 1 and 2, uncoupling protein 2 (UCP2) and mitochondrial transcription factor A (TFAM), which are important for the transcription and replication of mitochondrial deoxyribonucleic acid (DNA) (25,26).

1.4. Oxidative phosphorylation

OXPHOS represents a fundamental element of cell physiology being a key process of bioenergetics (27). This intricate biochemical pathway plays a pivotal role in generating ATP, the primary currency of cellular energy, through the coupling of electron transport across the mitochondrial inner membrane with the phosphorylation of ADP to ATP (28). This mechanism not fuels various cellular processes and therefore maintains cellular homeostasis and sustains life (29).

1.5. Molecular components of oxidative phosphorylation

The mitochondrial respiratory machinery involves a series of coordinated enzymatic reactions occurring within the electron transport chain (ETC) and the ATP synthase complex (30). The ETC comprises four multi-subunit protein complexes (I to IV) embedded in the inner mitochondrial

membrane, namely NADH dehydrogenase (Complex I), succinate dehydrogenase (Complex II), cytochrome c reductase (Complex III), and cytochrome c oxidase (Complex IV). Each complex, along with ubiquinone and cytochrome c as electron carriers, plays a distinct role in facilitating the sequential transfer of electrons along a series of redox reactions, ultimately leading to the generation of a proton gradient across the inner mitochondrial membrane and the subsequent synthesis of ATP by ATP synthase (also referred to as Complex V).

1.5.1. Complex I: NADH Dehydrogenase

NADH dehydrogenase, the largest and first complex of the electron transport chain, serves as the entry point for electrons derived from the oxidation of NADH molecules generated during glycolysis and the citric acid cycle (31). This multi-subunit enzyme complex catalyses the transfer of electrons from NADH to ubiquinone (coenzyme Q), a mobile electron carrier within the inner mitochondrial membrane (32). The transfer of electrons through a series of redox reactions within complex I is coupled with the translocation of protons across the inner mitochondrial membrane from the matrix to the intermembrane space, contributing to the establishment of the proton gradient.

1.5.2. Complex II: Succinate Dehydrogenase

Unlike the other complexes of the electron transport chain, succinate dehydrogenase (SDH) is not only a component of oxidative phosphorylation but also an integral part of the citric acid cycle (33). Located within the inner mitochondrial membrane, SDH catalyses the oxidation of succinate to fumarate while simultaneously reducing ubiquinone to ubiquinol (34). The electrons derived from succinate are transferred via flavin adenine dinucleotide (FAD) to the ubiquinone pool, bypassing complex I. Thus, complex II directly contributes to the generation of reducing

equivalents for the electron transport chain and the maintenance of the mitochondrial redox balance.

1.5.3. Complex III: Cytochrome c Reductase

Cytochrome c reductase, also known as complex III, functions as the next link in the electron transport chain, receiving electrons from ubiquinol and transferring them to cytochrome c, a soluble electron carrier located in the intermembrane space (35). This multi-subunit complex comprises cytochromes, iron-sulfur clusters, and other cofactors essential for electron transfer. The transfer of electrons through complex III is coupled with the translocation of protons across the inner mitochondrial membrane, further contributing to the establishment of the proton gradient (35).

1.5.4. Complex IV: Cytochrome c Oxidase

Cytochrome c oxidase, the terminal complex of the electron transport chain, catalyzes the final step of electron transfer, where molecular oxygen serves as the final electron acceptor, ultimately leading to the reduction of oxygen to water (36). This multi-subunit enzyme complex contains heme groups and copper ions critical for the transfer of electrons from cytochrome c to oxygen. The energy released during this process is utilised to pump additional protons across the inner mitochondrial membrane, contributing to the electrochemical gradient necessary for ATP synthesis (37).

1.5.5. Complex V: ATP Synthase

Completing the electron transport chain, ATP synthase acts as the final molecular machine responsible for ATP production, utilising the proton gradient established across the inner mitochondrial membrane. Structurally, ATP synthase consists of two main components: the F1 catalytic domain protruding into the mitochondrial matrix and the F0 proton-translocating domain embedded within the inner mitochondrial membrane (38).

The F1 domain, often referred to as the headpiece, comprises multiple subunits arranged in a hexameric structure. These subunits possess ATPase activity, catalysing the synthesis of ATP from adenosine diphosphate (ADP) and inorganic phosphate (Pi) through a process known as oxidative phosphorylation (39). The rotational movement of the γ subunit within the F1 domain, driven by the flow of protons through the F0 domain, induces conformational changes in the catalytic sites, enabling the synthesis of ATP.

In contrast, the F0 domain forms a proton channel spanning the lipid bilayer of the inner mitochondrial membrane. Protons translocate through this channel from the intermembrane space to the mitochondrial matrix, driven by the electrochemical gradient generated by the electron transport chain complexes. The flow of protons through the F0 domain powers the rotary motion of the γ subunit in the F1 domain, facilitating ATP synthesis.

Overall, ATP synthase represents a remarkable molecular complex that converts the energy stored in the proton gradient into the chemical energy of ATP, thus serving as the primary source of cellular energy in aerobic organisms. Dysregulation of ATP synthase activity can have profound implications for cellular metabolism and physiological function, highlighting its significance in health and disease (40).

1.6. Nicotinamide Adenine Dinucleotide

Nicotinamide adenine dinucleotide (NAD+) is a molecule which is essential for life in all organisms (41,42). It was discovered more than 100 years ago as a low-molecular weight “cozymase” which is present in boiled yeast extracts and is essential for yeast fermentation (43). NAD+ has been widely recognised for its central role in cellular respiration, the set of biochemical reaction that generate energy in the form of adenosine triphosphate (ATP) after intake of nutrients, by serving as cofactor for oxidation-reduction (redox) reactions (44). NAD+ is composed of two nucleotides: one with an adenine base and the other with a nicotinamide base and both are linked by their respective phosphate groups (Figure 1.1). It exists in an oxidised form (NAD+) and a reduced form (NADH) (Figure 1.2).

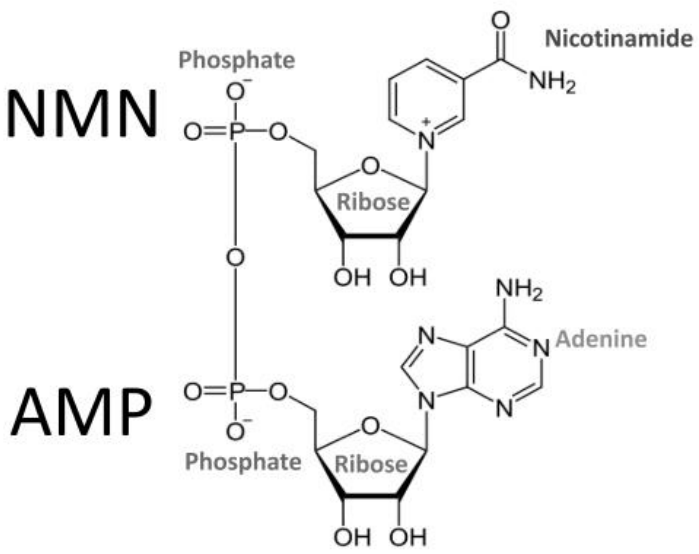

Figure 1.1: The molecular structure of NAD+.

NADH can be generated from the reduction of NAD+ in the sixth step of glycolysis when NAD+ serves as a cofactor for glyceraldehyde-3-phosphate dehydrogenase which converts

glyceraldehyde-3-phosphate to 1,3-biphosphoglycerate (45). In the presence of oxygen, NADH is carried across the mitochondrial membrane to the matrix through the malate-aspartate shuttle or the glycerol-3-3-phosphate shuttle. Pyruvate, the final product of glycolysis under aerobic settings, is decarboxylated to acetyl CoA with further NAD+ reduction to NADH (46). This oxidative reaction is catalysed by pyruvate dehydrogenase complex which is regarded as the convergence point in the regulation of the metabolic fine-tuning between glucose, fatty acid, and ketone oxidation. This is because fatty acid oxidation and oxidation of ketones can also produce acetyl CoA and NAD+ is also required as a cofactor in these processes (long-chain 3-hydroxyacyl-CoA dehydrogenase, hydroxyacyl-CoA dehydrogenase and D-β-hydroxybutyrate dehydrogenase) (47,48). NAD+ is also required as a cofactor for TCA cycle enzymes isocitrate dehydrogenase, α-ketoglutarate dehydrogenase and malate dehydrogenase (49). The generated NADH from these redox reactions drives the electron transport chain by donating electrons to Complex I, whilst FADH2, generated from the TCA cycle, donates electrons to Complex II of the chain to produce ATP (50) (Figure 1.3). When oxygen is limited, NADH facilitates the reduction of pyruvate to lactate to yield NAD+ (50).

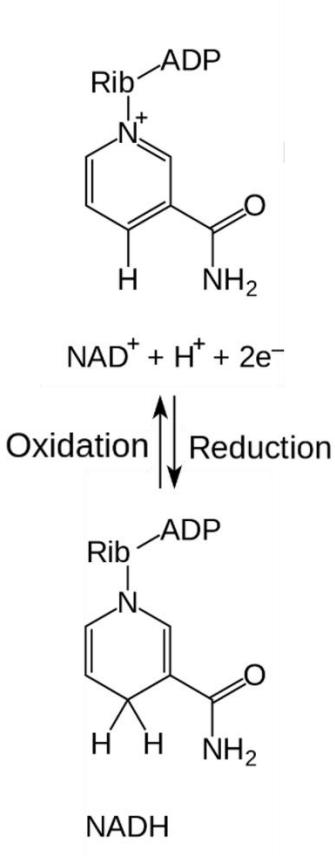

Figure 1.2: The structure of NAD (H)+ as redox factors.

Furthermore, NAD+ can also be phosphorylated by NAD kinase (NADK) which transfers a phosphate group, most often from ATP, to the adenosine ribose moiety of NAD+ to form NADP+ (51). Similar to NAD+, oxidised NADP+ accepts electrons from molecules and is therefore reduced NADPH. These electrons transfers enable oxidoreductase enzymes to catalyse transhydrogenase reactions (52). Generally, NAD+ frequently serves in energy generating catabolic reactions (e.g. glycolysis, fatty oxidation, TCA cycle) to become reduced to NADH. On the other hand, NADP+ is mostly involved in anabolic pathways such as cholesterol synthesis and fatty acid chain elongation (53). NADP+ and NADPH have cell protection roles in protecting against oxidative stress which results from an increase in the production of reactive oxygen species (ROS) through acting as a reducing factor for antioxidants such as glutathione which

clear hydrogen peroxide, a downstream ROS product (54). Therefore, they are maintained at high levels in the mitochondria and cytosol, compared to NADH which is depleted in the cytosol (55).

Given these crucial redox roles of NAD+, depression in its cellular levels can disturb glycolysis and oxidative phosphorylation leading to impaired cellular energy balance, ultimately leading to cell death (56–58). The critical role of NAD+ in mitochondrial intermediary metabolism suggests that variations in NAD+ concentrations in this compartment may affect metabolic efficiency, ageing, and ageing-associated diseases. This model is supported by the observation that components of the malate-aspartate NADH shuttle, which transfers reducing equivalent from NADH in the cytoplasm to NADH in the mitochondrial matrix, are required for life-span extension in response to dietary restriction in yeast (59).

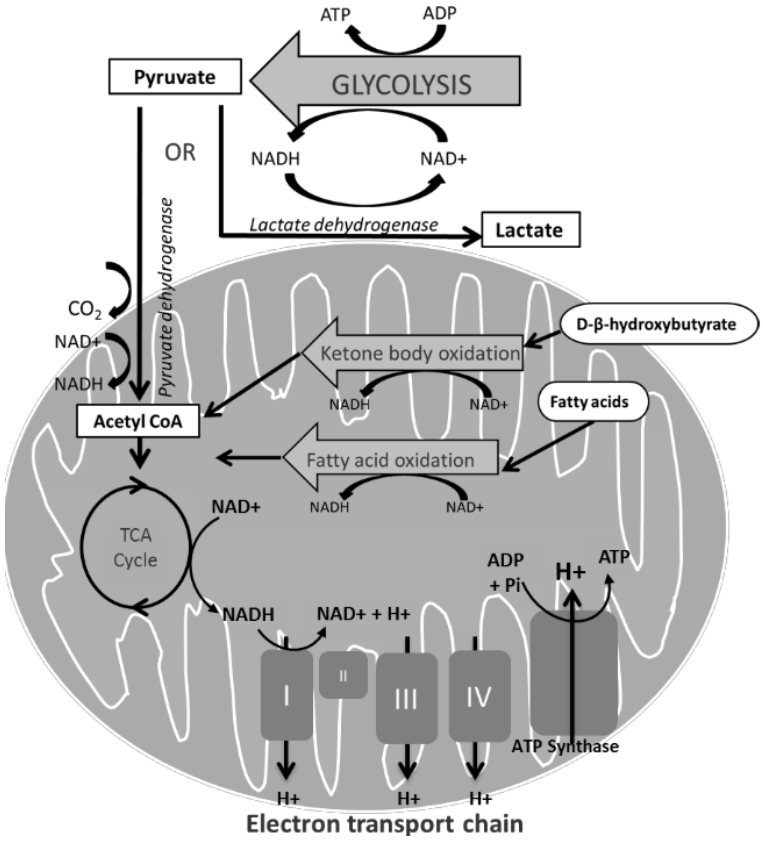

Figure 1.3: Schematic representation of the electron transport chain and the oxidative phosphorylation process leading to the formation of energy (ATP) from the different fuels via glycolysis, fatty acid oxidation, ketone bodies oxidation, and tricarboxylic acid cycle (TCA).

1.6.1. Non-redox Functions of NAD+

Eukaryotic chromatin is composed of DNA which is structurally wrapped around two copies of each of 4 nuclear proteins called histones (H2A. H2B, H3, and H4) (60,61). Modification of these histone proteins is an important mechanism of epigenetics by which genetic expression and activity are determined by factors other than the underlying DNA sequence (62). These covalent modifications include acetylation (addition of acetyl group), methylation (addition of methyl group), phosphorylation (addition of phosphoryl group), and ubiquitination (addition of ubiquitin) (63,64), which influence all the chromatin-dependant processes.

NAD+ has relatively recently been recognised for its non-redox cell signalling processes, conspicuously being a substrate for enzymes implicated in covalent modification of histones (52,65). These NAD+-dependant enzymes fall into 3 classes all of which involve cleavage of the glycosidic bond between nicotinamide and the adenosine diphosphate (ADP)-ribose. The ribose moiety donated by NAD+ is then transferred to an acceptor molecule such as amino acid residues of proteins resulting in modification and modulation of their function (66,67). The three classes are: sirtuins, poly-ADP ribose polymerases (PARPs), and cyclic ADP ribose synthases (CD38 and CD157) (Figure 1.4). The relative activity of these enzymes contributes to NAD+ consumption and therefore have an important influence on the activity of other cellular enzymes through modulating NAD+ availability, stressing the importance of considering the crosstalk between these distinct signalling pathways.

1.6.2. Sirtuins

Histone decateylases (HDACs) are enzymes that remove the acetyl group from ε-*N*-acetyl lysine amino acids on the histones (68–71). Sirtuins, named for their named for their similarity to the yeast Sir2 gene-silencing protein, are histone decatylases which are the most important class of

the NAD+-consuming enzymes in terms of cellular energy metabolism (72,73). Sirtuins consume NAD+ and transfer an acetyl group to the NAD+-donated ADP-ribose, resulting in an O-acetyl-ADP-ribose and a decaetylated lysine residue in the protein substrate (74,75). To date, seven sirtuins have been characterised in mammals (SIRT1 – SIRT7) which have diverse cellular localisation expression patterns, and biochemical and biological functions (76,77).

At the turn of the 21st century, there has been renascent interest in the field of NAD+ and sirtuins metabolism research. This is due to two seminal discoveries. First, the dependency of sirtuins on NAD+ as a consumed substrate was established (73). Second, was the finding that the yeast Sir2 protein is required for the lifespan extension mediated by calorie restriction (78), although this has been challenged in other studies (79).

In terms of expression and localisation, the seven sirtuins are ubiquitously expressed and share a conserved NAD+-binding and catalytic domain, called the sirtuin core domain, which consists of 275 amino acid sequence (80). Additionally, each sirtuin has unique N- and C-terminal domain (81). SIRT1, SIRT6, and SIRT7 are predominantly nuclear proteins with distinct subnuclear compartmentalisation and they modulate nuclear transcription factors and chromatin remodelling proteins (82,83). SIRT3, SIRT4, and SIRT5 are located in the mitochondria and they have critical roles in sensing the cellular redox state and triggering appropriate metabolic responses (84,85). Finally, SIRT2 is mainly cytoplasmic and can regulate transcription factors in the cytoplasm when inactive (86).

SIRT1 and SIRT3 are the most relevant from a metabolic perspective (87). SIRT1 is the most characterised sirtuin and in addition to its function as histone deacetylase, it also targets non-histone transcriptional factors and coactivators including forkhead box protein O1 (FOXO1) (88,89), PGC-1α (90), p53 (91), p300 (92), nuclear factor-KappaB (NF-κB) (93), and hypoxia-inducible factor(HIF)-1α (94). Worthwhile highlighting that SIRT1-mediated metabolic control is regulated by AMPK, the cellular fuel gauge, which can enhance SIRT1 activity by increasing

NAD+ levels (95). Contrariwise, SIRT1 activation can induce AMPK through deacetylating AMPK upstream kinase, LKB1 (96). SIRT1-mediated deacetylation of these substrates is important for mitochondrial biogenesis, metabolic regulation, and genomic stability and autophagy, favouring longevity (97).

SIRT3 is the key mitochondrial sirtuin. It was first characterised to deacetylate, and therefore activate, acetyl-CoA synthetase 2 (ACS2) which converts acetate to acetyl-CoA, ultimately entering the TCA cycle and contributing to energy production (98,99). Thereafter, it was discovered that SIRT3 decaetylates NDUFA9, a component of the electron transport chain (100), and promote fatty acid oxidation during fasting (101), the formation of ketone body by-products from acetyl-CoA (102), and α-ketoglutarate from the amino acid glutamate (103). Furthermore, SIRT3 deacetylates superoxide dismutase-2 (SOD2) which is essential in oxygen detoxification (104) and isocitrate dehydrogenase 2 (IDH2), a major source of NADPH in the TCA cycle (105). Taken together, SIRT3 stimulates metabolic and detoxification responses during fasting state when activated by low-nutrient levels (106).

Interestingly, overexpression of the nuclear sirtuin SIRT6 in mice induced skeletal atrophy although the mechanisms underlying this process are not very well understood (107).

1.6.3. Poly-ADP ribose polymerases

The PARP family of proteins are the most studied among the ADP-ribosyl transferases (108). These are nuclear enzymes that transfer NAD+-derived single moiety or polymers of ADPribose to their protein substrates (109,110). To date, 17 PARPs have been described, with PARP1 and PARP2 representing the main PARP activities in mammals (111). PARP1 represents the major NAD+-consuming enzyme permitting posttranslational modification of proteins by linking ADP-ribose groups to an amino acid receptor (112,113). PARPs activity is robustly enhanced by breaks

in DNA strand and therefore, they are typically described as DNA repair proteins (114–117). For instance, in acute DNA damage, sudden depletion of NAD+ due to PARP activation can be triggered (118). Corroborating the impact of PARPs as the major cellular NAD+ consumers, PARP inhibition increases cellular NAD+ content (119). Thus, by modulating NAD+ availability, PARPs are linked to cellular metabolism. PARPs activity has been reported to increase with ageing mice, contributing to the ageing phenotype (120). PARP1 knockout mice are metabolically healthier and had higher NAD+ content in skeletal muscle and brown adipose tissue (121). Similarly, PARP2 deletion in mice enhanced SIRT1, energy expenditure, and mitochondrial function (122). Additionally, PARP1 has been described as a regulator of circadian clock in mouse liver (123).

1.6.4. Cyclic ADP-Ribose Synthases

A wide spectrum of physiological functions are signalled and regulated by mobilisation of intracellular Ca^{2+} stores (124). The highly conserved cADP-ribose synthases (CD38 and CD157), are membrane-bound ectoenzymes that produce and hydrolyse the Ca^{2+}- mobilising second messenger cyclic ADP-ribose from NAD+ (125). Moreover, CD38 catalyses a base exchange of the nicotinamide of NADP+ with nicotinic acid to form nicotinic acid adenine dinucleotide phosphate (NAADP) which is also a hydrolytic substrate (126,127). Thus, CD38/CD157 and NAADP have distinct and crucial functions in intracellular calcium homeostasis and signalling (128,129). Several genetic studies highlighted the central role of CD38 as NAD+ consumer and its overarching role in metabolism. The knockout of CD38 increased NAD+ and activated SIRT1 in tissues (130) and protected against high fat diet induced obesity (131).

These three classes of NAD+-dependent signalling reactions are regarded as the “master regulators” of metabolism due to their central regulatory roles in cellular metabolism (132). The enhanced activity of these reactions and their downstream pathways has been associated with

improved cellular and organismal function (133,134). These non-redox roles of NAD+ have ignited the interest in further researching this molecule.

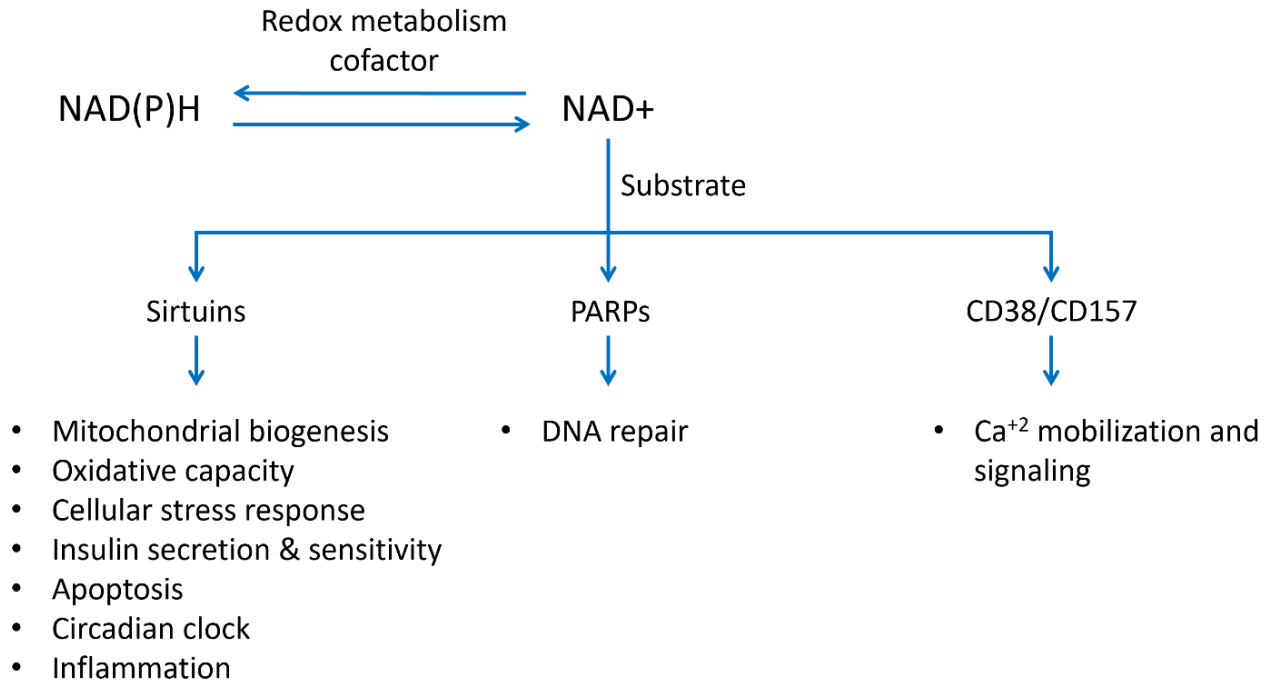

Figure 1.4: Summary of the non-redox functions of NAD+.

1.7. NAD+ biosynthesis pathways

Given the diverse and crucial cellular processes that involve NAD+ consumption, there is a requirement for continuous NAD+ synthesis to maintain its cellular levels. Pellagra, the disease of the 4"D's": dermatitis, diarrhoea, dementia, and death, illustrates the importance of sufficient NAD+ levels (135,136). In 1937, Conrad Elvehjem and colleagues identified that the factor that prevents and cures pellagra is the NAD+ precursor, nicotinic acid (137,138).

Intracellular concentration of NAD+ is believed to be 0.4 to 0.7 mM (139), however, NAD+ levels varies depending on the cell type and physiologic state being assessed. There is considerable

difference in NAD+ levels between the different cellular compartments. The mitochondria contain the largest NAD+ pool representing 70% to 75% of cellular NAD+ and 10- to 100-fold higher than cytosolic NAD+ (140,141). The NAD+ levels vary to adapt cellular physiology in response to changes in nutrient availability and energy demand. Illustrating this point, calorie restriction and exercise increase NAD+ levels in tissues (142–144), whilst high fat diet and ageing in mice reduce NAD+ levels (120,145–147).

Given the importance of adequate NAD+ homeostasis, numerous NAD+ biosynthesis pathways exist in humans to ensure that NAD+ turnover is matched with adequate supply. Impairment of these mechanisms can lead to NAD+ depletion and ultimately cell death (148).

1.7.1. De novo NAD+ synthesis

In humans, NAD+ can be synthesised via the de novo pathway, where nicotinamide is made from scratch, from the dietary amino acid tryptophan (149). The first steps of the de novo pathway, which comprise the so-called kynurenine pathway, transform tryptophan into amino-3-carboxymuconate semialdehyde (ACMS). ACMS subsequently undergoes spontaneous cyclisation to quinolinic acid. Quinolinate phosphoribosyltransferase (QPRT) catalyses the conversion of quinolinic acid to nicotinic acid mononucleotide (NAMN) which is then converted by the ubiquitous enzyme nicotinamide mononucleotide adenylyltransferase (NMNAT) to form nicotinic acid adenine dinucleotide (NAAD) (150). Eventually, NAAD is amidated via the enzyme NAD+ synthase (NADS) to form NAD+ (151).

Although the kynurenine pathway represents the main pathway for tryptophan breakdown (152), it is a poor NAD+ precursor in vivo and is insufficient to support physiological NAD+ concentrations in mammals (153,154). Additionally, its role in the maintenance of cellular NAD+ levels in human cells is regarded as insignificant (155). Thus, most organisms have alternative

pathways to synthesise NAD+ from non-amino acid dietary vitamin B3 precursors or from recycling of the nicotinamide molecule cleaved-off from NAD+ consuming reactions (156).

1.7.2. Vitamin B3 as NAD+ precursor molecules

As NAD+ is continuously spent in cell signalling processes, and de novo synthesis is insufficient to maintain homeostasis, NAD+ salvage is paramount to maintain the cellular NAD+ pool. The major precursors of NAD+ are from the vitamin B3 precursors nicotinic acid (NA), nicotinamide (NAM), and nicotinamide riboside (NR) which are found in the diet or as consumed NAD+ metabolites, with similar chemical structures to NAD+ (Figure 1.5). Different pathways exist that utilise these vitamin B3 precursors (139,155,157), however, the relative importance and tissue specificity of the different precursor molecules in NAD+ replenishment *in vivo* remains unclear

Preiss-Handler pathway

Nicotinic acid requires only three steps to be converted to NAD+ via the so-called Preiss-Handler pathway (Figure 1.6). NA is first coupled to 5-phosphoribosyl-1-pyrophosphate (PRPP) to form NAMN by nicotinic acid phosphoribosyltransferase (NAPT). NAMN then converges with the same NAD+ synthesis de novo pathway used by tryptophan where an adenylyl moiety from ATP is then added to NAMN by NMNAT to form NAAD, which in turn is amidated by NADS to form NAD+ (158,159). As the final step of both the de novo and Preiss-Handler pathways, NADS activity is rate-limiting for NAD+ biosynthesis by these routes. The degree of NADS enzymatic activity varies across tissues, with highest activity levels demonstrated in the liver and kidneys. However, NADS activity is undetectable in skeletal muscle and the lungs and very low in brain homogenates, reflecting limited roles of the de novo and Preiss-Handler pathways in NAD+ synthesis in these tissues (160).

NAMPT salvage pathway

As NAD+ contains a NAM molecule that cannot be synthesised by most tissues de novo, most mammalian cells must instead rely on a salvage pathway to locally reproduce degraded NAD+ (Figure 1.6). In this two-step salvage pathway, the Nam moiety is recycled back into NAD+ to ensure that the continuous NAD+ consumption is matched by supply. Through the action of the ubiquitously expressed rate-limiting enzyme nicotinamide phosphoribosyltransferase (NAMPT), NAM is coupled to PRPP to form nicotinamide mononucleotide (NMN) in an ATP dependant reaction. NMN is then converted by the enzyme NMNAT to form NAD+ (155). This NAMPT-mediated direct NAD+ recycling mechanism is sensitive to various cellular physiological and stress states (161,162).

NAMPT activity has been described in 1957 (163). However, its molecular activity was first described as being equivalent to a previous cytokine called PBEF (164,165) that was initially cloned from a cDNA library of activated peripheral blood lymphocytes (166). NAMPT role was later redefined as an adipokine, called visfatin (167–169). However, this NAMPT role as an insulin-mimetic has been challenged (170). It is also worthwhile mentioning that the paper published in *Science* in 2004 and described the insulin-mimetic properties of visfatin has been retracted.

NAMPT is found in both the intracellular (mainly in the cytosol and nucleus) and extracellular compartments, which supports a more systemic role of NAMPT in the distribution of NAD+ and metabolism in general (171,172). Highest levels of NAMPT expression were reported in myocytes, hepatocytes, and adipocytes (166). Illustrating the importance of intracellular NAMPT, loss of its function markedly reduces NAD+ and causes cell death (173). NAMPT can be released from several cell types, including from adipose tissue, liver, heart, leucocytes, beta cells, and

neuronal cells (174). Although the mechanism of this extracellular NAMPT (eNAMPT) secretion and its role remains unclear, increased activity has been reported in response to cell death and the release of ATP and PRPP into the circulation (161,175), and it has been suggested that eNAMPT activity is relevant in metabolism and cancer (176–178). Yoshida et al reported in 2019 that eNAMPT is contained exclusively in extra-cellular vesicles and supplementing eNAMPT in vesicles improved physical activity and increased life-span in mice (176). It has also been questioned whether eNAMPT has NAD+ biosynthetic role via NMN and Hara et al showed that NAMPT did not increase NMN in the blood plasma suggesting NAD+-independent effects (175).

Interestingly, NAMPT seem to exhibit circadian rhythmicity and guides a circadian clock feedback mechanism through NAD+-dependant SIRT1 activation of the key clock regulatory complex, CLOCK:BMAL1 (179–181).

Nicotinamide riboside kinase (Nrk) salvage pathway

In addition to the long-established NAMPT salvage pathway, a more recent additional salvage pathway has been discovered when Bieganowski and Brenner challenged the belief eukaryotic NAD+ biosynthesis only flows through NAMN (via the Preiss-Handler pathway)(182) (Figure 1.6). They reported that NR, a known NAD+ precursor in bacteria (183,184), is a eukaryotic NAD+ precursor in a previously undiscovered NAD+ synthesis pathway. They characterised two human nicotinamide riboside kinase enzyme isoforms (Nrk1 and Nrk2) (182) that phosphorylate NR on the 5′-OH of the ribose ring, using as ATP as phosphate donor, to form NMN which is subsequently adenylated by NMNAT to form NAD+(182).

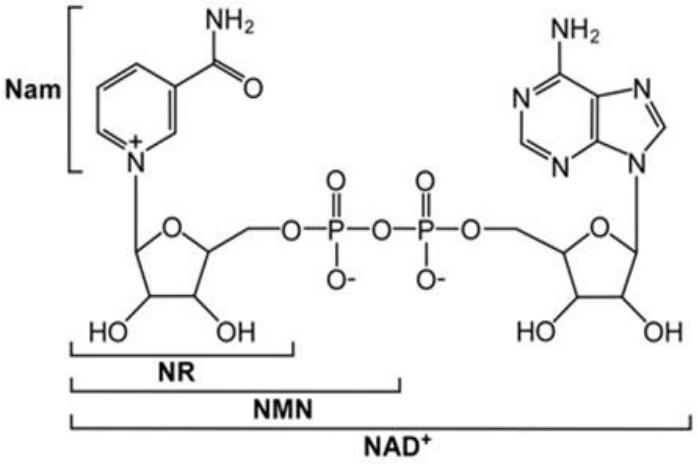

Figure 1.5: The structure of NAD+ and its precursors. (Adapted from Bogan et al 2008 (185)).

Nicotinic acid riboside (NAR) is an NAD+ precursor (least studies of the NAD+ precursors) in yeast and human cells where it can also be phosphorylated by Nrk to NAMN and subsequently to NAD+ (186).

Substrate specificity of Nrk1 and Nrk2 differ but both have high affinity for NR (187,188). Nrk1 is ubiquitously expressed whereas Nrk2 appears to be highly specific to skeletal muscle (189,190). Interestingly, several cellular stress states are associated with NRK2 overexpression (191–193).

Relatively recently, it has been shown that the human cytoplasmic 5'-nucleotidases (5'-NTs) are capable of dephosphorylating NAMN and, to a lesser extent, NMN thereby generating intracellular ribosides pool. Thus, NAR can be generated from NA via NAPT-mediated NAMN formation. NAMN, in turn, is then dephosphorylated to NAR by 5'-NTs(186). Therefore, these ribosides turnover forms an integral part of NAD metabolism. This intracellular NR and NAR generation was first observed in yeast mediated by the cytoplasmic 5'-nucleotidase (5'-NTs) Isn1 and Sdt1 (194). 5NTs also exist extracellularly where NMN is dephosphorylated to NR in order to penetrate into the cell (155). The presence of NMN in plasma has been a matter of debate (175). Therefore, it is plausible that NR, rather than NMN, is the molecule taken up by the cell, and then re-

phosphorylated inside the cell to NMN by NRK. Of note, the presence of NMN transporter has been characterised (195), whilst no such transporter for NR has been reported.

In summary, in human cells, there are five distinct entry points into NAD+ biosynthesis (Figure 1.6): NA, Nam, NR, NAR, and Tryptophan. All of these converge at the step of NAD+ and NAAD formation by NMNATs. It is important to note, however, that not all these pathways are active in each cell and at all times. This is dependent on tissue and cell-type specific enzyme expression (185). For instance, cells must express the enzymes involved in the de novo pathway to utilise Tryptophan, must express the Preiss-Handler pathway to utilise NA, and must express either NRK or nucleoside phosphorylase and the NAMPT pathway to utilise NR. Because tissue and cell-type specific enzyme expression differences exist in metazoans, the precursors are differentially utilised in the gut, brain, blood and other organs (185). The de novo pathway is clearly active in liver, neurones, and immune cells. The pathway from NA is expressed in the liver, kidney, heart, and intestine. While vertebrates do not possess the nicotinamidase enzyme that converts NAM to NA, intestinal bacteria in the vertebrate gut use nicotinamidase to convert NAM to NA, which in turn is used to synthesise NAD+ via the Preiss-Handler salvage pathway. The NAMR salvage pathway is expressed in neurons and in cardiac and skeletal muscle (185)

Importantly, the entire NAD+ pool is consumed and replenished several times each day, balanced by the different NAD+ synthesis pathways (196). Due to its constant utilisation, the half-life of NAD+ in mammals is only up to 10 hours (197–199). The NAD+/NADH levels vary to adjust cellular and tissue physiology in response to changes in nutrient availability and energy demand.

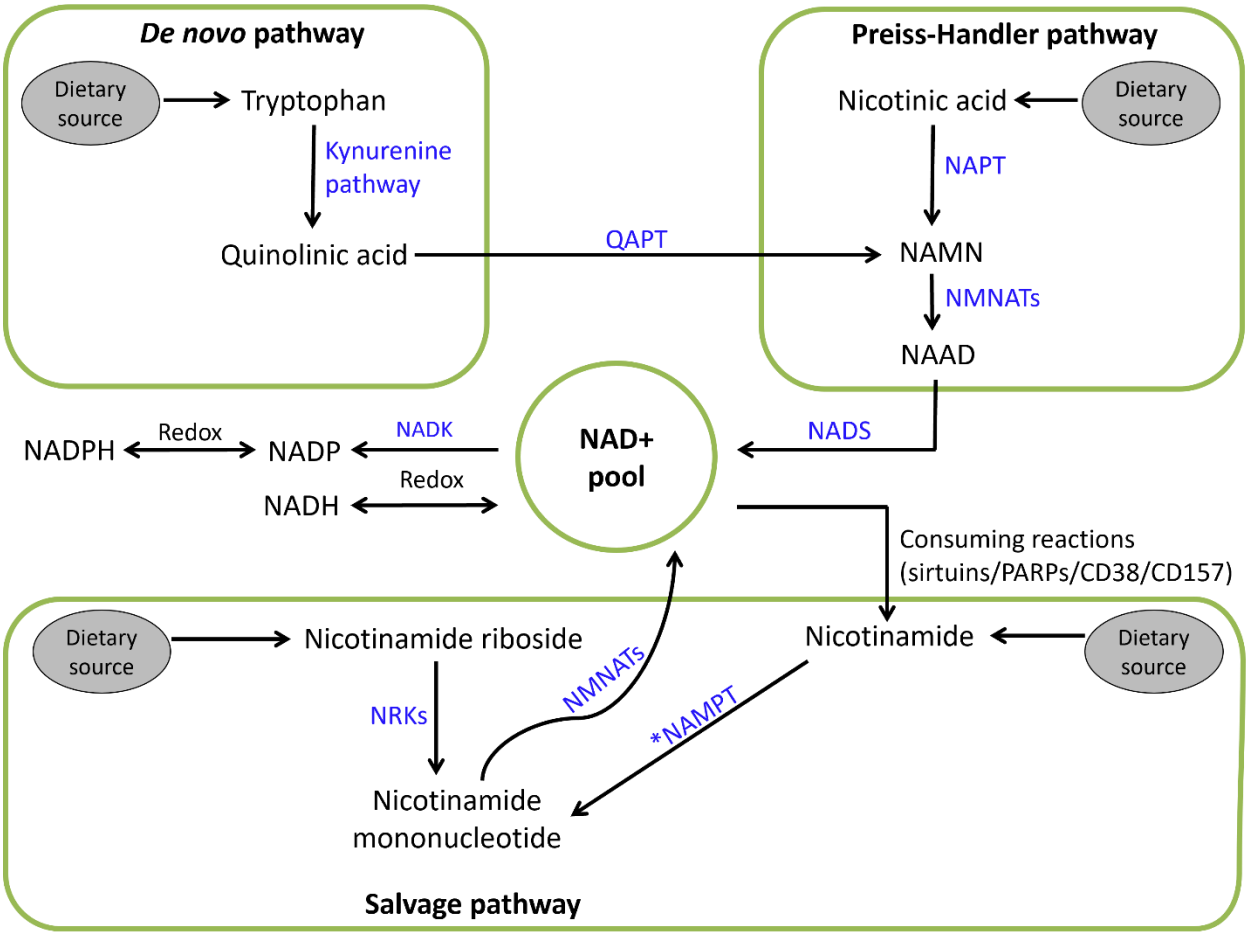

Figure 1.6: Schematic representation of the NAD+ biosynthesis pathway in the cell cytoplasm. The five entry points for NAD+ synthesis are de novo pathway by Tryptophan, Preiss-Handler pathway by Nicotinic acid, and Salvage pathway through Nicotinamide riboside. NAD is consumed by C38, CD157, PARP, and Sirtuins, and the result of NAD+ breakdown is Nicotinamide which is converted to nicotinamide mononucleotide to enter the NAD+ synthesis pathway. NAAD, nicotinic acid adenine dinucleotide; NADK, NAD kinase; NAPT, nicotinic acid phosphoribosyl-transferase; NADS, NAD+ synthase; NMNAT, nicotinamide mononucleotide adenylyl-transferase; QAPT, quinolinic acid Phosphoribosyl-transferase.

1.8. NAD+ boosting strategies

The recommended daily allowance of niacin, collective term for NA and Nam, is 16 mg/day for men and 14 mg/day for women (200) which can be achieved through the diet. The main sources of dietary niacin are meat, fish, eggs, some vegetables, nuts, fortified foods (e.g. cereals), and dairy products (201–203). More recently, the presence of NR in cow's milk was confirmed (182,204). Intake of these diets is sufficient to prevent pellagra. However, substantial lines of evidence suggest that greater rates of NAD+ synthesis is beneficial by supporting pathways that require NAD+ as a substrate. Higher NAD+ levels can be achieved through the provision of higher concentration of the dietary vitamin B3 precursors (145,146,205,206), NAD+ biosynthesis enzymes augmentation (95,142), and inhibition of the NAD+-consuming enzymes (131,207,208).

1.9. Vitamin B3 precursor supplementation

The most obvious strategy to increase cellular NAD+ is via the supplementation of the different Vitamin B3 precursors, all of which can increase NAD+ concentrations in human and animal tissues. This approach is the most tractable because NAD+ precursors are naturally occurring in the diet and are readily available in synthetic isolated forms. This nutritional approach to increase NAD+ metabolism *in vivo* can potentially provide a relatively inexpensive strategy with low toxicity and limited side effects (209,210).

1.9.1. Niacin

NA is the most therapeutically characterised NAD+ precursor via the Preiss-Handley pathway (211) and it has been studied since the 1950s in the treatment of hyperlipidaemia. In fact, it appears to be the most powerful drug capable of increasing high-density lipoprotein (HDL) cholesterol (212–214). It is appreciated that for nutrients there is an intake threshold above which the risk of adverse effects

increases, called tolerable upper intake level (200). Therefore, the intake of niacin in the diet is problematic, whilst pharmacological doses of NA are commonly associated side effects, leading to poor compliance. This is because NA is a ligand for G-protein-coupled receptor GPR109A that is expressed in epidermal Langerhans cells (215). NA binds GPR109A and induces calcium flux to result in the formation of prostaglandins causing troublesome flushing in addition to other vasodilatory side effects such as headaches, low blood pressure, and itching (216). Due to the side effects and the reduced treatment adherence, the National Institute for Health and Care Excellence (NICE) now recommends against the use of NA for the prevention of cardiovascular disease (217). However, the American College of Cardiology/American Heart Association guideline on the treatment of blood cholesterol acknowledges NA as a treatment option (218). Noteworthy, however, a recent study showed that increased niacin metabolism and its breakdown products increased vascular inflammation and increased the risk of cardiovascular disease (219). This “niacin paradox” requires further studies to understand the boundaries between therapeutic benefit and potential harm.

Nam is the principal endogenous NAD+ precursor via the salvage pathway (139), however its utility as exogenous NAD+ precursor is limited by three lines of evidence. Whereas in the literature Nam has been used at doses as high as 3 grams per day for a variety of therapeutic applications, high dose Nam supplementation has toxic potential, particularly hepatotoxicity (220). Second, Nam can inhibit sirtuins by feedback regulation (221,222). Finally, early reports suggested that Nam is less effective than NA as an NAD+ precursor (139,223). However, under high fat diet metabolic challenge, Nam was more powerful as NAD+ precursor and sirtuin activator than NA (224). In contrast to NA, Nam is not a ligand for GPR109A and therefore the prostaglandin-mediated vasodilatory side effects are not usually expected with its use (225).

1.9.2. Nicotinamide riboside and nicotinamide mononucleotide

The contemporary NAD+ precursors NR and NMN attracted great attention in the field of metabolic research. The finding that NR is present in milk and the identification of the two human Nrk isoenzymes that synthesise NAD+ From NR (182,210) sells the promising concept of nutritional preventative or therapeutic interventions targeting NAD+ metabolism (Figure 1.7). Several studies confirmed that NR can increase intracellular NAD+ in human and animal tissues in a dose-dependent manner (204,226,227).

NMN is also a key NAD+ biosynthesis intermediate and product of the NAMPT reaction. It is the least studied NAD+ precursor, but several studies confirmed that NMN can increase intracellular NAD+ concentrations (145,147,228,229). NR and NMN are advantageous because of their ability to efficiently elevate NAD+ levels without inhibiting the sirtuins activity or causing flushing through the activation of the GPR109A receptor (146,230).

A relatively recent publication reported that dihydronicotinamide riboside (NRH), which has never been investigated before as a precursor in NAD+ metabolism, increases cellular NAD+ levels in mammalian cell and mouse tissues (231). It was already known that the enzyme quinone oxidoreductase (NQO2) which converts quinones to dihydroquinone, preferentially uses NRH as the upstream reductant (232,233).

1.9.3. Augmentation of NAD+ biosynthesis enzymes

Activation of NAMPT (the rate limiting enzyme in NAD+ biosynthesis) and AMPK (the main energy sensor within the cell) is another strategy to enhance cellular NAD+ and downstream metabolism (Figure 1.7). The most studied is the nonflavonoid polyphenol resveratrol that is present in red grapes and wine which activates AMPK and SIRT1 in humans and other species and therefore improves metabolic health status (234–237). Such metabolic efficiency could not be fully proven

in human clinical trials and a systematic review concluded that evidence is not sufficient enough to recommend resveratrol to humans beyond the dose that is available through the diet (238).

Metformin is a widely prescribed anti-diabetic drug which has a multitude of favourable effects on various body organs. Although the exact mechanism of action is debated, AMPK activation is an important action of metformin mediating its beneficial effects (239). Treatment of the mouse skeletal muscle cell line C2C12 with metformin increased AMPK activity and cellular NAD+ levels thereby regulating energy metabolism (95).

Several other compounds can potentiate NAMPT activity to increase NAD+ concentrations. The neuroprotective chemical P7C3 was discovered by *in vivo* screening of 1000 drug-like compounds during the search for a compound capable of enhancing neuron formation in the hippocampus of adult mice (240,241). Later, it has been reported that P7C3 binds NAMPT, increasing NAD+ levels (242). Some antioxidants also showed NAMPT activation properties. Troxerutin, a flavanol derived from rutin increased NAD+ levels and SIRT1 activity via activating NAMPT in mouse liver (243). Proanthocyanidins, the most abundant polyphenol in the food, steadily increased NAD+ levels in the rat liver via increased expression of the NAD+ biosynthetic enzymes (244,245). Supplementation of the dietary amino acid leucine in mice also potentiated NAMPT expression levels and NAD+ concentrations (246).

MicroRNAs (miRNAs), class of small non-coding RNA molecules, represent a hot topic in research as they appear to be implicated in several metabolic and non-metabolic disease (247). Interestingly, the inhibition of miR-34a in the mouse liver increase the expression of NAMPT, cellular NAD+, and SIRT1 activity (248).

1.9.4. Inhibition of the NAD+-consuming enzymes

Inhibiting the consumption of NAD+ by non-sirtuin pathways also boosts NAD+ levels and promotes the activity of sirtuins (Figure 1.7). Preclinical studies showed that inhibition of the non-sirtuin NAD+ consumers, PARPs and CD38, reduced the enzymatic competition for their shared substrate thus increased NAD+ levels and sirtuins activity leading to enhanced mitochondrial gene expression and more favourable metabolic profile and enhanced (131,208,249–252). PARP inhibitors have found their way into clinical practice as effective anti-cancer agents through DNA damage repair and enhanced oxidative metabolism, thereby opposing the Warburg effect (253–255).

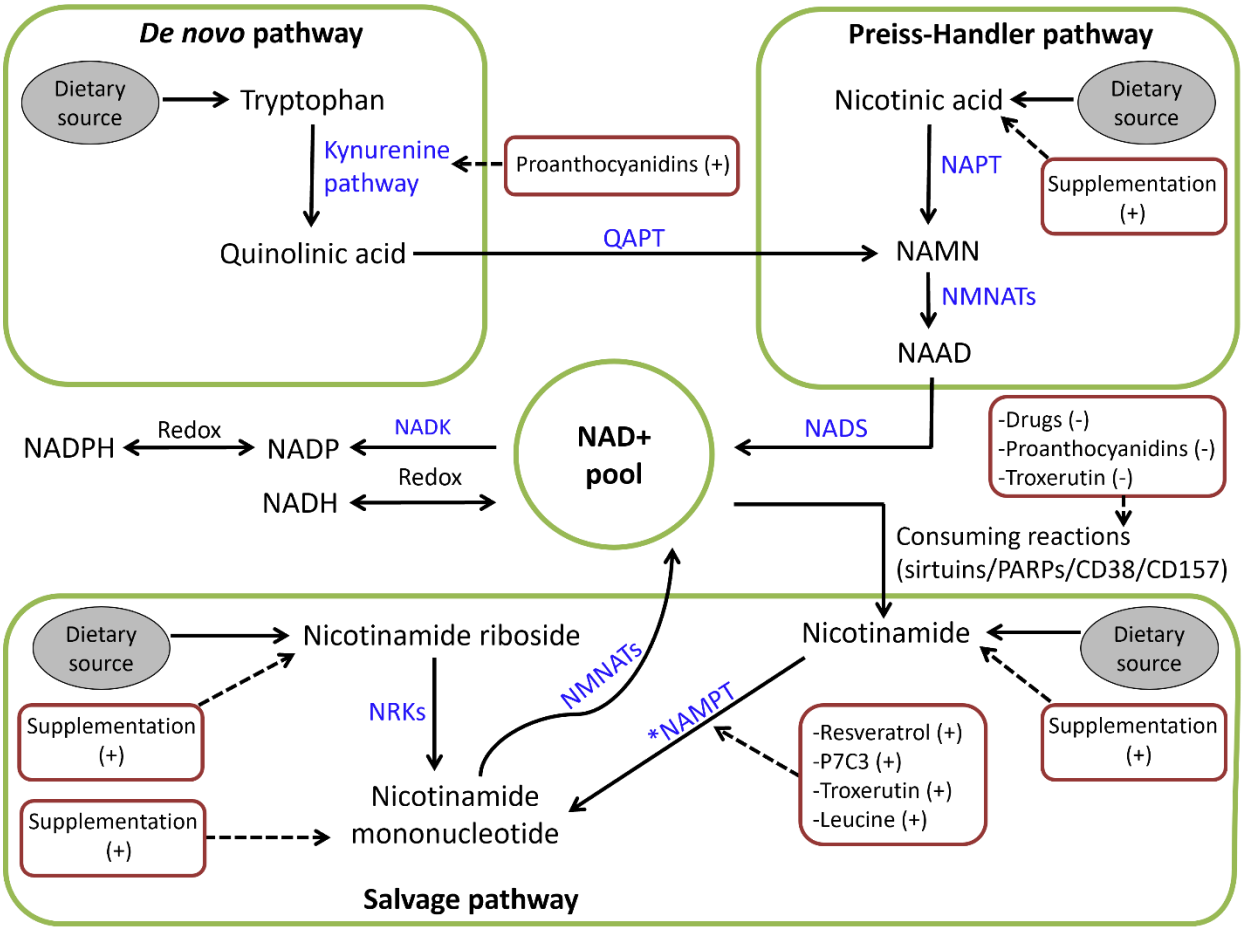

Figure 1.7. Schematic representation of the NAD+ biosynthesis pathway in the cell cytoplasm with an illustration of the different NAD+-boosting strategies.

1.10. Role of NAD+ in metabolic disease

Metabolic diseases represent a global health burden, characterised by aberrations in energy metabolism, insulin signalling, and lipid homeostasis. NAD+ serves as a vital coenzyme in redox reactions and enzymatic processes, participating in key metabolic pathways such as glycolysis, oxidative phosphorylation, and the TCA cycle. Emerging evidence suggests that NAD+ depletion or dysregulation contributes to the pathogenesis of metabolic disorders, making it an intriguing target for therapeutic interventions (256,257).

1.10.1. Age-related metabolic decline

Biologically, ageing can be defined as an age-progressive deterioration in the physiological function of the body systems as a result of diverse deleterious changes in cells and tissues disposing individuals to an increased risk of disease and eventually death. Several theories have been proposed as the driver of the ageing process including inflammation (258), immunosenescence (259), and mitochondrial dysfunction (260). Due to advancing science and technology, the proportion of ageing population continues to rise, particularly in low mortality countries. It is projected in the UK that by the year 2035, a quarter of the population will be aged over 65 years old and 5% will be aged 85 years or over (261). Similarly in the United States, it is projected that by the year 2050, there will be 83.7 million people over the age of 65 years (262). Therefore, there remains a need to identify strategies that can maintain health span and reduce the undesirable consequences of ageing.

Sarcopenia, derived from the Greek word meaning "poverty of flesh," consistently emerges as a consequence of ageing, linked with frailty, metabolic disorders, cardiovascular issues, and significant healthcare expenses (263,264). Undoubtedly, there is a pressing need for strategies targeting sarcopenia and age-related ailments. Disruptions in NAD+ homeostasis are recognised

as contributors to the ageing process (265,266). Notably, NAD+ and sirtuins play pivotal roles in regulating various pathways associated with ageing and longevity (78,120,267–269), ultimately converging on supporting mitochondrial functionality (270). Indeed, mitochondrial dysfunction and impaired cellular energy signalling are identified as crucial factors in ageing and age-related metabolic conditions like type 2 diabetes mellitus (T2DM), non-alcoholic fatty liver disease (NAFLD), and sarcopenia (118). Specifically, disturbances in mitochondrial homeostasis, stemming from decreased NAD+ and SIRT1 activity, are highlighted as hallmarks of muscle ageing (147). Moreover, restricting NAD+ in the skeletal muscle of mice led to muscle mass and function decline (i.e., sarcopenia)(56). The age-related decrease in NAD+ levels is attributed to various mechanisms, including accumulated DNA damage (resulting in chronic PARPs activation) (271,272) and increased CD38 expression, which depletes NAD+ and induces mitochondrial dysfunction (128). Additionally, chronic inflammation (273), a consistent feature of ageing, diminishes NAMPT expression and the capacity to replenish adequate NAD+ across multiple tissues (274).

More recent studies underscored the potential of NAD+ supplementation in promoting healthy ageing. For instance, NAMPT overexpression in aged mice restored NAD+ levels and muscle characteristics akin to those of young mice (56). Furthermore, mice overexpressing SIRT1 were protected against age-related diabetes and exhibited a reduced cancer incidence (275). Administration of NMN in aged mice revived NAD+ levels and mitigated age-related declines in mitochondrial function (147). From a different perspective, NR supplementation boosted PGC-1α expression in the brain of an Alzheimer's disease mouse model, significantly ameliorating cognitive decline (276). These findings reinforce the notion that declining NAD+ levels contribute to the ageing process and suggest that NAD+ supplementation holds promise in preventing and potentially treating age-related diseases.

1.10.2. Type 2 diabetes mellitus

The ongoing global challenge of obesity, insulin resistance, and T2DM remains a significant threat to public health, contributing to heightened risks of cardiovascular disease and premature mortality (277). A multitude of studies affirm the close association between compromised mitochondrial structure and function and the development of insulin resistance and T2DM (278–286). The predominant proposed mechanism involves impaired mitochondrial fatty acid oxidation, leading to intracellular accumulation of fatty acid metabolites and reactive oxygen species, ultimately reducing insulin sensitivity (287–291). Moreover, disrupted OXPHOS directly contributes to insulin resistance (292). Obesity further exacerbates these issues by diminishing mitochondrial enzymatic activities (293,294) and fostering metabolic inflexibility (295), which is the inability to switch from fatty acid to carbohydrate oxidation in response to diet and insulin stimulation (296–299).

Disrupted NAD+-mediated sirtuin signalling, particularly defective SIRT1 activity, is implicated in impaired insulin sensitivity (300–306). Furthermore, evidence supports the role of metformin and resveratrol in improving insulin sensitivity through hepatic SIRT1 activation (307,308). Of note, SIRT1 appears to modulate PGC-1α in the liver to promote gluconeogenesis (90). Knockdown of hepatic SIRT1 caused hypoglycaemia, increased systemic glucose and insulin sensitivity, and decreased glucose production (309).

Lifestyle modifications such as caloric restriction and exercise alleviate insulin resistance and T2DM via common pathways involving AMPK activation, leading to increased NAMPT-mediated NAD+ production and enhanced SIRT1 activity, thereby improving mitochondrial function (6,142,310,311). Additionally, NAD+ and SIRT1 regulate glucose-stimulated insulin secretion in pancreatic β cells, with NAMPT inhibition and SIRT1 deficiency resulting in β cell dysfunction (274,312,313). Moreover, NAMPT inhibition and the lack of SIRT1 resulted in pancreatic β cell dysfunction (172,314–317). SIRT1 also modulates circadian clock components (*CLOCK and*

BMAL1) (318,319); the induction of circadian misalignment in mice reduced hepatic *BMAL1* and *SIRT1* levels and induced insulin resistance (308). Furthermore, SIRT6 in pancreatic β cells increased FOXO1 deacetylation and increased the expression of glucose-dependent transporter 2 and therefore the glucose-sensing ability of pancreatic β cells and systemic glucose handling (320). Pancreatic SIRT3 also appears to be relevant with a study showing that pancreatic SIRT3 deficiency promoted hepatic steatosis by enhancing 5-hydroxytryptamine synthesis in rodents with diet-induced obesity (321).

These findings advocated for strategies to boost cellular NAD+ levels, with NAD+ precursors which demonstrated efficacy in enhancing insulin sensitivity and mitigating metabolic abnormalities in preclinical models (145,322). NMN administration restored β cell glucose-stimulated insulin secretion and insulin sensitivity in mouse models of glucose intolerance (145,172,229). Moreover, Nam promoted sirtuin-induced mitochondrial biogenesis and improved insulin sensitivity in obese rats with T2DM (224). Similarly, NR supplementation alleviated obesity-induced insulin resistance and improved lipid profiles in mice (146,322).

Human clinical data, however, remain limited, with acipimox and resveratrol showing inconsistent results in improving insulin sensitivity and glycaemic control, likely due to variations in study populations, treatment regimens, and assessment methods (323–330). To illustrate, acipimox administration in individuals with obesity reduced free fatty acids and fasting glucose with a possible positive effect on fasting insulin and HOMA-IR (331), but this could not be confirmed in patients with T2DM (332) speculatively due to a rebound increase in free fatty acids after short-term treatment with acipimox (333).

Relevant to this thesis which will focus on skeletal as a research model, it is important to remind that skeletal muscle is the primary tissue contributing to whole-body insulin-mediated glucose disposal and skeletal muscle mass and function have been linked with insulin resistance and diabetes mellitus (334). Skeletal muscle has been suggested to be implicated in the

pathophysiology of type 2 diabetes through abnormal fibre type distribution, abnormal lipid accumulation, and altered secretion of myokines (such as IL-6) (334).

1.10.3. Non-alcoholic fatty liver disease

NAFLD stands as the predominant liver ailment in Western societies, encompassing a range of liver diseases like simple steatosis, non-alcoholic steatohepatitis, cirrhosis, liver failure, and hepatocellular carcinoma (335). The accumulation of fat in the liver, termed lipotoxicity, triggers cellular dysfunction, forming the core of NAFLD development (336–338). This leads to metabolic adaptations such as increased β oxidation, which fosters metabolic inflexibility and triggers oxidative stress and mitochondrial dysfunction seen in NAFLD (339–342).

Maintaining adequate levels of NAD+ is crucial for effective mitochondrial fatty acid oxidation (343,344), and reduced NAD+ levels due to lipid overload can induce lipotoxicity in mice(345). Research indicated that hepatic NAD+ levels decline with age in humans and mice, potentially explaining susceptibility to NAFLD during ageing (346). Moreover, impaired hepatic SIRT1 and SIRT3 signalling are implicated in NAFLD (101,345,347–349) with evidence suggesting that enhancing these signals, such as through SIRT1 overexpression, can reverse hepatic steatosis (350,351). Disruptions in NAD+ metabolism have also been linked to alcoholic hepatic steatosis and hepatocellular carcinoma (352–354).

Various strategies targeting NAD+ metabolism to boost sirtuin signalling have shown promise in mitigating NAFLD pathology. Compounds like Nam, and resveratrol have demonstrated protective effects against liver stressors in vitro (205,355), while in vivo studies have shown NR's ability to improve mitochondrial function and decrease inflammation and hepatic lipid accumulation (146,356). Additionally, PARP inhibition in NAFLD mice corrects NAD+ deficiency, enhancing mitochondrial function and insulin sensitivity while reducing liver fat buildup and liver

enzyme levels. Interestingly, NR demonstrated the ability to target various molecular aspects of NAFLD development, such as reducing the expression of inflammatory genes in the liver, decreasing blood levels of tumour necrosis factor-alpha, and mitigating hepatic infiltration by CD45 leukocytes (356,357). In mice with NAFLD, PARP inhibition has been used to correct NAD+ deficiency, enhancing mitochondrial function and insulin sensitivity, and alleviating hepatic lipid accumulation and transaminitis (358).

Given the current data and the absence of approved therapies for NAFLD, the strategy of replenishing hepatic NAD+ levels to activate sirtuins and address mitochondrial dysfunction holds promise for future clinical trials.

The following sections of the introduction will focus on the compartmentalisation of cellular NAD+ and the interaction with a key enzyme in the metabolism of crucial hormones, term glucocorticoids.

1.11. NAD+ availability and 11β-HSD1 mediated glucocorticoid regeneration in skeletal muscle cells

1.11.1. Cellular compartmentalisation of NAD+

The intracellular NAD+ pool is split by cellular compartments that are not uniformly distributed within the subcellular organelles reflecting the various intracellular necessities of NAD+ utilisation (Figure 1.8) (359). Nuclear/cytosolic and mitochondrial pools are maintained by NAD+ biosynthesis in these compartments. NMNAT has 3 isoforms that catalyse the generation of NAD+ from NMN; NMNAT1 in the nucleus, NMNAT2 at the surface of the Golgi apparatus, and NMNAT3 within the mitochondria (360). Given that the majority of NAD+ biosynthesis enzymes and NAD+-dependent processes occur in the cytosol or the nucleus, it is accepted that NAD+ can freely mobilise between those two compartments i.e., without diffusion barriers (360). The mitochondrial

membrane is impermeable to NAD+ and the mitochondrial NAD+ pool is maintained through intracompartmental NAD+ biosynthesis (mainly via NMNAT3). Besides, the malate-aspartate NADH shuttle is a prominent a source of NADH in the mitochondria (361). The presence of a mitochondrial NAD+ transporter has also recently been characterised (362). Regarding the endoplasmic reticulum (ER), a prevalent debate exists around the mechanisms that underpin molecular transport across the ER membrane. Several observations suggested that the ER membrane is separated from the cytosolic pool by a selective barrier that permits the transport of selective molecules (363–365).

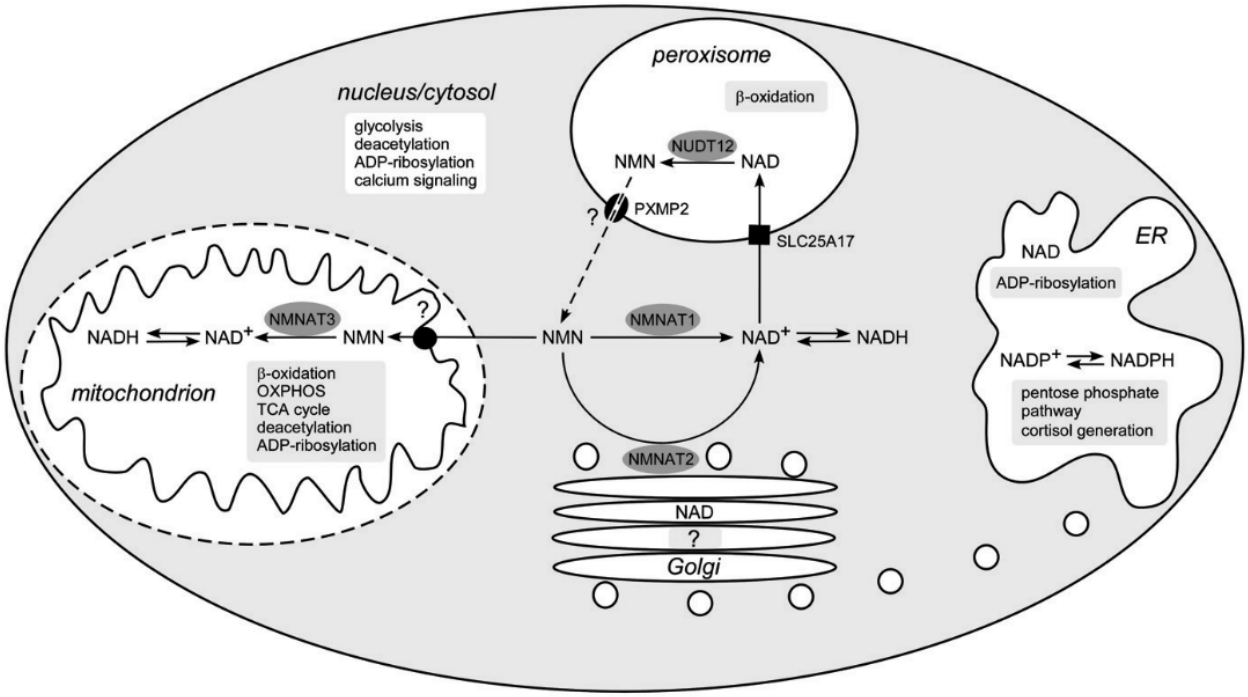

Figure 1.8: Compartmentalisation of the intracellular NAD+ pool outlining four subcellular NAD+ pools: nuclear/cytosolic, mitochondrial, peroxisomal and ER/Golgi). Adapted from Nikiforov et al. 2015 (360).

1.11.2. Maintenance of the ER pyridine nucleotide pool

Along with pre-receptor GC metabolism, other metabolic pathways are localized to the ER. These pathways are linked to carbohydrate metabolism, biotransformation, and protein processing, and

they require cytosolic substrates and cofactors (366). Therefore, it is indispensable that some molecules cross the ER membrane. However, it is accepted that the ER membrane acts as a barrier confining a separate metabolic compartment, and that compounds do not diffuse passively. This is supported by the findings that G6P is unable to enter the ER lumen unless it is mediated by a specific transporter (367,368) and that inactivating mutations in the H6PD gene result in cortisone reductase deficiency syndrome suggesting that luminal cortisone reduction is dependent on local NADPH generation (369,370). More specifically, in liver microsomes, the ER membrane appears to be impermeable to pyridine nucleotides(371,372). However, others reported an increased 11β-HSD1 activity in liver microsomes incubated with NADPH (373).

An important observation is that H6PDH knockout mice exhibited a severe skeletal myopathy characterised by switching of type II to type I (slow) fibres and demonstrated reduced locomotor activity. In these mice, a set of adaptive processes ensued in the muscle including a marked increase in Nrk2 expression, a key enzyme in cytosolic NAD+ biosynthesis(374). This might suggest that the cytosol sensed the reduction in the ER NADPH/NADP+ ratio and that the ER and cytosolic pools are not entirely separated.

1.11.3. Glucocorticoids

Adrenal corticosteroids, crucial for sustaining life, are categorised into three primary types: glucocorticoids (produced in the zona fasciculata), mineralocorticoids (synthesised in the zona glomerulosa), and sex steroids (generated in the zona reticularis) (375).

Cortisol, the principal active glucocorticoid in humans, is produced by the zona fasciculata of the adrenal cortex (corticosterone in rodents), meticulously regulated by the hypothalamic-pituitary-adrenal (HPA) axis. Corticotrophin releasing hormone (CRH) is formulated and released from the hypothalamus, prompting the synthesis and release of ACTH (adrenocorticotrophin) from the pituitary gland, which acts on the zona fasciculata of the adrenal cortex. Classic endocrine

feedback loops govern the secretion of glucocorticoids, orchestrating a tightly regulated process within the hypothalamus and pituitary gland (375) (Figure 1.9).

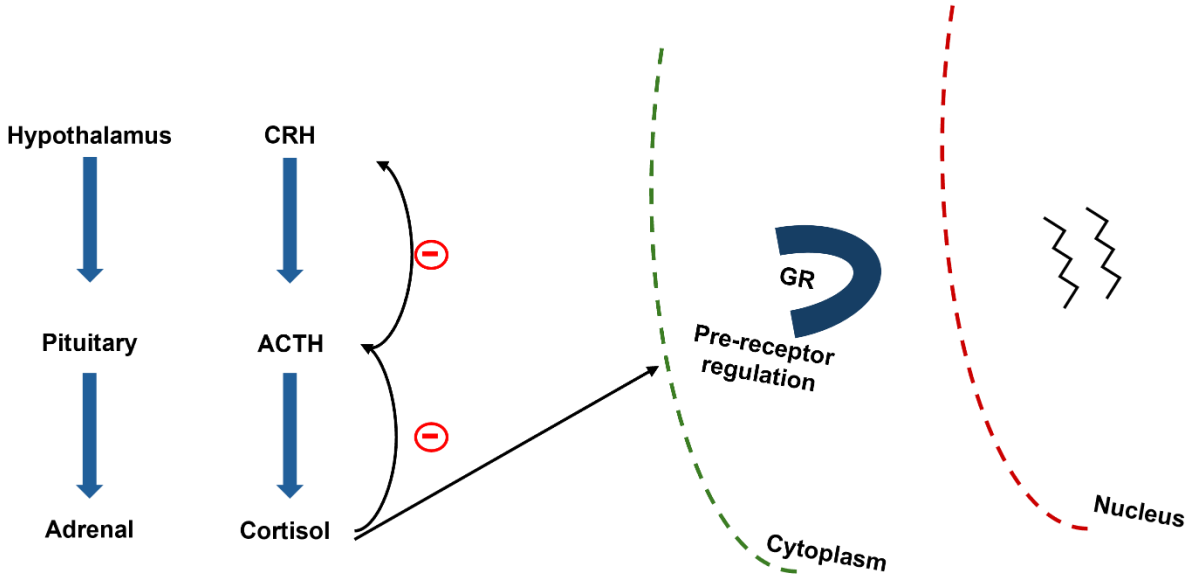

Figure 1.9: Schematic illustrating the hypothalamic pituitary adrenal axis. Corticotrophin releasing hormone (CRH) produced from the hypothalamus stimulates the anterior pituitary gland to produce adrenocorticotrophic hormone (ACTH) which in turn stimulates cortisol production from the adrenal gland. Cortisol exerts negative feedback at the level of the hypothalamus and pituitary. Circulating cortisol eventually binds the glucocorticoid receptor (GR).

1.11.4. The glucocorticoid receptor

The glucocorticoid receptor (GR), a member of the nuclear receptor family (375), plays a crucial role in different body systems. Upon binding to a glucocorticoid (GC) ligand, the GR undergoes a conformational change, leading to dissociation from the chaperones and translocation of the GR-ligand complex into the cell nucleus (375). Once inside the nucleus, the GR dimerises and binds to specific DNA sequences called glucocorticoid response elements located in the promoter region of target genes (376). These GREs regulate the expression of hundreds of GC-responsive genes (375).

1.11.5. Pre-receptor glucocorticoid metabolism and the 11 β-hydroxysteroid dehydrogenases

Circulating GCs are centrally modulated by the HPA axis. However, GCs are also further modulated at local tissue level via the 11 β-hydroxysteroid dehydrogenases (11β-HSDs). 11β-HSD has two isoenzymes that catalyse the interconversion of hormonally active cortisol [corticosterone (CORT) in rodents] and inactive cortisone [11-dehydrocorticosterone (11-DHC) in rodents]; 11β-HSD1 and 11β-HSD2 (377).

11β-HSD1 is expressed in key metabolic tissues including liver, adipose tissue, and skeletal muscle where it primarily acts as a oxoreductase converting inactive cortisone to active cortisol (11-DHC to CORT in rodents), a reaction that is dependent on NADPH as cofactor (378) (Figure 1.10).

11β-HSD2 is predominately expressed in the kidney, colon, and salivary gland and catalyses the inactivation of cortisol to cortisone (CORT to 11DHC in rodents), a reaction that requires NAD+ as a cofactor (379). This protects the mineralocorticoid receptor (MR) from being activated by cortisol which has similar affinity to MR as mineralocorticoids.

1.11.6. Hexose-6-phosphate dehydrogenase

Within skeletal muscle, 11β-HSD1 is localised to the sarcoplasmic reticulum (SR) lumen and is dependent on an another enzyme hexose-6-phosphate dehydrogenase (H6PDH)(380) (Figure 1.10). H6PDH catalyses the first two steps of the pentose phosphate pathway converting glucose-6- phosphate (G6P) to 6-phosphogluconolactone (6-PGL) with the concomitant production of NADPH that confers electrons for the reductase activity of 11β-HSD1(381). The link between H6PDH and the activity of 11 β-HSD1 was investigated in the study of the H6PD knock-out mice. The oxo-reductase activity of 11 β-HSD was depleted in murine H6PD gene knock-out, and

metabolite of 11 DHC was only seen in the urine analysis (382). These findings suggest the role of H6PD as a regulator of the 11 β-HSD1 oxo-reductase activity in the ER/SR.

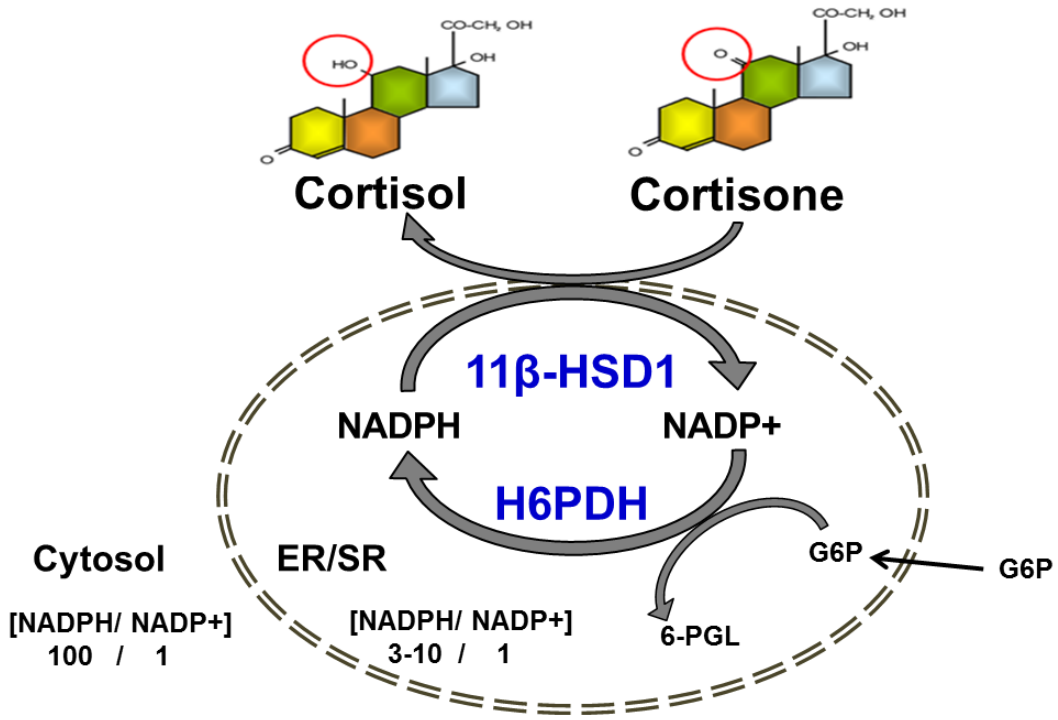

Figure 1.10. Schematic representation of the interaction between H6PDH and 11β-HSD1 within the SR. H6PDH generates NADPH by conversion of glucose-6-phosphate (G6P) to 6-phosphogluconate (6PG) within the ER. 11β-HSD1 uses the NADPH as cofactor, allowing the conversion of cortisone to cortisol.

1.12. Thesis Rationale

NAD+ decline leads to a reduction in energy metabolism disposing individuals to metabolic disease and overall decreased later-life health. Our goal is to ascertain the prospect of boosting tissues NAD+ in humans using the more contemporary NAD+ precursor, NR, with potential implications for metabolic disease.

Skeletal muscle is richly endowed with mitochondria and will therefore be used as an accessible large metabolic organ and to assess the mitochondrial function.

Human ageing is used as a model for metabolic (and possibly NAD+) decline.

Readouts will include systemic and tissue-specific parameters.

The thesis will also illuminate the possibility of a crosstalk between the cytosolic and SR NAD+ pool. This may have implications for understanding how fluctuations in NAD+ may have impact on subcellular hormone reactions the regulation of which is poorly understood.

1.13. Hypothesis

- Oral NR is safe and well-tolerated in humans and can increase skeletal muscle NAD+ and benefits whole-body and muscle specific metabolic readouts.
- Manipulating cytosolic NAD+ impacts the SR pyridine nucleotide tool and the enzymatic activity of 11β-HSD1 can be used as a readout.

Aims

- Assess the safety and tolerability of oral NR.
- Assess the effects of NR supplementation on the whole body and skeletal muscle NAD+ metabolome.
- Assess the effects of NAD+ boosting in whole-body and muscle-specific metabolic readouts.
- Examine the cytosolic/SR NAD+ crosstalk.

Chapter 2: Methodology

2.1. Clinical study

2.1.1. Study conduct and population

The study was conducted at the National Institute for Health Research/Wellcome Trust Clinical Research Facility at the Queen Elizabeth Hospital Birmingham, UK. The target population were aged volunteers who met the inclusion and exclusion criteria (outlined in the next Chapter). The design was a single centre, double blind, placebo-controlled, and crossover study. Aim was to obtain complete assessments from 12 aged individuals.

2.1.2. Methods

Intervention

Single centre, randomised, double blind, placebo-controlled, crossover study (Figure 3.1).

Volunteers were randomised to receive 21 days treatment with either;

Placebo

1000mg NR- (250mg, two tablets twice daily).

NR was supplied as 250 mg capsules by the manufacturer (Niagen®, ChromaDex, Irvine, CA). Participants received NR 500mg twice daily or matched placebo for 21 days with 21 days washout period before crossover to the other treatment arm.

Randomisation and blinding

Participants were allocated to either NR or placebo. A randomisation list was held by the clinical trials pharmacist at the clinical research facility, Queen Elizabeth Hospital Birmingham. The study investigators, nurses, and participants were all blinded to the intervention allocation during the trial.

Recruitment and inclusion and exclusion criteria

Participants recruited from the Birmingham 1000 Elders group. All participants fulfilled the inclusion criteria including male sex, age 70–80 years, BMI 20–30 kg/m^2, able to discontinue aspirin for 3 days prior to the muscle biopsy, and able to discontinue statins and vitamin D supplements for a week before the study and for the duration of the study. Exclusion criteria included: serious active medical conditions including inflammatory diseases or malignancies, significant past medical history including diabetes mellitus, ischaemic heart disease, cerebrovascular disease, respiratory disease requiring medication, or epilepsy, blood pressure >160/100mmHg, or treatment with oral anti-coagulants.

2.1.3. Study endpoints

Primary outcome

Skeletal muscle, blood, and urine NAD+ metabolome levels using targeted metabolomics.

Secondary outcomes

NAD+ boosting using NR supplementation may also have system wide effects in aged humans due to integrated action not only in muscle, but also at the level of the liver and adipose tissue. There the secondary end points included:

1) Mitochondrial function using high-resolution respirometry (Oroboros technology). If NAD+ boosting is successful, increased oxygen consumption in response to glucose may be observed.

2) Assess glucose tolerance and insulin sensitivity following oral glucose tolerance test (OGTT). NR supplementation may improve glucose handling as a function of improved insulin sensitivity and whole-body glucose disposal.

3) NAD+ boosting may improve lipid profile as a function of liver and adipose effects and increased capacity of muscle to use lipids.

4) We employed the muscle arterio-venous difference analysis. This allowed us to examine muscle-specific metabolite trafficking, oxygen consumption, CO2 production, which may reflect a favourable metabolic profile.

5) Used muscle biopsy tissue to ascertain adaptive gene expression profiles associated with NAD+ boosting.

Additional outcomes

Local capacity in clinical research (NIHR/Wellcome Trust Clinical Research Facility) and metabolic analysis offered the opportunity to develop a greater characterisation of our study. On this basis, also assessed:

1) Nutrient portioning using indirect calorimetry, allowing us to test changes in the glucose and lipid metabolism during fasting and the GTT in response to NAD+ boosting

2) We assessed 24-hour urine collection for changes in steroid metabolism using Gas chromatography/ mass spectrometry. Steroidogenesis is sensitive to changes in NAD+ and its metabolites. Using this analysis, we can test whether production of steroids and enzyme activities are improved.

2.1.4. Study design and schedule of study visits

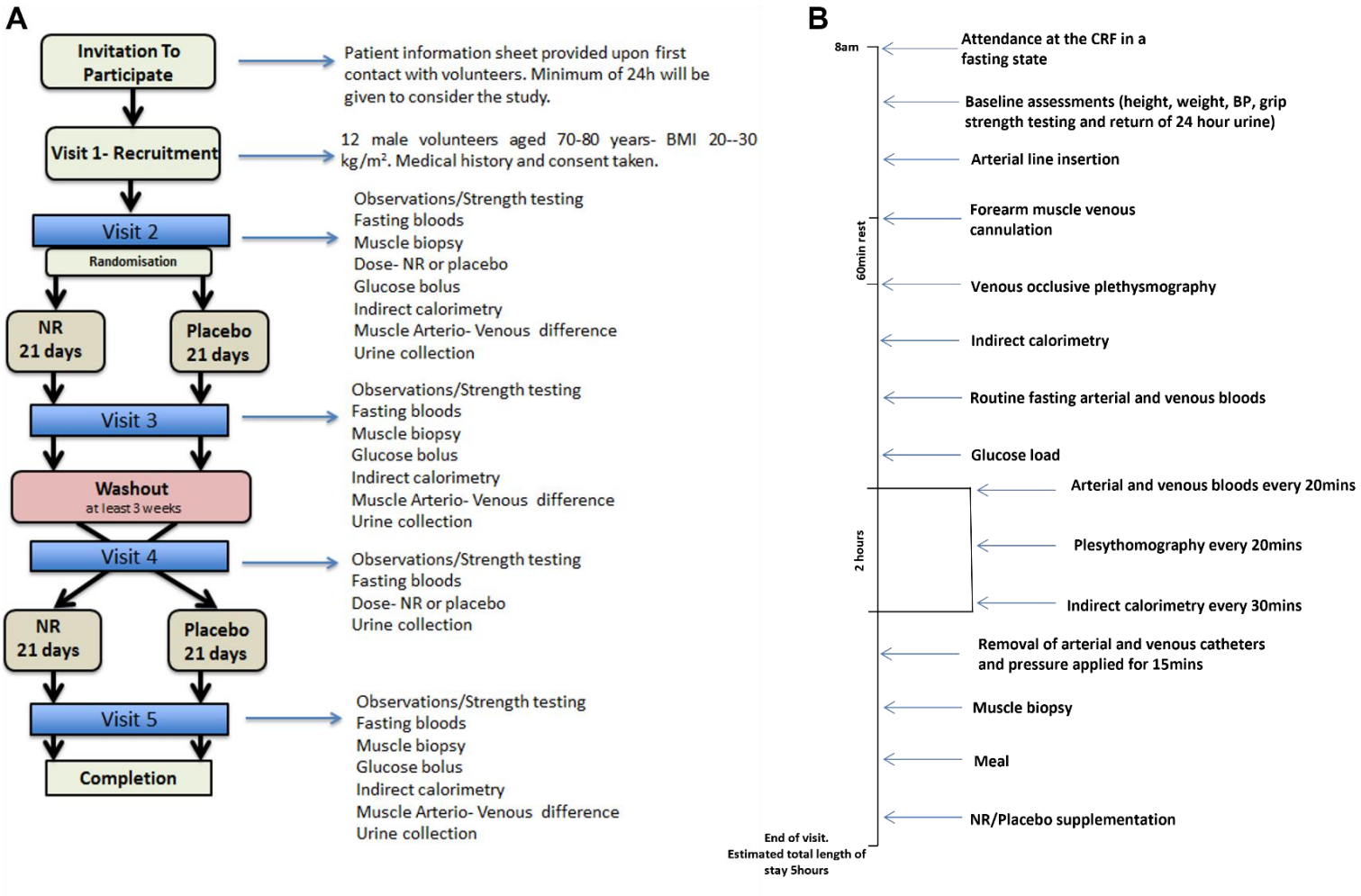

Figure 2.1: NADMet study design. (A) The overall study design- from participant recruitment, study visits, treatments, and crossover. (B) A typical day protocol to demonstrate the flow of primary and secondary outcome data collection.

Visit 1 was a screening and enrolment visit, while visit 4 was after the washout period and only fasting blood and 24hr urine were collected. The protocol design for visits 2, 3, and 5 included muscle biopsy, fasting blood analyses, glucose tolerance test, muscle arterio-venous difference technique, venous occlusive plethysmography, and indirect calorimetry analysis.

2.1.5. Blood pressure measurement

Blood pressure was measured at the start of each visit after an overnight fast using an automated machine (Welch Allyn, USA). At the trial visits, participants were instructed to rest for 15mins in a supine position before blood pressure measurement was undertaken. For optimal accuracy of the blood pressure measurements, an appropriately sized cuff was used to encircle 80% of the arm and the same was used for all participants, and on the same arm. Blood pressure was measured three times, and the mean was logged.

2.1.6. Hand-held dynamometry

To measure the hand-grip strength, the peak absolute strength (in kilograms) and relative hand-grip strength (kilograms of force per kilogram of body weight) were measured in triplicate in both hands using a dynamometer (Takei Instruments, Japan). The highest measurement values were captured.

2.1.7. Muscle biopsy

Vastus lateralis muscle biopsies were obtained by me using the percutaneous Bergstrom technique as previously described (383) under local anaesthesia (1% lignocaine). The biopsies were undertaken whilst the participants were lying down. Biopsy samples (100–150mg) were immediately dried on clean filter paper and around 10mg of tissue was split and placed on ice cold BIOPS buffer for the high-resolution respirometry analysis. The remainder of the skeletal muscle tissue was immediately snap frozen in liquid nitrogen and stored at -80°C for further analyses.

2.1.8. Arterio-venous (AV) difference technique

An arterial catheter was placed into a non-dominant limb radial artery and a retrograde cannula was inserted into in a deep antecubital vein draining a forearm muscle, on the opposite side of the arterial line. To avoid contamination of the muscle venous blood with the mixed arteriovenous blood from the hand, a wrist cuff was inflated to 200mmHg for 3 mins before sampling. Blood was simultaneously drawn from the arterial and venous catheters at fasting and then every 20mins following an oral glucose load for a duration of 120 min.

2.1.9. Indirect calorimetry

Participants were requested to lie in a supine position for at least 60 mins after insertion of the arterial and venous catheters. Whilst in a comfortable supine position, a transparent ventilated canopy was placed over the head. Plastic sheet attached to the hood was placed around the participants to create a tight seal (Figure 2.1). The room temperature, humidity and barometric pressure were measured by a digital thermo-hygrometer (Oregon Scientific, USA). During the measurement acquisition period, participants were instructed to remain supine and breathe normally. Respiratory measurements, including resting oxygen consumption (VO_2) and carbon dioxide production (VCO_2) and respiratory exchange ratio (VCO_2/VO_2) were obtained using the mixing chamber mode of the metabolic cart (AEI MOXUS II Metabolic System, USA). Measurements were captured at a fasting state and then every 30 minutes for 120 minutes following a 75g oral glucose load. Measurements for each period lasted 15 mins so the first and last 5 minutes could be disregarded, and the mean value for the middle 5 minutes was captured.

Figure 2.2: Picture of the Moxus metabolic cart for indirect calorimetry. Picture on the left is the MOXUS metabolic cart showing the O2 and CO2 analysers, gas cylinders, mixing box, canopy, and the associated laptop and software for data acquisition and analysis. Picture on the right showing an example of a participant's positioning under the canopy.

2.1.10. Venous occlusive plethysmography

Forearm muscle blood flow was measured by venous occlusive plethysmography (Hokanson, USA) (384) as previously described (385) (Figure 2.2). The principle of this method is to arrest the venous flow completely for a few seconds without interrupting the arterial flow and a record is made of the changes in volume in the forearm between the level of venous occlusion and a distal cuff inflated to a pressure intended to arrest the circulation in all vessels. Practically, a cuff was tightly applied to the wrist and a second cuff applied to the arm (site of usual blood pressure measurement). A mercury-in-rubber strain gauge was applied to the forearm between the two cuffs and connected to the data acquisition box and analysis software. The arm cuff was intermittently inflated and deflated, whilst the wrist cuff was inflated, and measurements of blood flow were undertaken. Changes in the strain length between inflating and deflating the arm cuff give information on how much blood flows in and out of the forearm. The initial rate of swelling during venous occlusion is the apparent rate of arterial inflow, and the assumption is made that this rate is the same as the actual undisturbed rate of arterial inflow immediately before the venous

occlusion (385). The blood flow measurements were obtained immediately after each blood sampling.

Figure 2.2: Picture showing the venous occlusive plethysmography with the wrist and arms cuffs and the strain gauge.

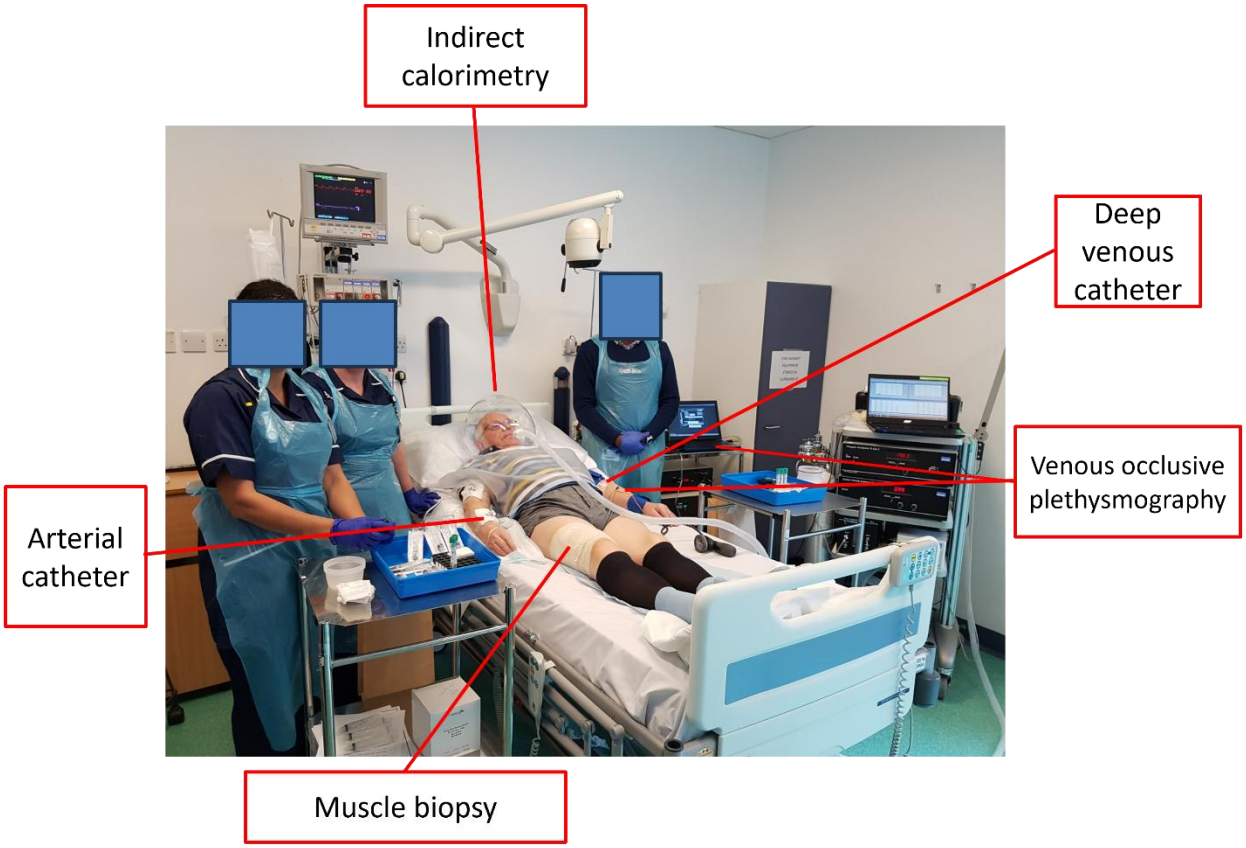

Figure 2.3: Photograph showing the research team (two research nurses and myself) the complex setup of the study interventions in each study visit. The participant's permission was obtained for the photograph.

2.1.11. Sample size and statistical analysis

Sample size was determined based on previous studies using the same methodological design (332), in which the sample size detected significant differences at the 5% level. Outcome data are reported as mean ± SEM, or median and quartiles where appropriate. Comparisons of participants between the NR and phases were undertaken using paired t-tests. Furthermore, we undertook further data analyses considering the period effect by dividing the participants based on whether they were randomised to NR first or second. This is to look for carryover effect across all analyses. Wherever relevant, area under the curve was calculated using the trapezoid method. Data were analysed using IBM SPSS Statistics version 22 and GraphPad Prism version 7.0.

2.1.12. NAD+ metabolomics

Skeletal muscle

Muscle tissue was pulverised and around 10 mg was used for each of the acidic (A) and basic (B) metabolite extraction. Internal standard mixtures for each of A and B were prepared for each sample. The extraction was undertaken using 0.2 ml of ice-cold liquid chromatography-mass spectrometry (LC-MS/MS) grade methanol and kept on ice followed by the addition of 0.3ml of internal standard made in LC-MS grade water. Samples were sonicated in an acetone water bath at -4 °C for 20 seconds, placed back on ice, and then incubated at 85 °C with constant shaking at 1050 rpm for 5 minutes. Samples were then placed on ice for 5 min and centrifuged (16.1k x g, 10 minutes, 4 °C). The supernatant was transferred to fresh tubes and then dried using a speed vacuum. The dried extract was resuspended in 30 µl of either LC-MS grade water for acidic extract or 10 mM ammonium acetate for alkaline extract and centrifuged (16.1k x g, 3 minutes, 4 °C). The supernatant was carefully transferred to a Waters Polypropylene 0.3 ml plastic screw-top vial. The skeletal muscle pellet was then dried using a speed vacuum, pellet was weighed, and later used to normalise the data which were finally reported as pmol/mg.

Blood

To analyse nucleotides, samples were thawed in small batches. Working in batches of four, samples were vortexed for 2mins and aliquoted into duplicate 100 µL samples using a positive displacement pipette; the second sample was immediately frozen on dry ice to store for analysis of nicotinamide and related analytes. 20 µL of internal standard working solution was added, followed by 400 µL of 3:1 0.25N trichloroacetic acid: acetonitrile. Samples were vortexed and stored on ice until up to 24 samples had been processed to this point. After the last sample had been on ice 5 minutes they were transferred onto a heater/shaker for 3 minutes at 55 °C.

Samples were centrifuged for 12 minutes at 4 °C and 16.1 rcf. The supernatants were transferred to new 1.5 mL microcentrifuge tubes which were stored at 4 °C until the entire daily load of samples was complete. The remaining samples were processed in a second batch in the same manner. Standards and controls were prepared by adding internal standard and the appropriate amount of standard working solution to microcentrifuge tubes. In batches of 4, 100 µL of human blood was added to each and 400 µL of 3:1 0.25N trichloroacetic acid: acetonitrile added. Samples were processed further as described above. Six blank zero samples were containing only blood and internal standard were also prepared in the same fashion. When all samples were completed, the tubes containing the supernatants were transferred to a Centrivap at room temperature and a reduced pressure of ~ 0.03 bar and solvent removed overnight. The dried samples were stored at -20 °C until reconstitution immediately prior to the analytical run.

To analyse Nam, NR, 1-methylnicotinamide (MeNam), NA, N- methyl-4-pyridone-3-carboxamide (Me-4-py), N- methyl-2-pyridone-5-carboxamide (Me-2-py), and Nam oxide, 20 µL of internal standard working solution containing stable labelled analogues of NR, Nam, MeNam, and Me-4-py was added to the previously frozen aliquots of sample. From this point on, the samples were handled as above for the nucleotides, except the standards prepared contained the analytes for this analysis.

Urine

Urine was thawed on ice, 2 x 100 µL and 1 x 10 µL were pipetted into 1.5 mL microcentrifuge tubes. The 10 µL and one of the 100 µL tubes were frozen on dry ice and stored at -80 °C. For the remaining aliquot, 20 µL of working internal standard solution in 5% formic acid was added to each sample. Standards and controls were prepared in a synthetic urine matrix containing urea, creatinine, sodium chloride, and potassium nitrate at physiological relevant

concentrations. Previous work has shown that nucleotides are not found in urine above the detection limit.

2.1.13. Blood biochemical analyses

Blood was collected from the arterial and venous catheters into heparinised blood tubes. Plasma was quickly separated by centrifugation at 4°C and was then snap frozen. Plasma non-esterified fatty acids (NEFA), glucose, and lactate concentrations were measured using commercially available kits on an ILAB 650 Clinical Chemistry Analyser (Werfen Ltd, UK). Insulin was measured using a commercially obtainable assay as per the manufacturer's instructions (Mercodia, Sweden). Homeostasis model assessment of insulin resistance (HOMA-IR) was calculated using the formula [fasting glucose (mmol/L) × fasting insulin (mU/L)/22.5] (386).

Full blood count was measured on a Beckman Coulter DxH analyser (USA). Lipid profile, urea and electrolytes, and thyroid function tests were all measured on the Roche Modular Platforms (Roche, Switzerland).

2.1.14. High-resolution respirometry on permeabilised muscle fibres

Ex vivo mitochondrial function was determined by measuring oxygen consumption polarographically using a two-chamber Oxygraph (OROBOROS Instruments). Oxygen consumption reflects the first derivative of the oxygen concentration (nmol/ml) in time in the respiration chambers and is termed oxygen flux [pmol/(s*mg)], corrected for wet weight muscle tissue (2–5 mg) introduced into the chamber. To evaluate oxidative phosphorylation, different on carbohydrate- and lipid-derived substrates and inhibition protocols were used. A small portion of the muscle biopsy sample was kept on cold biopsy preservation buffer (BIOPS; 50 mM K-MES, 20 mM taurine, 0.5 mM dithiothreitol, 6.56 mM $MgCl_2$, 5.77 mM ATP, 15 mM phosphocreatine, 20

mM imidazole, 10 mM Ca-EGTA, 0.1 µM free calcium, pH 7.1) until processed for the measurement according to Pesta and Gnaiger, 2012 (387). Briefly, approximately 4-6 mg was placed in a drop of BIOPS on a small Petri dish and the muscle fibres were mechanically separated during the standardised period of 5 min with a pair of sharp forceps under the preparative microscope. Processed sample was then permeabilised for 30 min in 2 mL of BIOPS/saponin (50 ug/mL) by gentle agitation in the cold room and then washed in 2 mL of MiR media (110 mM sucrose, 60 mM K^+-lactobionate, 0.5 mM EGTA, 3 mM $MgCl_2$, 20 mM taurine, 10 mM KH_2PO_4, 20 mM HEPES, 1g/L BSA essentially fatty acid free, pH 7.1) for 10 min. Washed sample was divided in 2, gently blotted onto filter paper to dry off the extra buffer and the wet weight was read (usually between 1 and 3 mg). Samples were then transferred in the oxygraph chambers filled with MiR media supplemented with catalase (280 U/mL), the stoppers were inserted incompletely and approximately 5 mL of medical gas mixture (95 % O_2, 5 % CO_2) were injected in the chamber to elevate the oxygen concentration in the media to approximately 400 µM and chamber was closed. Two protocols were run in parallel in one oxygraph and the experiment repeated 3-4 times during the day of biopsy collection. For protocol 1, the titrations used were: 2 mM malate, 10 mM glutamate, 4-5 mM ADP, 10 mM succinate, 10 µM cytochrome c, sequential addition of 0.5 µM FCCP, 0.5 µM rotenone and 2.5 µM antimycin A. For protocol 2: 0.05 mM malate, 0.2 mM octanoyl-carnitine, 4-5 mM ADP, 2 mM malate, 10 mM glutamate, 10 mM succinate, 10 µM cytochrome c, sequential addition of 0.5 µM FCCP, and 0.5 µM rotenone. When the oxygen concentration during the experiment dropped below 240 µM, the reoxygenation was done by injection of 2 mL of 200 mM hydrogen peroxide. Experiments in which the addition of cytochrome c resulted in more than 15 % increase of respiration were excluded from the final evaluation. Data were also corrected for mitochondrial DNA (mtDNA) copy number and citrate synthase activity.

2.1.15. Mitochondrial density assessments

mtDNA copy number was determined using quantitative real time PCR (qPCR). mtDNA copy number was calculated using the ratio of NADH dehydrogenase subunit 1 (ND1) to lipoprotein lipase (LPL) (mtDNA/nuclear DNA) as previously described (282).

For citrate synthase activity (388), 5mg of snap frozen human muscle biopsy was placed in 200 µl homogenisation buffer (HEPES 20 mM, EDTA 1 mM, Triton X-100 0.1% v/v) and homogenised with tissue lyser (Qiagen, Hilden, Germany) at 20 beats/s for 20s. Samples were then centrifuged 380 x g for 30 seconds at 4°C. Supernatant was collected into a fresh tube and re-centrifuged at Vmax, 10 min, 4°C. Again, the supernatant was collected, and protein concentration of tissue homogenate was measured by the DC protein assay (BioRad). Samples were diluted to 200 µg/ml in the homogenisation buffer. Citrate synthase activity was then quantified with a reaction mix composed of Tris 20 mM, 5,5'-dithiobis- 2-nitrobenzoic acid 1.01 mM and acetyl-CoA 12.2 mM, pH 7.5. The mix was incubated at 30°C for 15 minutes for baseline measurements, then the reaction was initiated by the addition of oxaloacetate 10 mM, pH 7.5 and after 15 minutes incubation, the absorbance was measured on plate reader at 412 nm. Citrate synthase activity was determined in triplicates by subtraction of baseline values without oxaloacetate.

2.1.16. RNA sequencing

This was undertaken with support from Dr Ildem Akerman, at the Institute of Metabolism and Systems Research, University of Birmingham. Figure 2.4 is a pictorial representation of the steps involved in RNA sequencing. RNA was extracted from frozen skeletal muscle tissue using Tri Reagent (Sigma-Aldrich) following manufacturer's instructions. Sequencing libraries were prepared using RNA (RIN >7) with the Lexogen Quantseq3 FWD kit. Libraries were sequenced

using HiSeq2000 across 4 flow cells generating 75bp long single ended reads (average read depth of 6-10M/sample, which is higher than the 4M reads / sample required for analysis for this type of library). All samples were prepared and sequenced as a single pool. Trimmomatic software (v0.32) and bbduk.sh script (Bbmap suite) were used to trim the ILLUMINA adapters, polyA tails and low quality bases from reads. Trimmed reads were then uniquely aligned to the human genome (hg38) using STAR with default settings (v2.5.2b) and the Gencode (v28, Ensembl release 92) annotation as the reference for splice junctions. Mapped reads were quantified using HT-seq (v0.9.1) using Gencode (v28) genes (intersection-nonempty flag). Differential gene expression was obtained using DEseq2 with paired baseline and treatment samples. In the analysis we did not use a cutoff to remove lowly expressed genes. Inclusion of lowly expressed genes (at arbitrary cut-offs) had little bearing on our results (97.8% of differentially expressed genes at $p < 0.05$ were identical between no cutoff, and a cut-off of > 3). Of note, volcano plot was drawn with a cut-off (>3) in order to visualise the typical “V” shape using R. Differentially expressed genes between baseline (control) and NR treated samples at p-value = <0.05 were annotated using Biological processes (BP) gene sets with DAVID tool (389,390). We obtained similar results using gene annotation tool within Gene Set Enrichment Analysis (GSEA) suite (391,392) for gene sets from KEGG pathways and C5-Biological processes. In addition, we have used GSEA analysis tool to interrogate specific gene sets against our pre-ranked expression data (Control vs NR treatment). GSEA calculates an Enrichment Score (ES) by scanning a ranked-ordered list of genes (according to significance of differential expression (-log10 p-value), increasing a running-sum statistic when a gene is in the gene set and decreasing it when it is not. The top of this list (red) contains genes upregulated upon NR+ treatment while the bottom of the list (blue) represents downregulated genes. Each time a gene from the interrogated gene set (i.e. Glycolysis, mitochondria, TCA cycle) is found along the list, a vertical black bar is plotted (hit). If the “hits” accumulate at the bottom of the list, then this gene set is enriched in upregulated genes (and vice versa). If interrogated genes are distributed

homogenously across the rank ordered list of genes, then that gene set is not enriched in any of the gene expression profiles (i.e. control gene sets of similar expression levels to interrogated gene sets). GSEA was used in pre-ranked mode with parameters -norm meandiv -nperm 1000 -scoring_scheme weighted. 10 gene sets of equal size and similar expression levels to the interrogated gene sets were generated using a custom pipeline in R (available upon request). We have interrogated the following gene sets: GO0048870; cell motility, GO0030029; actin filament based process, GO0022610; Biological cell adhesion, (also GO0007155 cell adhesion with similar results), M15112: Wong Mitochondria gene module, M3985: KEGG citrate cycle TCA cycle, merge of M15109: BIOCARTA Glycolysis pathway and M5113: REACTOME glycolysis.

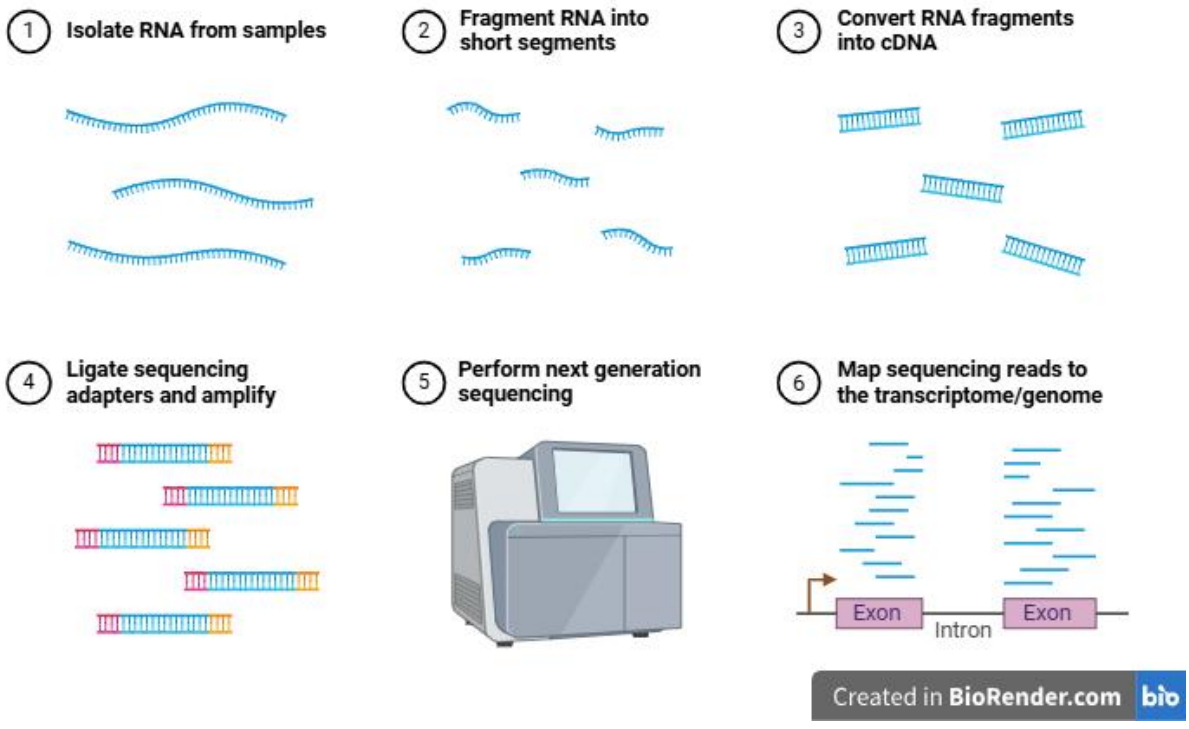

Figure 2.4: Pictorial representation of the steps involved in RNA sequencing.

2.1.17. Protein immunoblotting

Muscle biopsies were homogenised in ice-cold sucrose lysis buffer (50 mM Tris/HCl (pH 7.5), 250 mM Sucrose, 10mM Na-β-Glycerophosphate, 5mM Na-Pyrophosphate, 1mM Benazmidine, 1 mM EDTA, 1 mM EGTA, 1% Triton X-100, 1 mM Na3VO4, 50 mM NaF, 0.1% β-Mercaptoethanol, supplemented with protease inhibitor cocktail). Samples (40-100µg of protein extract) were loaded into 4-15% Tris/Glycine precast gels (BioRad) prior to electrophoresis. Proteins were transferred onto PVDF membranes (Millipore) for 1h at 100V. A 5% skimmed milk solution made up with Tris-buffered saline Tween-20 (TBS-T, 0.137M NaCl, 0.02M Tris-base 7.5pH, 0.1% Tween-20) was used to block each membrane for 1h before being incubated overnight at 4°C with appropriate primary antibodies. Membranes were washed in TBS-T for three rounds prior to incubation in horse radish peroxidase-conjugated secondary antibody at room temperature for 1 hour. Membranes were then washed in TBS-T prior to antibody detection via enhanced chemiluminescence horseradish peroxidase substrate detection kit (Millipore). Images were undertaken using a G:Box Chemi-XR5 (Syngene, India).

2.1.18. Inflammatory cytokines

We utilised a commercially available multiplex cytokine bead assay using the Bio-Plex Pro Human Cytkine 17-plex panel analysed with a flow-cytometry based Luminex 200 reader. The levels of IL-1b, IL-2, IL-4, IL-5, IL-6, IL-7, IL-8, IL-10, IL-12, IL-13, IL-17, G-CSF, GM-CSF, IFN-g, MCP-1, MIP-1b, and TNF-α were measured on the participants' sera as per the manufacturer's instructions. Highly sensitive CRP was measured using CRPHS: ACN 217 on COBAS 6000 analyser (Roche, USA). All measurements were undertaken in duplicates.

2.2. In vitro studies

2.2.1. Cell culture

All cell culturing procedures were conducted using a lamina flow hood in an aseptic environment, and all materials used in the hood were sterilized with Ethanol 70% (v/v).

2.2.2. C2C12

The C2C12 cell line is derived from mouse myoblasts and represents an established model of both skeletal muscle proliferation and differentiation. Cryofrozen C2C12 myoblasts (passage <20 to ensure they retained adequate myoblast/myotube characteristics) were purchased from the European Collection of Cell Cultures (Salisbury, UK). Originally, the C2C12 line was created through serial passaging of myoblasts isolated from the thigh muscles of C3H mice 70 hours after a crush injury (393–395).

2.2.3. Cell culture

C2C12 myoblasts were maintained in 75cm3 TC flasks (Corning, Surrey, UK) in growth media [Dulbecco's Modified Eagle's Medium (DMEM) supplemented with 10 % foetal bovine serum (FBS) and 1% Penicillin/Streptomycin (PS)]. At 60-70 % confluence, cells were split by removing the media and washing with sterile phosphate-buffered saline (PBS). To detach the cells, 3 ml of TrypLETM Express trypsin enzyme (GibcoTM, UK) was added to the flask and incubated at 37°C. After 5-7 min incubation, 7 ml of fresh DMEM was added and transferred to a 10 ml falcon tube and centrifuged at 1300 rpm for 5 min. The pellet was then resuspended with 10 ml of media and reseeded into fresh flasks. To prepare well plates for experiments, cells were seeded at the

desired density into 6 or 12-well plates (Corning, Surrey, UK), and the media was replaced every 48 hours with fresh proliferation media.

2.2.4. Cell differentiation

When myoblasts reached 60-70% confluency, cell differentiation was triggered by replacing growth media with differentiation media [DMEM supplemented with 5 % horse serum and 1% PS]. Differentiation media was replaced every 48 hours. All cell culture was maintained in incubators at 37°C under a 5% CO2 atmosphere. After 5 days, myoblasts had fused to form multinucleated myotubes. Media were replaced every other day until myotubes had fused and formed multinucleated myotubes (usually 6-8 days) (Figure 2.4). Experiments and treatments started when cells started to form multinucleated myotubes.

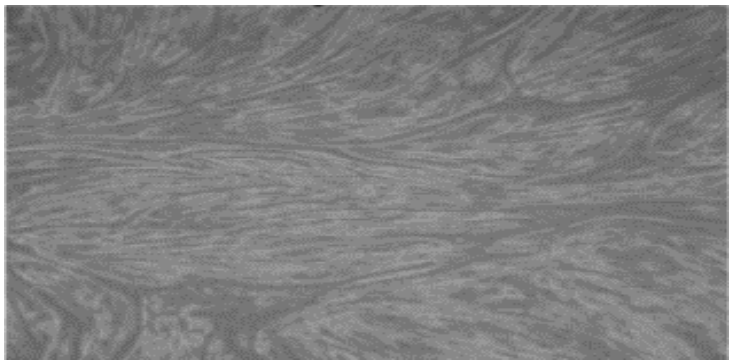

Figure 2.5: Image of C2C12 differentiated myotubes obtained during an experiment.

2.2.5. Freezing down

Freezing down C2C12 cells permitted long-term storage and kept the cells at low passage numbers for future use. At 60-70% confluence, cells were treated with trypsin and resuspended in 9 ml of proliferation media supplemented 10 % FCS, and 1 % P/S and then centrifuged at 1300

rpm for 5 min. The cell pellet was then resuspended in 3 mL of FCS supplemented with 10% DMSO. The cells were aliquoted into 1 ml cryotubes (Nalgene, Hereford, UK), pre-cooled overnight in a Mr. Frosty TM freezing container (Sigma, UK), and transferred to liquid nitrogen at -200°C for long-term storage. To start a new culture of C2C12, the cryopreserved cells were thawed in a water bath at 37°C and transferred to a new 10ml falcon tube with 10 ml DMEM. Cells were centrifuged and the pellet was resuspended and transferred to new flasks.

2.2.6. Primary mouse myotubes

Primary mouse culture represents a better reflection of muscle cell characteristics than in vitro study of C2C12. Cells were collected from the gastrocnemius muscle and washed with DMEM for 1 hour supplemented with 1% P/S. To stimulate the proliferation of satellite cells, media containing 0.5 % CEE, 10% HS, and 1% P/S was added to the plate and left in the incubator for 24 hours. Media was replaced with differentiation DMEM media supplemented with % HS, 0.5% CEE, and 1% P/S. At this stage, the medium was replaced every 48 hours until the cells differentiated to form myotubes (approximately 7 days). Cells were extracted from gastrocnemius muscle and cultured in Dulbecco's modified Eagle's medium (DMEM) supplemented with 2% (v/v) HS, 0.5% (v/v) chicken embryo extract (CEE), and 1% (v/v) P/S for 7 days to differentiate and form multinucleated myotubes.

2.2.7. NAD+ modulation with FK866 and NR

After 5 days of C2C12 myotubes differentiation, cells were left as control (no FK866 or NR), or treated with the NAMPT inhibitor, FK866 (Sigma-Aldrich, UK) at concentrations of 100 nM for 48 hours (Figure 2.5). This concentration was adequate to deplete NAD+ as indicated by the dose-response curve published (396). NR (Chromadex, USA) treatment was at a dose of 0.5 mM

(146). FK866 and NR doses were repeated every 24 hours in experiments of more than 24hours treatment duration.

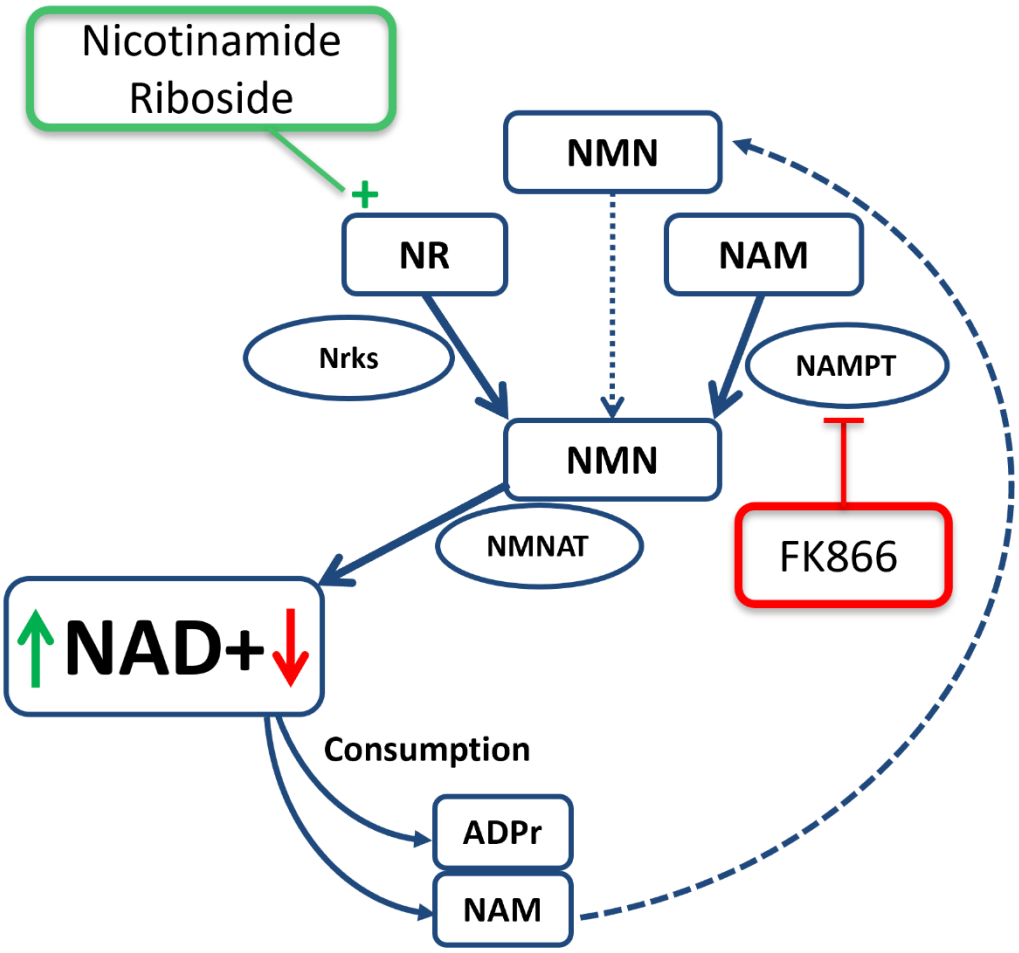

Figure 2.6: A schematic representation of the NAD+ biosynthesis salvage pathways showing the effects of FK866 (NAMPT inhibitor) and Nicotinamide Riboside (NR; NAD+ precursor).

2.2.8. NAD+ in vitro measurement assay

NAD+/NADH concentrations were determined using the BioVision colorimetric NAD+/NADH quantification kit (Cambridge Bioscience, UK). C2C12 cells were extracted with 400µl of NADH/NAD+ extraction buffer by freeze/thaw two cycles (20min on dry ice, then 10 mins at room temperature), vortexed for 10secs and centrifuged at 16,100 g for 5min. The extracted NADH/NAD+ supernatant was transferred into a labelled tube.

To make a standard curve (Figure 2.6), 10 µL of the 1nmol/µL NADH standard was diluted with 990 µL NADH/NAD+ extraction buffer in order to generate 10pmol/µL standard NADH which was added (0,1, 2, 4, 8, 10 µL) into a 96-well plate in duplicate. The final volume to 50 µL was made up with NADH/NAD+ extraction buffer. Subsequently, 50 µL of extracted samples were transferred into a 96-well plate.

To detect NADH, NAD+ was decomposed in 200µL of the extracted samples by heat shock at 60^{o}C for 30mins before reaction. The samples were cooled down on ice, and 50 µL of NAD+ decomposed samples were transferred into a plate. 100µL of NAD+ cycling mix (100µL of NAD+ cycling buffer and 2µL of NAD+ cycling enzyme mix) was added into each well to convert NAD+ to NADH followed by the plate incubation at room temperature for 5 mins. Finally, 10 µL of NADH developer was added into each well, and the readings at OD 450 nm were taken at room temperature after 1 to 4 hours of incubation.

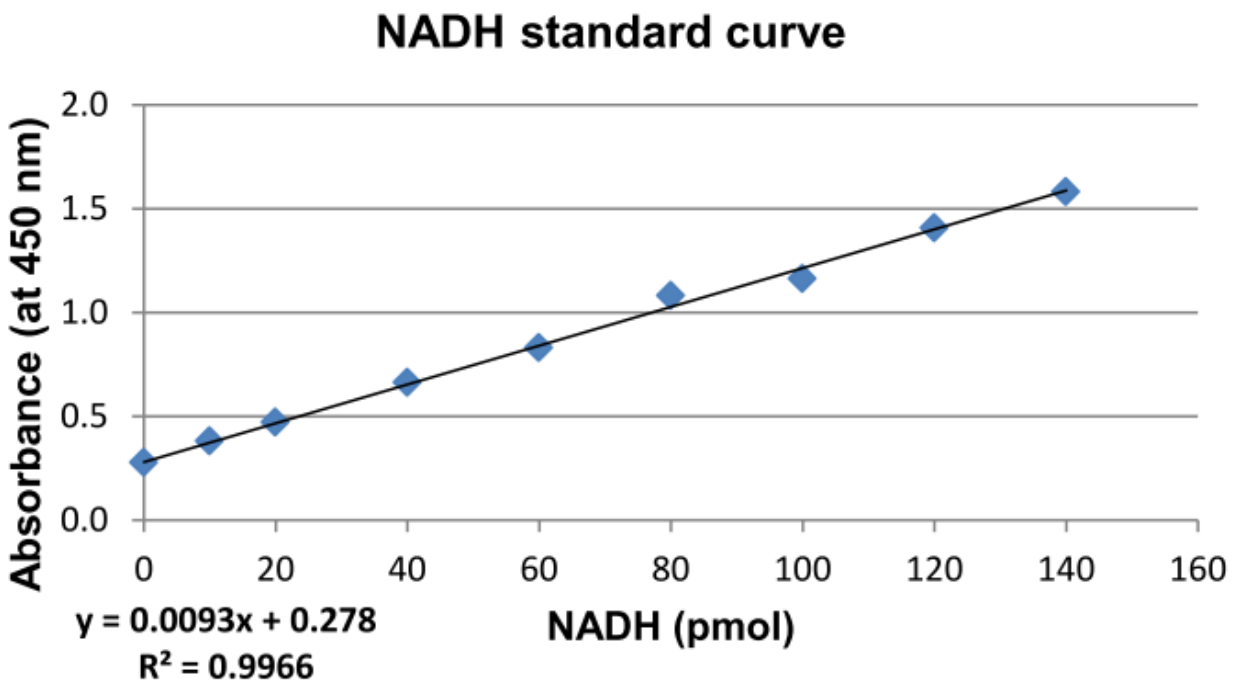

Figure 2.7: NAD/NADH cycling assay standard curve. Following the NAD/NADH cycling assay an NADH standard curve was plotted using the absorbance of NADH at known concentrations. Sample concentrations were determined by extrapolating absorbance values to the standard curve.

2.2.9. Cell viability assay

Cellular viability and apoptotic activity were determined using the ApoLive-GloTM Multiplex assay (Promega, USA). As the aim of this conducted experiment was to determine cell viability in response to depleting and increasing NAD+ content, this assay was specifically chosen because the reactions are not NAD+ dependent.

Cells were plated into 96 well plates at a density of 15,000 per well and differentiated for 6 days, before they were treated with FK866 and NR for 24, 48 or 72 hours with a final well volume of 100 µl. Hydrogen peroxide (1 mM and 100 µM) and ionomycin (100 µM) were added as controls to initiate cell death.

Cell viability: 10 µl of glycyl-phenylalanyl-amino fluorocoumarin substrate (cleaved by protease activity limited to viable cells) was added to 2 ml of assay buffer provided to make the viability reagent. Then 20 µl of the reagent was added to the wells and the plate was mixed using a shaker at 300 rpm for 30 seconds. The plate was then incubated for 30 minutes at 37°C. Fluorescence was measured at 400EX/505EM with the signal proportionate to the number of viable cells. *Induction of apoptosis*: determined by measuring the activity of the apoptotic marker caspase-3/7. 100 µl of the Caspase-Glo® was added to the wells and mixed using a shaker at 300 rpm for 30 seconds. The plate was incubated for 30 minutes at room temperature and then luminescence was measured with an increase in signal proportional to caspase-3/7 activity.

2.2.10. RNA extraction

After removal of cell media, C2C12 cells were washed on ice with PBS. 500ul of TRIreagent (Sigma- Aldrich, UK) was added per well and cells were incubated at room temperature (RT) for 5 minutes and then the cell lysates were transferred into Eppendorfs. 100ml of chloroform was added to the Eppendorfs and the tubes were shaken for 10 seconds at RT, following which they were allowed to stand at RT for 15 minutes. The Eppendorfs were then transferred to a refrigerated centrifuge and centrifuged at 12,000g for 10 minutes at 4^{o}C. The aqueous phase containing RNA was then transferred to a fresh Eppendorfs. 250ul of isopropanol was added and tubes were mixed by inverting 5 times and placed at -20^{o}C overnight. Following that, they were centrifuged at 12,000g at 4^{o}C for 10 minutes. The supernatant was carefully removed and the pellet was washed with 75% ethanol, following which the Eppendorfs were vortexed and subsequently centrifuged at 12,000g for 5minutes at 4^{o}C. The ethanol supernatant was removed and the RNA pellet was allowed to air dry for 10 minutes and then re-suspended in 30ul of RNAase/Nuclease free H20 and put on a heating block at 55^{o}C to aid dissolving of the pellet. Finally, the RNA was stored in a - 80^{o}C freezer until further use.

2.2.11. RNA quality and quantification

The quality of the RNA was assessed by gel electrophoresis on a 1% agarose gel with GelRed Nucleic acid Gel Stain (Figure 2.7). The gel was visualised under a UV light in a G:Box gel documentation system (Syngene, UK). RNA separates in the gel according to its molecular mass and the resultant bands were visualised under UV light. Intact RNA shows two sharp bands corresponding to the highly abundant 28S and 18S rRNA.

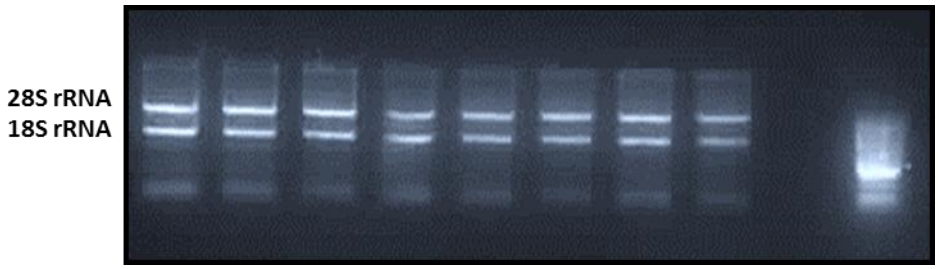

Figure 2.8: Gel electrophoresis of the RNA extracted from C2C12 myotubes and used for gene expression analysis in this work.

RNA was quantified using NanoDrop ND-1000 UV-Vis Spectrophotometer (Thermofisher, UK). The absorbance of 1.5µl of RNA at 260nm and 280nm was determined where 1 OD260 = 40µg/mL of RNA and the OD260/OD280 ratio indicates the RNA purity. Only OD260/OD280 ratios in the range of 1.8-2 were used. All measurements were made with respect to a blank consisting of the nuclease free water in which the RNA was suspended.

2.2.12. Reverse transcription and polymerase chain reaction

Reverse transcription polymerase chain reaction (RT-PCR) reactions were carried out using Applied Biosystems High-Capacity Reverse Transcription Kit (Applied Biosystems, Warrington, UK). The following reagents were combined in Eppendorfs to generate a 2x RT master mix:

RT Buffer – 2µl per sample

dNTP mix – 0.8 µl per sample

10X Random Primers – 2µl per sample

MultiScribe Reverse Transcriptase – 1µl per sample

RNase inhibitor - 1µl per sample

Nuclease-free H2O - 3.2µl per sample

1µg of RNA was diluted with nuclease free water to a volume of 10µl before 10µl of 2x RT master mix was added giving a final volume of 20µl. The 20µl samples were loaded onto a PCR thermal cycler (Applied Biosystems, UK) and subjected to 25^{o}C for 10 mins followed by 37^{o}C for 120 mins, and finally 95°C for 5 minutes to terminate the reaction. Samples were then stored in -80^{o}C freezer.

2.2.13. Real-Time PCR

The reactions were set up in triplicate by combining: 5 µL of 2x Master Mix, 0.5µL of either 18S (housekeeping gene) or gene of interest, 100 ng of cDNA and nuclease free water to a final volume of 10 µL per well. Plates were sealed with a clear adhesive film (Life Technologies, UK) and finally run on 7500 real-time PCR system (Life Technologies, UK). All data were expressed as Ct values and used to calculate ΔCt (Ct of gene of interest – Ct of 18S). For ease of data

interpretation and graphical representation, all the ΔCt values were converted to arbitrary units (AU = $1000x2^{-\Delta Ct}$).

The list of primers used in this thesis are included in the table below@

Resource	Source	Identifier
ACTN1 Primers Fwd CCACCCTCTCGGAGATCAAG Rev TCCCTTCGCTTCTGAGTTAGG	Sigma-Aldrich	Cat#VC00021
ANXA1 Primers Fwd CTAAGCGAAACAATGCACAGC Rev CCTCCTCAAGGTGACCTGTAA	Sigma-Aldrich	Cat#VC00021
GAPDH Primers Fwd TGCACCACCAACTGCTTAGC Rev GGCATGGACTGTGGTCATGAG	Sigma-Aldrich	Cat#VC00021
GPD1 Primers Fwd GCCATCTGAAGGCAAACGC Rev GCCAATGGTTGTCTCACAGAAC	Sigma-Aldrich	Cat#VC00021
HPRT Primers Fwd CACCCTTTCCAAATCCTCAG Rev CTCCGTTATGGCGACCC	Sigma-Aldrich	Cat#VC00021
ITGA1 Primers Fwd CTGGACATAGTCATAGTGCTGGA Rev ACCTGTGTCTGTTTAGGACCA	Sigma-Aldrich	Cat#VC00021
KLF12 Primers Fwd CGGCAGTCAGAGTCAAAACAG Rev CGGCTTCCATATCGGGATAGT	Sigma-Aldrich	Cat#VC00021
LPL primers Fwd CGAGTCGTCTTTCTC CTGATGAT Rev TTCTGGATTCCAATGCTTCGA	Sigma-Aldrich	Cat#VC00021
MSN Primers Fwd GAGGATGTGTCCGAGGAATTG Rev GTCTCAGGCGGGCAGTAAA	Sigma-Aldrich	Cat#VC00021
MYL9 Primers Fwd TCTTCGCAATGTTTGACCAGT Rev GTTGAAAGCCTCCTTAAACTCCT	Sigma-Aldrich	Cat#VC00021

MYO6 Primers Fwd TGGGACAAGACCACCTCATGT Rev CCGGCTCCTGATTCTCCAGA	Sigma-Aldrich	Cat#VC00021
NAMPT Primers Fwd CGGCAGAAGCCGAGTTCAA Rev GCTTGTGTTGGGTGGATATTGTT	Sigma-Aldrich	Cat#VC00021
ND1 primers Fwd CCCTAAAACCCGCCACATCT Rev GAGCGATGGTGAGAGCTAAGGT	Sigma-Aldrich	Cat#VC00021
NDUFS2 Primers Fwd GTCCGATTGCCGATTCAGC Rev GCTTGGGTACATAACAGCTCC	Sigma-Aldrich	Cat#VC00021
NMNAT1 Primers Fwd GGTGGAAGTTGATACATGGGAAA Rev AGCAGCTTGACCTTTGGCA	Sigma-Aldrich	Cat#VC00021
NMNAT3 Primers Fwd AGAGCGTAAAGTACCTGATTCCC Rev CTCTGGGTGCTTTTGCCTT	Sigma-Aldrich	Cat#VC00021
NMRK1 Primers Fwd TATCAGCCTCCAGACTCTCCG Rev GTACACAACTTCCCATGTGATGT	Sigma-Aldrich	Cat#VC00021
NMRK2 Primers Fwd ACTGCTGCGTGATCCATCAG Rev TCCCACTGTTTGAAGCCGTC	Sigma-Aldrich	Cat#VC00021
NNMT Primers Fwd GAGATCGTCGTCACTGACTACT Rev CACACACATAGGTCACCACTG	Sigma-Aldrich	Cat#VC00021

2.2.14. Protein extraction and measurement

C2C12 cells were washed on ice with cold PBS. For 12 well plates, 30 µl of RIPA buffer (1 mM EDTA, 150 mM NaCl, 0.25% SDS, 1% NP40, 50 mM Tris pH 7.4) was added to each well and the cells were scraped using a cell scraper and the resultant cell lysate was transferred into an

Eppendorf and incubated at -80ºC for 20 minutes and thawed on ice. The lysate was then centrifuged at 14000g for 15 minutes at 4°C. The supernatant containing soluble proteins was transferred to fresh eppendorf tubes and stored at -80°C prior to further protein concentration assessment.

Protein concentration was assessed according to the manufacturer protocol (BioRad, UK) in a 96 well plate. The protein standards were made by dissolving bovine serum albumin (BSA) in RIPA buffer. The range of standards was 0, 0.25, 0.5, 1, 2, 4, 8 and 10mg/ mL of BSA in RIPA buffer. 25ml of solution A (alkaline copper tartrate) with 20µl of solution S per ml of solution A was initially added followed by 200µl of solution B (Folin reagent). Once the solutions were added the plate was incubated at room temperature for 10 minutes and the absorbance read at 690nm on a Victor3 1420 multi-label counter (PerkinElmer, UK). Protein concentration in the sample was then calculated according to the slope of the standards curve.

2.2.15. Immunoblotting

20µg of protein was combined with an appropriate volume of 5 x loading buffer and denatured at 98ºC for 3 mins. Proteins were separated with 10-12% gradient SDS-PAGE gel (BioRad, UK) using Precision Plus Protein Standard (BioRad, UK) as a marker. The samples were run at 140 V for 1 h 30 mins, and protein transfer to nitrocellulose membrane (GE Healthcare, UK) was conducted at 140 mA for 1 -2 h. To visualise the protein bands, the membrane was incubated in Ponceau stain with agitation for 60 secs and rinsed with water. Electrophoresis and protein transfer were carried out in BioRad mini protein 3 apparatus (BioRad, UK). The membranes were blocked in 10 mL of blocking buffer containing 5% milk at room temperature for 1 h, followed by overnight incubation with the primary antibody at 4ºC. After washing with 10ml of washing buffer for 15 mins three times, the membranes were incubated with the secondary antibody at room

temperature for 1 h. Subsequently, the membranes were washed with 10 mL of washing buffer for 15 mins three times. Antigen-antibody complexes were detected using Enhanced Chemiluminescence (ECL; GE Healthcare, Bucks, UK). The reaction mixture (1 ml per membrane for 5 mins) was made by combining both substrate A and substrate B at a 50:50 ratio. Finally, photographic film (Perkin Elmer, Surrey, UK) was placed over the membranes in the dark and exposed for 30 secs to 30 mins followed by development on Compact X4 automatic film processor (Xograph Imageing Systems, Gloustershire, UK). To remove bound primary/secondary antibodies, the membranes were stripped by incubating them in stripping buffer (2% SDS, 100 mM β-mercaptoethanol, 50 mM Tris, pH 6.8) at 50°C for 1 h with gentle agitation. Afterwards, the membranes were washed with 10mL of washing buffer 3 times for 15 mins followed by re-probing with a different primary antibody.

2.2.16. 11 β-hydroxysteroid dehydrogenase type 1 activity assay

11βHSD1 activity was measured using Thin Layer Chromatography (TLC); a technique that is based on a separation principle to isolate nonvolatile mixtures on a sheet of aluminium foil coated with a thin layer of adsorbent material. The separation is determined by the affinity of compounds that move in the mobile phase to the surface of the stationary phase. At the end of separation, the individual compounds show as a spot on the TLC plate at variable locations.

A mixture of 1ml serum free DMEM media containing 100nM of either 11-DHC enriched with 20000cpm/reaction 3H-11DHC or corticosterone enriched by 20000cpm/reaction of 3H-corticosterone (GE Healthcare, Bucks, UK) was added to each well of 6 well plates. Incubations were carried out at 37°C under a 5 % CO2 atmosphere for 15 minutes. Media was then transferred to a glass test tube and 5mL of dichloromethane was added. The cells were retained in 30 µl RIPA and stored at -80°C for protein quantification. Steroids were extracted from media by

vortexing the tubes for 10 seconds. Aqueous and organic phases were separated by centrifugation at 1000 g for 10 minutes. The aqueous phase was aspirated off and the organic phase containing the steroids was evaporated at 55°C using an air blowing sample concentrator (Techne, New Jersey, US). Steroids were resuspended in 60 µl of dichloromethane and spotted onto a silica coated thin layer chromatography plate (Thermofisher, Surrey, UK) using a glass Pasteur pipette followed by spotting of 2 µl of non-radiolabelled 11-DHC/corticosterone or cortisone/cortisol (10mM in ethanol) as a cold standard. Each spot was separated by 1.5 cm from adjacent samples and 2 cm from the bottom of the plate. The TLC plate was placed in a glass beaker with the solvent (chloroform 92% and Ethanol 8%) for 1.5 hours to separate the steroids based on their relative affinity in a mobile phase. Radioactivity of the separated 3H-11-DHC/3H-corticosterone or 3H-cortisone/3H-cortisol was measured using a Bioscan 200 Imaging Scanner (LabLogic, Sheffield, UK) for 10 minutes per lane. The plates were placed under UV light to visualise the position of the cold standards to assign the correct glucocorticoids.

Percentage conversion was calculated using region counts for the individual peaks. Enzyme activity was expressed in pmol of steroid converted per mg of protein per hour (pmol/mg/h). Calculation for steroid conversion (V):

Steroid conversion = % conversion/100 x S x (1000/P)/T

S = substrate concentration in reaction volume; e.g. if 100 nM of substrate used in 0.1 ml volume, S=100 pmol/reaction, P= protein concentration in well in mg, T = time in hours

2.2.17. Production of tritiated 11-dehydrocorticosterone (3H- 11DHC)

Unlike tritiated corticosterone (3H-corticosterone), tritiated 11-dehydrocorticosterone (3H-11DHC) is not commercially available; consequently tritiated corticosterone [3H-corticosterone (GE Healthcare, UK) was used to generate 3H-11DHC by a dehydrogenase reaction employing 11β-HSD2 dehydrogenase activity present in mouse placenta. Initially, mouse placenta was homogenised with a homogeniser in 2 ml of 0.154 M KCl. Then the homogenate was centrifuged at 1500rpm for 10 min at 4oC and supernatant aliquoted into eppendorfs and stored at -80^{o}C until required (at this stage protein concentration was measured using BioRad method).

In glass tubes, 20 µl of 3H-corticosterone (1mCi/mL) was incubated with 250 µg of homogenised mouse placenta in 500 µl of 0.1 M phosphate buffer (pH7.4), with 500 µM NAD+. Conversion was carried out overnight in a shaking water bath at 37°C. Steroids were extracted by addition of 5mL of dichloromethane and vortexing the tubes for 10 seconds. Aqueous and organic phases were separated by centrifugation at 1000 g for 10 minutes. The aqueous phase was aspirated off and the organic phase containing the steroids was evaporated at 55°C using an air blowing sample concentrator (Techne, US). Steroids were resuspended in 5µl of dichloromethane and spotted onto a single point of a silica coated thin layer chromatography plate (Thermofisher, UK) using a Pasteur pipette. Cold standards of corticosterone and 11-dehydrocorticosterone were spotted onto the plate 5cm cm distant to the spotted hot steroids, to avoid contamination. Steroids were then separated by thin layer chromatography using 200mL of cholorform:ethanol (ratio of 92:8) as the mobile phase for 1.5 hour. To establish the position of 3H-11DHC, the silica plates were read using a Bioscan 200 Imaging Scanner (LabLogic, UK). The silica at the corresponding position to 3H- 11DHC was pencil marked and then scraped into a glass test tube and eluted in 500mL of ethanol overnight at 4°C. The eluted 3H-11DHC and silica were separated by centrifugation at 1000 g for 5 minutes. Radioactivity of 3H-11DHC was determined by spotting

2μL of stock by thin layer chromatography and number of counts determined using the Bioscan 200 Imaging Scanner. Stock was then diluted in ethanol to give ~1000 counts/μL.

Chapter 3: Safety, Tolerability, And Effects of Oral Nicotinamide Riboside Supplementation on The Human NAD+ Metabolome

Parts of this chapter have been published as:

Nicotinamide Riboside Augments the Aged Human Skeletal Muscle NAD+ Metabolome and Induces Transcriptomic and Anti-inflammatory Signatures

Elhassan YS et al.

Cell Reports. 2019 Aug 13;28(7):1717-1728.e6

DOI: 10.1016/j.celrep.2019.07.043

3.1. Introduction

Ageing is defined by a decrease in metabolic and physiological functions across all organs in the body. A key characteristic of ageing is the gradual reduction in skeletal muscle mass and function, which may progress to sarcopenia, linked with significant morbidity, mortality, and health economic burden (264,397). While exercise is commonly advocated to counteract age-related muscle decline (398), dietary interventions also present a promising avenue to mitigate age-related health decline and support healthy muscle ageing (185).

Maintaining NAD+ homeostasis is crucial for cellular and organismal functions. A decline in NAD+ availability and signalling has been associated with ageing in several species (120,147), however, there is a paucity of data to confirm that this is the case in human ageing. NR and NMN were observed to extend life span and enhance metabolism in aged mice (399,400). Enhancing NAD+ availability through NR supplementation has emerged as a potential strategy to bolster tissue-specific NAD+ levels and improve physiological function (182,210,257). Several physiological stresses in mice associated with NAD+ depletion have been prevented or reversed with NR supplementation including noise-induced hearing loss (401), weight gain (146), dysglycaemia, fatty liver, neuropathy (322), cardiac dysfunction (402), and prevention of cortical neuronal degeneration (403). However, data in mice tracing NAD^+ fluxes questioned whether oral NR has the ability to access muscle (404). NR supplementation studies in humans have so far focussed on safety, cardiovascular, and systemic metabolic endpoints (405–407). Doubts exist regarding the ability of oral NR to access muscle tissue in humans, and the impact of NR supplementation on human skeletal muscle NAD+ metabolome remains uncertain.

To address these gaps, we conducted a randomised, double-blind, placebo-controlled crossover trial involving a 21-day NR supplementation intervention in a cohort of men aged 70–80 years (Figure 3.1).

3.1.1. Hypothesis, aims, and objectives

Hypothesis: NR supplementation in aged humans may increase skeletal muscle NAD+ bioavailability. If NAD+ boosting is successful, we may observe NAD+ metabolome profiles that reflect improved metabolic status of the muscle.

Aims: To exploit a novel dietary supplementation strategy (Nicotinamide Riboside-NR) in order to increase endogenous NAD+ availability in aged individuals which can potentially be used to prevent and treat age-related metabolic decline.

Objectives: This study is designed to assess the physiological consequences of elevating NAD+ availability using NR supplementation in skeletal muscle tissue and examine its effect upon muscle metabolic phenotype *in vivo*.

The detailed methodology of the clinical study was included in Chapter 2.

3.2. Results

3.2.1. Study approvals

Over a 12 months' period, I have established a protocol for this clinical study, prepared all the essential documents, and obtained NHS ethical approval from the Solihull NRES Committee (REC reference number 16/WM/0159) and the local R&D and Clinical Research Facility Scientific Advisory committee approvals (REC reference 16/WM/0159, IRAS ID 183388). All participants provided written informed consent. The study was registered on www.clinicaltrials.gov (Identifier: NCT02950441). The study was undertaken according to the principles of the Declaration of Helsinki and followed the principles of Good Clinical Practice.

3.2.2. Oral NR safety and tolerability in aged men

Following screening, twelve aged men (median age 75 years) were recruited. The participants were marginally overweight (median BMI 26.6 kg/m^2; range 21 - 30), but otherwise healthy. The baseline characteristics of participants are shown in Table 1.

Table 1: Cardiometabolic parameters at baseline and after NR and placebo. Data are presented as median (1st quartile, 3rd quartile).

Parameter	Baseline	NR	Placebo
Age (years)	75 (72, 78)	-	-
Weight (kg)	82.6 (76.5, 90.1)	83 (76.3, 89.9)	82.6 (77.0, 89.6)
BMI (kg/m^2)	26.6 (25.0, 30.0)	26.9 (24.9, 29.5)	26.9 (25.1, 29.3)
Systolic blood pressure (mmHg)	139 (136, 154)	138 (130, 147)	134 (126, 155)
Diastolic blood pressure (mmHg)	86 (83, 93)	84 (79, 93)	81 (77, 90)
Fasting glucose (mmol/L)	5.88 (5.63, 6.31)	6.04 (5.81, 6.23)	5.85 (5.67, 6.30)
Fasting insulin (mU/L)	7.07 (7.27, 8.67)	6.27 (5.47, 7.07)	7.06 (5.47, 8.67)
Cholesterol (mmol/L; reference range <5.0)	4.8 (3.6, 5.2)	4.6 (3.9, 5.6)	4.6 (4.2, 5.3)
HDL cholesterol (mmol/L; reference range >1.55)	1.4 (1.2, 1.5)	1.3 (1.2, 1.5)	1.4 (1.1, 1.5)
Triglycerides (mmol/L)	1.0 (0.6, 1.2)	1.0 (0.8, 1.2)	1.0 (0.7, 1.2)

NR chloride (Niagen ®) and placebo were provided as 250 mg capsules (ChromaDex, Inc., USA) and subjects were instructed to take two tablets in the morning and two tablets in the evening. The whole participants completed the five study visits and assessments according to the approved study protocol. NR was well tolerated and safe according to several clinical biochemistry safety parameters including renal, liver, and thyroid functions (Table 2). No adverse events were reported by the participants during the study on either of the NR or placebo phases.

Table 2**:** Safety parameters at baseline and after nicotinamide riboside (NR) and placebo. Data presented as median (1st quartile, 3rd quartile). ALT, alanine aminotransferase; TSH, thyroid stimulating hormone; Free T4, free thyroxine.

Parameter	Baseline	NR	Placebo
Haemoglobin (g/L; reference range 130-171)	139 (129, 145)	133 (128, 139)	136 (131, 149)
White cell count (x10^9/L; reference range 3.26-11.20)	6.2 (5.5, 7.0)	6.2 (5.3, 6.9)	6 .2 (5.7, 7.1)
Platelets (x10^9/L reference range 150-400)	187 (174, 233)	184 (169, 221)	203 (171, 231)
Sodium (mmol/L; reference range 133-146)	140 (139, 143)	139.5 (137, 142)	141 (137, 142)
Potassium (mmol/L; reference range 3.5-5.3)	4.2 (4.0, 4.3)	4.3 (4.1, 4.4)	4.2 (4.1, 4.5)
Urea (mmol/L; reference range 2.5-7.8)	6.0 (4.2, 6.5)	4.6 (4.0, 5.8)	5.1 (4.4, 6.0)
Creatinine (µmol/L; reference range 64-104)	74 (64, 78)	71 (67, 85)	74 (67, 79)
Calcium (mmol/L; reference range 2.20-2.60)	2.3 (2.2, 2.4)	2.3 (2.2, 2.4)	2.3 (2.2, 2.3)

Albumin (g/L; reference range 35-50)	43 (42, 44)	42 (40, 42)	42 (39, 43)
Total protein (g/L; reference range 60-80)	65 (63, 70)	65 (63, 67)	65 (62, 67)
Alkaline phosphatase (u/L; reference range 30-130)	56 (45, 62)	55 (46, 61)	52 (48, 62)
Bilirubin (umol/L; reference range <21)	7 (6, 10)	8 (6, 10)	8 (6, 9)
ALT (u/L; reference range 0-55)	17 (14, 17)	14 (12, 15)	16 (13, 19)
TSH (mIU/L; 0.40-4.90)	1.7 (1.0, 2.7)	1.8 (1.3, 2.8)	1.6 (1.1, 2.5)
Free T4 (pmol/L; 9-19)	14.0 (12.1, 15.1)	13.7 (13.4, 17.4)	14.8 (13.1, 17.5)

3.2.3. Oral NR augments skeletal muscle and systemic NAD+ metabolome

To evaluate the effects of NR supplementation on NAD+ metabolism, we employed a targeted LC-MS/MS method (408) to measure the NAD+ metabolome in skeletal muscle, whole venous blood, and urine.

We examined the NAD+ metabolome in skeletal muscle biopsies from all participants in a fasted state at baseline and after the NR and placebo phases, 14 hours after the last dose and prior to the physiological assessments. Samples were collected 14 hours after the last dose to enable the participants to attend the Clinical Research Facility in a fasted state and to evaluate the effects of longer-term NR administration rather than those of an acute dose. Eleven metabolites in total were measured in the muscle. NR was detectable without being elevated in the NR supplementation period (NR 1.4 pmol/mg µM vs. placebo 1.25 pmol/mg; p = 0.23). We found that

NR resulted in a two-fold increase in muscle NAAD (NR 0.73 pmol/mg vs. placebo 0.35 pmol/mg; p = 0.004), without increasing NAD+ (NR 210 pmol/mg vs. 197 pmol/mg; p = 0.22). NR supplementation did not affect muscle NAM (NR 92.0 pmol/mg vs. placebo 86.5 pmol/mng; p = 0.96). However remarkably, we detected 5-fold increases in the products of NAM methylation clearance pathways; N-methyl nicotinamide (MeNAM; NR 1.45 pmol/mg vs. placebo 0.35 pmol/mg; p = 0.006), N1-Methyl-2-pyridone-5-carboxamide (Me-2-py; NR 6.6 pmol/mg vs. placebo 1.1 pmol/mg; p = < 0.001), and N1-Methyl-4-pyridone-5-carboxamide (Me-4-py; NR 1.6 pmol/mg vs. placebo 0.3 pmol/mg; p = < 0.001) (Figure 3.2).

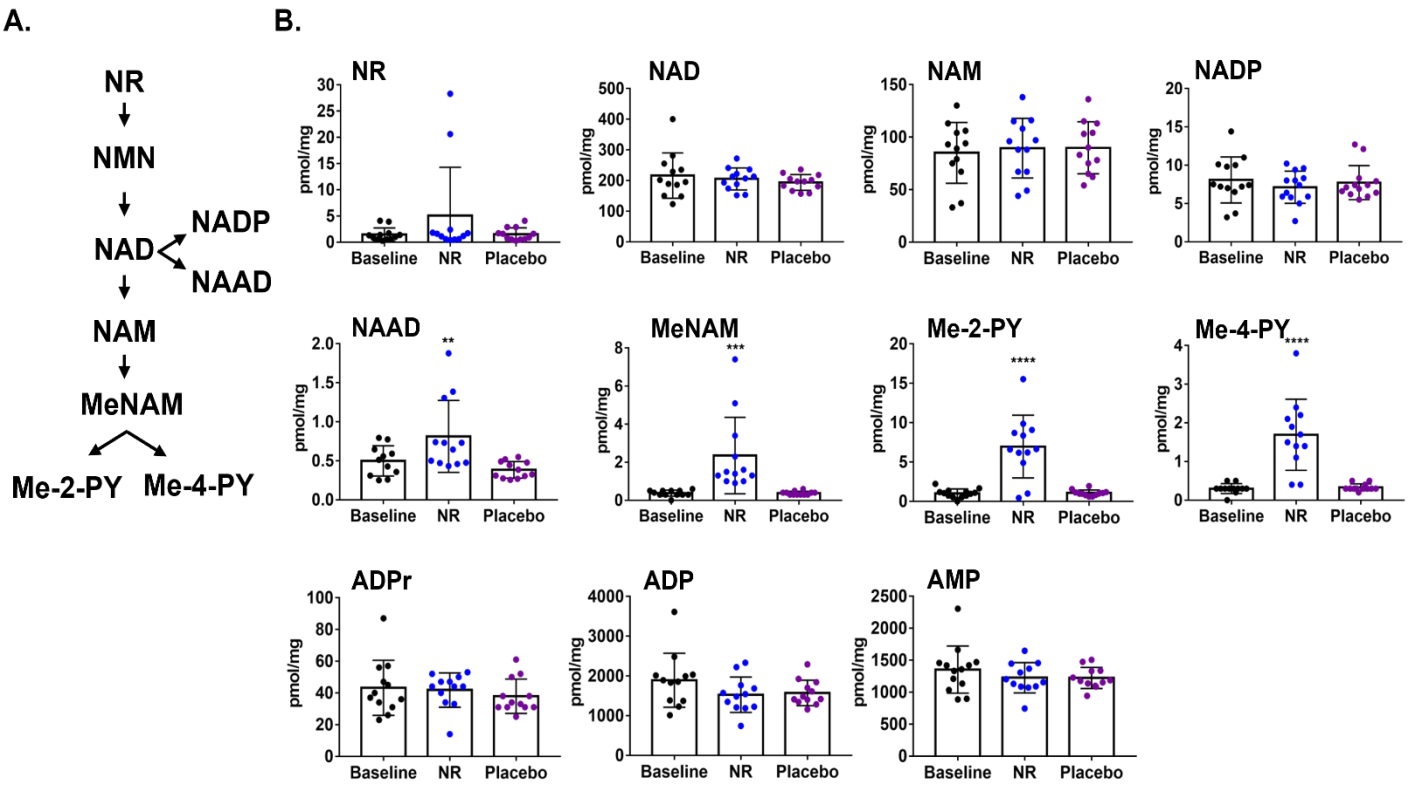

Figure 3.2: Skeletal muscle NAD+ metabolomics. Schematic representation of NR metabolism within the NAD+ metabolome, accompanied by the detected metabolite levels measured using LC-MS in skeletal muscle at baseline and after each of the NR and placebo periods. NAD+ metabolomics data at the end of the washout period are not shown as they are indistinguishable from baseline and placebo. Data were normalised to the weight of muscle pellet used for extraction. NMN, nicotinamide mononucleotide; NAAD, nicotinic acid adenine dinucleotide; NAM, nicotinamide; MeNAM, N-methyl nicotinamide; Me-2-py, N1-Methyl-2-pyridone-5- carboxamide; Me-4-PY, N-methyl-4-pyridone-3-carboxamide. Significance was set at p <0.05 with * <0.05; ** <0.01; *** <0.001; **** <0.0001.

In the blood, we measured 12 metabolites from each participant at baseline and following each of the NR, placebo, and washout periods. NR was also detectable in the blood but was not increased compared to placebo at 14 hours after the last dose of NR (NR 0.16 µM vs. placebo 0.15 µM; p = 0.31). NR increased the concentrations of NAD+ > 2-fold (NR 47.75 µM vs. placebo 20.90 µM; p = <0.001) and NMN 1.4-fold (NR 1.63 µM vs. placebo 1.13 µM; p = <0.001). NR supplementation did not elevate NAM in the blood (NR 10.60 µM vs. placebo 9.50 µM; p = 0.41). Again, NAM urinary clearance pathways were enhanced with NR supplementation manifesting

as excessive MeNAM (NR 0.66 µM vs. placebo 0.10 µM; p = <0.001), Me-2-py (NR 7.69 µM vs. placebo 1.44 µM; p = <0.001), and Me-4-py (NR 3.82 µM vs. placebo 0.48 µM; p = <0.001). NR elevated blood NAAD levels by 4.5-fold (NR 0.18 µM vs. Placebo 0.04 µM; p = <0.001) (Figure 3.3).

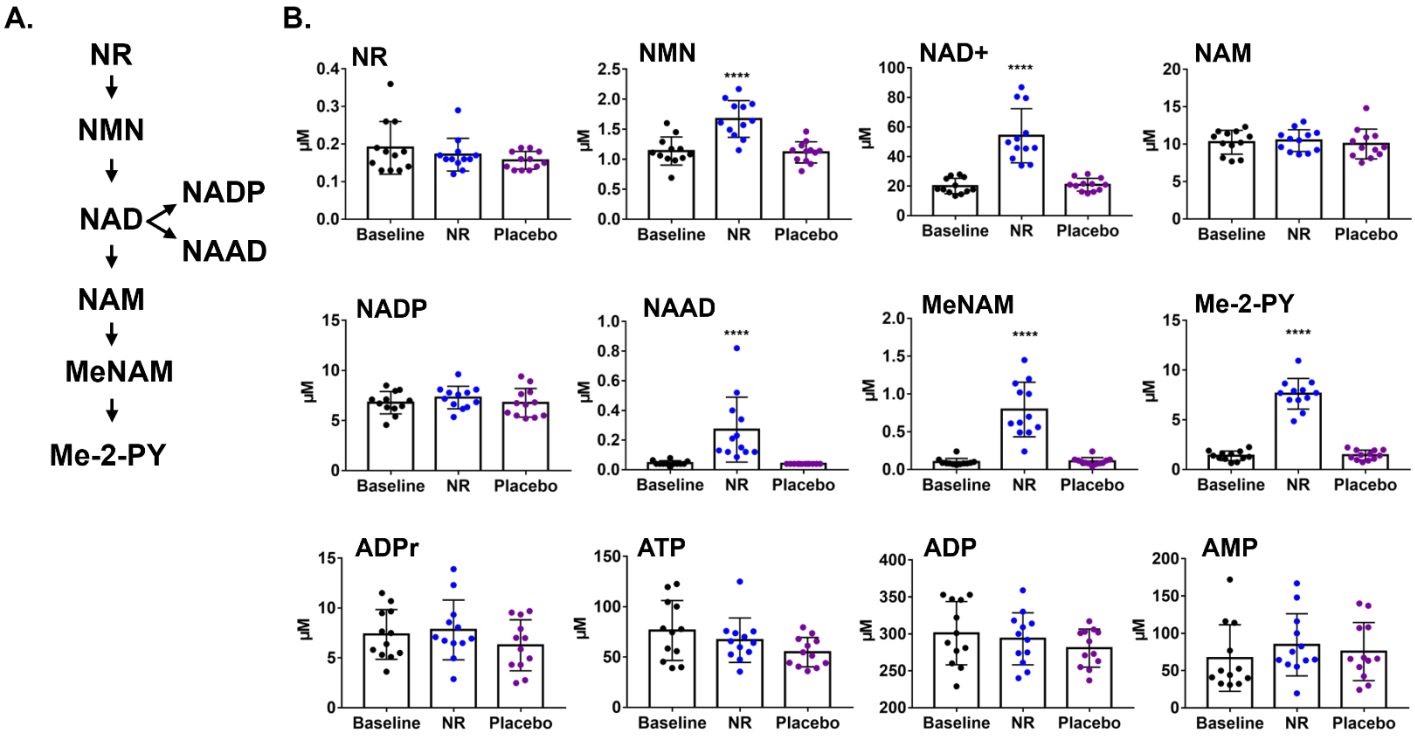

Figure 3.3: Whole blood NAD+ metabolomics. Schematic representation of the whole blood NAD+ metabolome at baseline and after each of the NR and placebo periods. NMN, nicotinamide mononucleotide; NAAD, nicotinic acid adenine dinucleotide; NAM, nicotinamide; NAMOx, nicotinamide N-oxide; MeNAM, N-methyl nicotinamide; Me-2-py, N1-Methyl-2-pyridone-5-carboxamide; Me-4-PY, N-methyl-4-pyridone-3-carboxamide. Significance was set at p <0.05 with * <0.05; ** <0.01; *** <0.001; **** <0.0001.

Urinary NAD+ metabolomics revealed that NR was detectable and augmented with NR supplementation (NR 41.5 µmol/mol creatinine vs. Placebo 31.7 µmol/mol creatinine; p = 0.02). Furthermore, a near 20-fold increase in nicotinic acid riboside (NAR; NR-185.5 µmol/mol creatinine vs. placebo-10.3 µmol/mol creatinine; p = 0.001) was observed. Unlike muscle and

blood, NAM was elevated in the urine 2.5-fold (NR-282 µmol/mol creatinine vs. Placebo-106.5 µmol/mol creatinine; p = 0.004) (Figure 3.4).

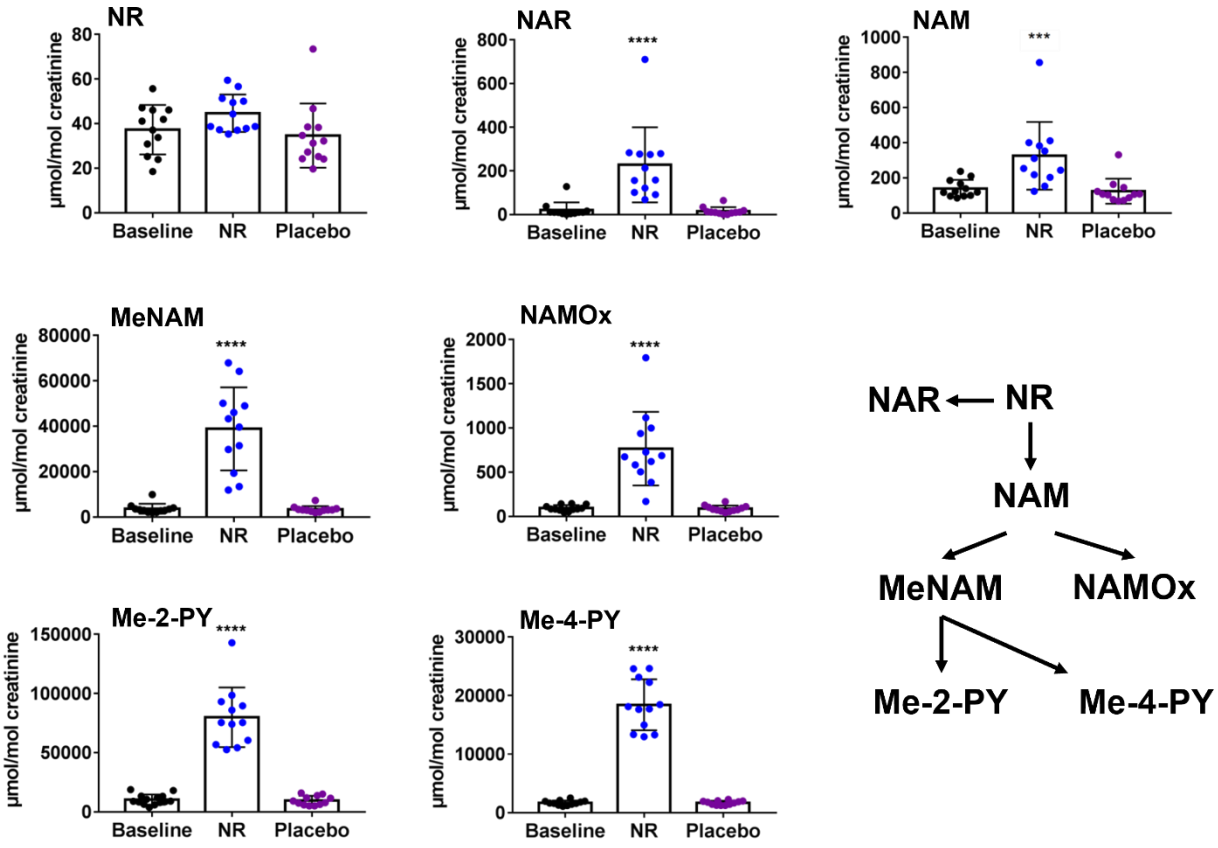

Figure 3.4: Urine NAD+ metabolomics. Schematic representation of the urinary NAD+ metabolome at baseline and after each of the NR and placebo periods. Data were normalised to urinary creatinine. NAM, nicotinamide; NAMOx,, nicotinamide N-oxide; MeNAM, N-methyl nicotinamide; Me-2-py, N1-Methyl-2-pyridone-5- carboxamide; Me-4-PY, N-methyl-4-pyridone-3-carboxamide. Significance was set at p <0.05 with * <0.05; ** <0.01; *** <0.001; **** <0.0001.

3.2.4. Discussion

These data establish that oral NR administration in humans is safe and well tolerated and paved the path for possible preventative or therapeutic applications. Although a 3-week supplementation period may not be sufficiently long to address longer-term adverse events, these results are indeed encouraging especially considering the age of the study cohort.

The data also depicts the extent and breadth of changes to NAD+ metabolites in human skeletal muscle, blood, and urine after NR supplementation. We confirm that oral NR greatly enhanced the whole blood NAD+ metabolome. We also detected an increase in tissue NAD+ metabolism, specifically in skeletal muscle. We also saw an increase in the disposal of NAM urinary clearance products as a result of oral NR supplementation. Interestingly, a recent study reported that the NAM clearance products, Me-2-PY and Me-4-PY, were associated with increased cardiovascular risk (219). The authors reported that Me-4-PY in mice increased the expression of vascular adhesion molecule 1 (VCAM-1) and leukocyte adherence to vascular endothelium (219). Although we did not detect adverse cardiometabolic profiles following NR supplementation and increased Me-2-PY and Me-4-PY in our study, a longer-term supplementation strategy would be required with outcomes specifically addressing cardiovascular risk.

A previous study in mice reported that oral NR is rapidly metabolised in the liver to NAM, which then becomes the main circulating product of the orally administered NR, to subsequently enhance the tissue NAD+ metabolome (404). However, chronic oral NR supplementation in humans in the present study did not boost the circulating NAM in the blood. However, we saw increases in whole blood NMN and NAD+ following NR supplementation; ideally a study of the liver NAD+ metabolome would be needed to better understand these dynamics.

The concentration of NR was detectable in skeletal muscle, blood, and urine, but the levels were not higher after NR supplementation compared to baseline and placebo. This is not surprising as

the studied C_{max} for NR is around 3 hours (409). Additionally, a study in mice suggested a high first pass metabolism in the liver for orally administered NR (404).

Nicotinic acid adenine dinucleotide (NAAD) was conistently increased in the muscle and blood following NR supplementation. These data confirm the previous observation that NAAD appears to be a highly sensitive biomarker of NR supplementation and enhanced rate of NAD+ synthesis than measuring NAD+ *per se* (204).

The 20-fold NR-mediated increase in urinary NAR is also interesting. This finding may support the speculation that NR supplementation leads to retrograde production of NAAD, nicotinic acid mononucleotide (NAMN), and NAR (204). However, direct NR transformation into NAR remains plausible.

Ideally, further studies are needed to better understand the dynamics in the NAD+ metabolome following the oral administration of the different NAD+ precursors (NR, NMN, NAM, NA). These studies would need to assess the NAD+ metabolome in several tissues, including the liver. However, these studies are likely to be challenging to undertake in terms of safety (e.g., of a liver biopsy) and accurate methodology.

Chapter 4: Effects of Oral NAD+ Supplementation on Human Skeletal Muscle

Parts of this chapter have been published as:

Nicotinamide Riboside Augments the Aged Human Skeletal Muscle NAD+ Metabolome and Induces Transcriptomic and Anti-inflammatory Signatures

Elhassan YS et al.

Cell Reports. 2019 Aug 13;28(7):1717-1728.e6

DOI: 10.1016/j.celrep.2019.07.043

4.1. Introduction

The previous chapter addressed the effects of NR supplementation on systemic and tissue NAD+ and demonstrated an increase in the skeletal muscle NAD+ metabolome. This chapter assessed whether the NR-mediated increase in NAD+ metabolism in human skeletal muscle alters the muscle mitochondrial bioenergetics, substrate utilisation, physical function, and tissue transcriptome.

4.1.1. Effects of oral NR supplementation on skeletal muscle bioenergetics

We undertook a detailed evaluation of skeletal muscle mitochondrial respiration on biopsies before and after NR supplementation. No differences were observed between the NR and placebo groups in skeletal muscle complex I and complex II mediated oxidative phosphorylation and maximal respiratory capacity, with and without the prior addition of the fatty acid conjugate octanoyl-carnitine (Figure 4.1). To account for the mitochondrial content in the sample, we corrected the data to the activity of the mitochondrial enzyme, citrate synthase, and the mtDNA copy number. The results remained unchanged whether the respiration rates were corrected for citrate synthase activity or mtDNA copy number.

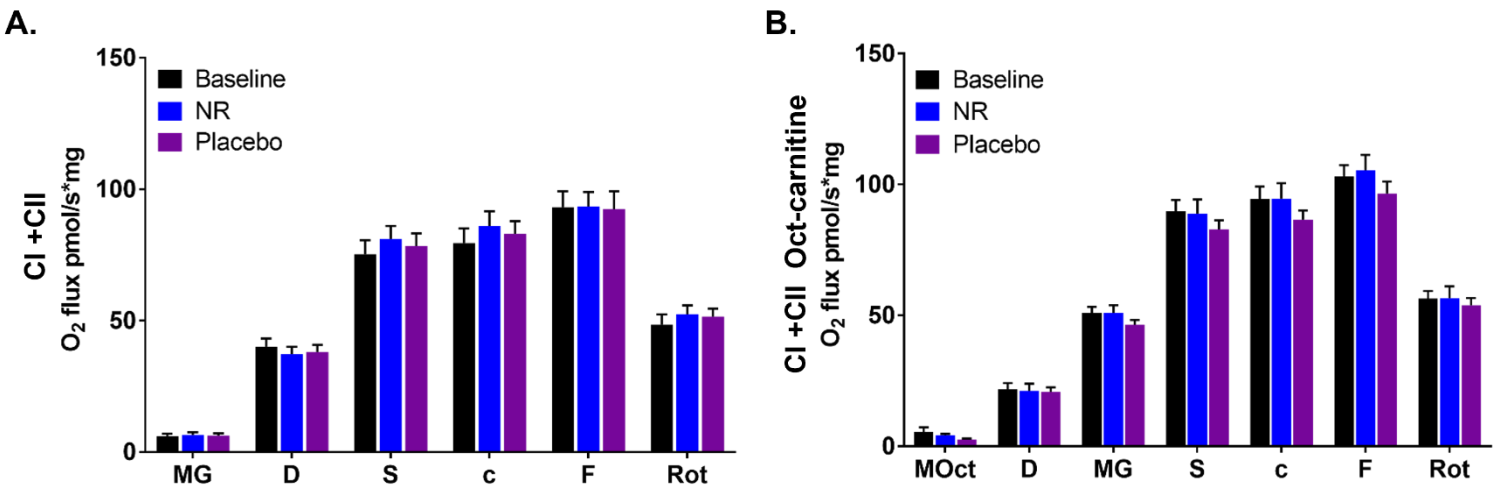

Figure 4.1: High resolution respirometry. Mitochondrial respiration of permeabilised muscle fibres after the addition of complex I and complex II substrates at baseline and after 3 weeks of supplementation of NR and placebo. MG, malate and glutamate; D, ADP; S, succinate; c, cytochrome C; F, FCCP; Rot, rotenone. Data are normalised to muscle fibre weight. (B) Mitochondrial respiration as per (A), but with the prior addition of the fatty acid conjugate octanoyl-carnitine to malate (MOct).

In support of the above finding, the activity of the enzyme citrate synthase, which is commonly used as a quantitative measure of mitochondrial content (410), and mtDNA (282) were unchanged with or without NR supplementation (Figure 4.2).

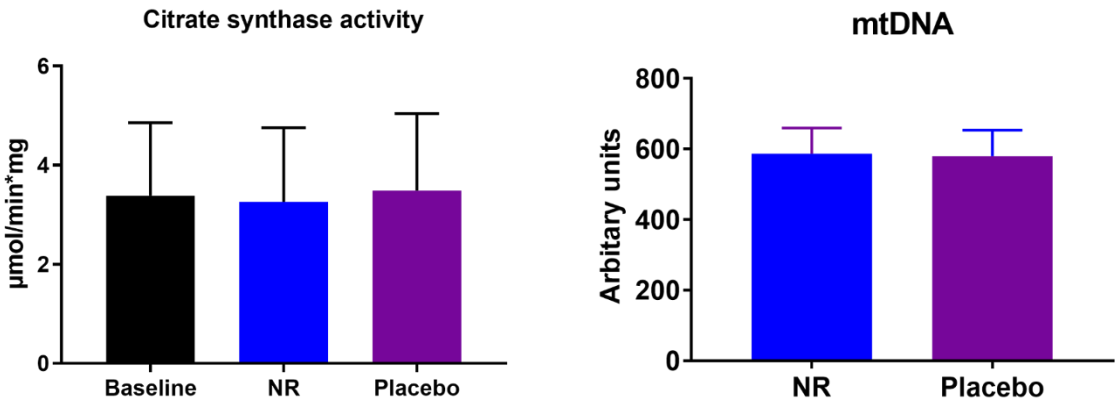

Figure 4.2: Citrate synthase activity and mtDNA. Left: Citrate synthase activity in human skeletal muscle at baseline and after NR and the placebo. Right: Relative PCR expression of mitochondrial DNA (mtDNA) to nuclear DNA (nDNA) at after NR and the placebo, expressed as arbitrary units

Furthermore, the levels of skeletal muscle mitochondrial resident proteins, which are implicated in the electron transport chain, were also unchanged with or without NR supplementation (Figure 4.3).

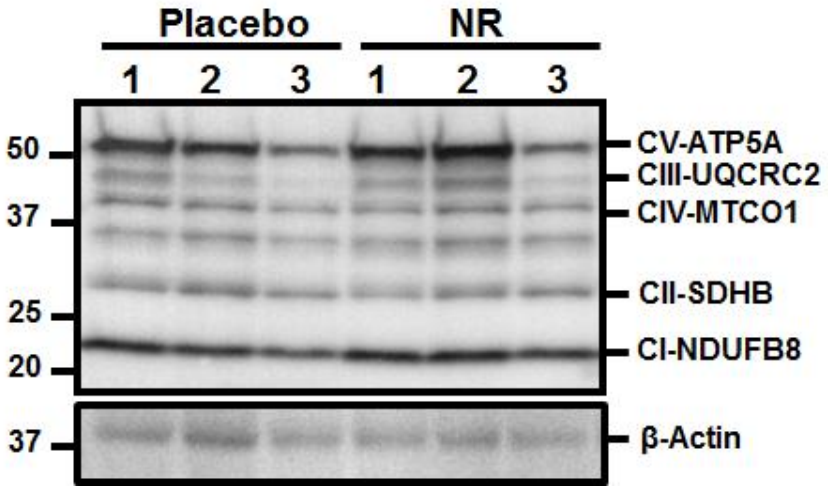

Figure 4.3: Western blot revealing the expression of selected mitochondrial proteins in skeletal muscle lysates when compared to β-actin as a housekeeping protein.

We then evaluated whether boosting the NAD+ metabolome with NR results in higher sirtuin-mediated deacetylation and undertook western blotting to look at the pan-acetylation status. Similarly, no NR-mediated changes to muscle protein acetylation were detected (Figure 4.4).

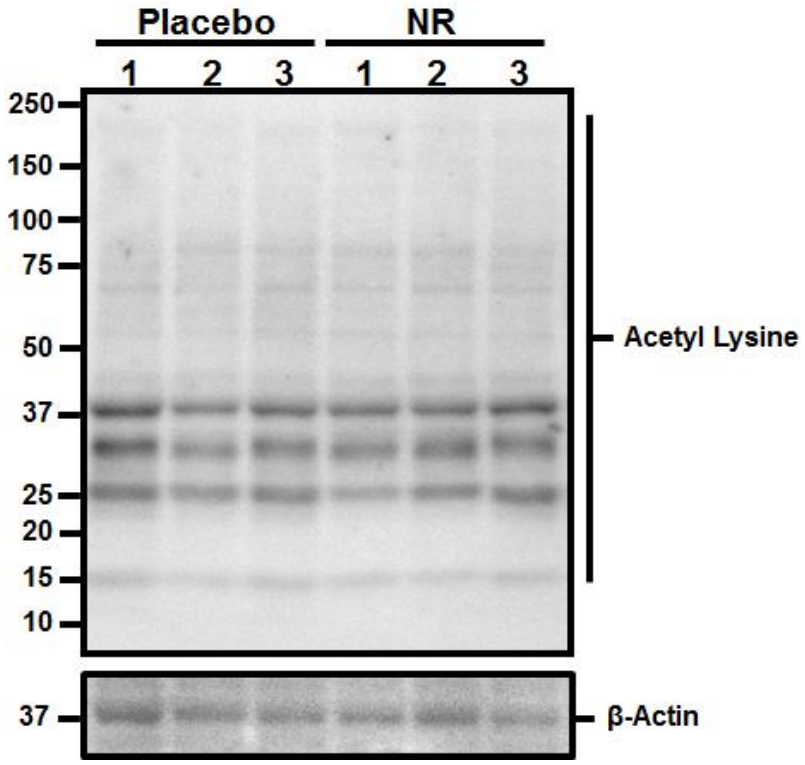

Figure 4.4: Western blot revealing the expression of acetylation proteins in skeletal muscle lysates when compared to β-actin as housekeeping protein

.

4.1.2. NR-mediated skeletal muscle transcriptomic changes

RNA sequencing accompanied by differential gene expression (DGE) analysis of the skeletal muscle biopsies identified 690 upregulated genes compared with 398 downregulated genes that differentiated the baseline and NR supplementation phases. We applied gene annotation analysis (DAVID and GSEA) (389–391,411) and found that the genes significantly downregulated with NR supplementation were enriched in pathways linked to energy metabolism including glycolysis, TCA cycle, and mitochondria. Conversely, pathways upregulated after NR supplementation prominently belonged to the gene ontology categories of cell adhesion, actin cytoskeleton organisation, and cell motility (Figure 4.5).

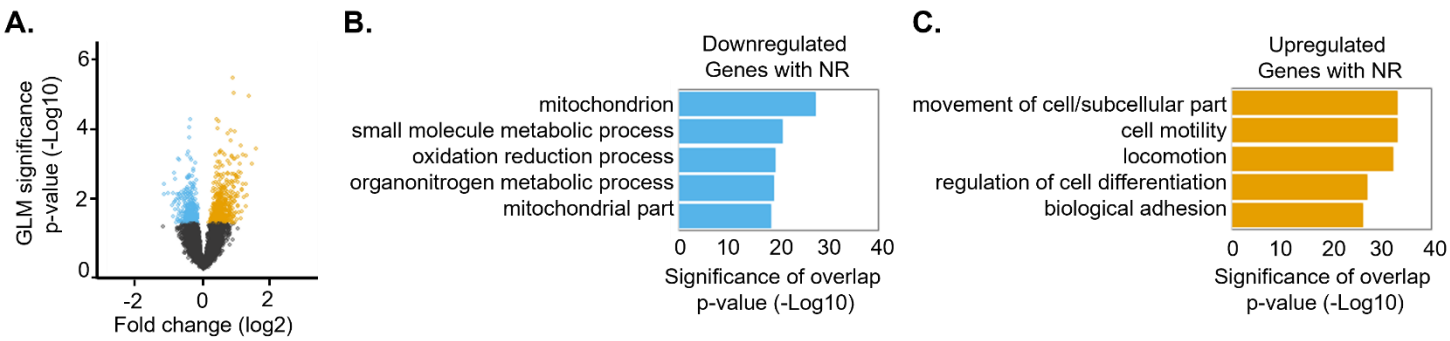

Figures 4.5: RNA sequencing of skeletal muscle biopsy. (A) Differential gene expression analysis skeletal muscle comparing the baseline and NR periods. Volcano plot of differential gene expression between baseline and NR treated human muscle samples. Fold change of gene expression is plotted against p value for differential gene expression (–Log10, y axis). Coloured dots represent Ensembl genes that are either upregulated (in orange) or downregulated (in blue) after NR supplementation at a p value < 0.05. (B and C) Gene Ontology analysis of significantly dysregulated genes after NR supplementation for downregulated genes (in blue) and upregulated genes (in orange). Gene Ontology analysis was performed using GSEA. Bars represent the p value (–Log10) of overlap from hypergeometric distribution.

We also examined all the genes belonging to the Glycolysis, TCA cycle, and Mitochondria pathways and detected that they were downregulated upon NR supplementation when compared to control of 10 gene sets of the same size and expression level. Again, we also found that the genes belonging to the gene ontology terms “actin filament-based process”, “cell motility”, and “biological cell adhesion”, were mainly upregulated upon NR supplementation (Figure 4.6).

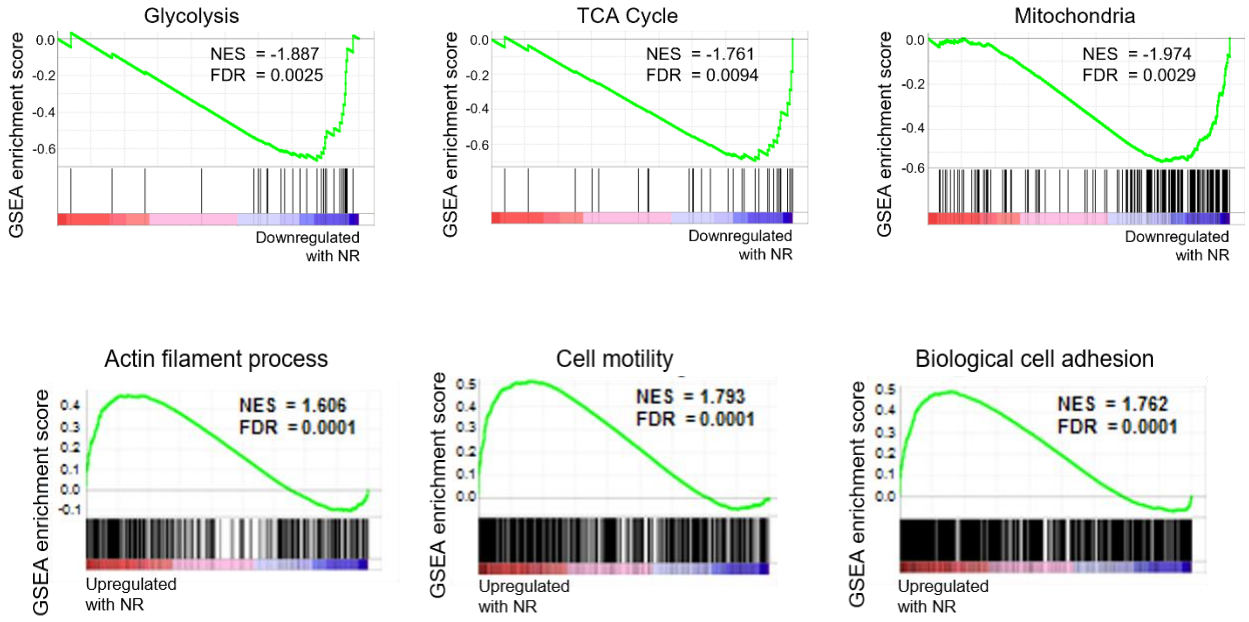

Figure 4.6: Gene set enrichment analysis (GSEA) suggests that the genes belonging to the gene set “glycolysis”, “TCA cycle” and “mitochondria” are downregulated upon NR supplementation whilst the gene sets “actin filament process”, “cell motility”, and “biological cell adhesion” are upregulated after NR supplementation. Normalised enrichment score (NES) and nominal p-value is noted on the graph.

For validation, we then undertook qPCR which also showed downregulation of selected genes implicated in energy metabolism (Figure 4.7).

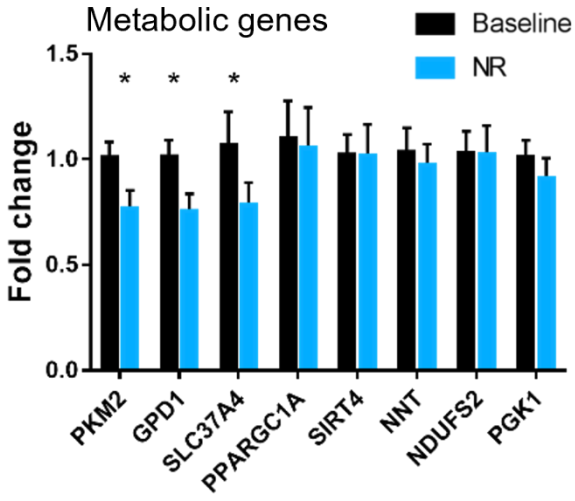

Figure 4.7: A qPCR analysis of a selected panel of NR-induced downregulated genes from the glycolysis, TCA cycle, and mitochondria gene sets identified through differential gene expression analysis. GAPDH was used as housekeeping gene.

Importantly, we found no transcriptional changes in key genes involved in NAD+ metabolism, including NMRK 1/2, NAMPT, NNMT, and NMNAT 1/3 (Figure 4.8).

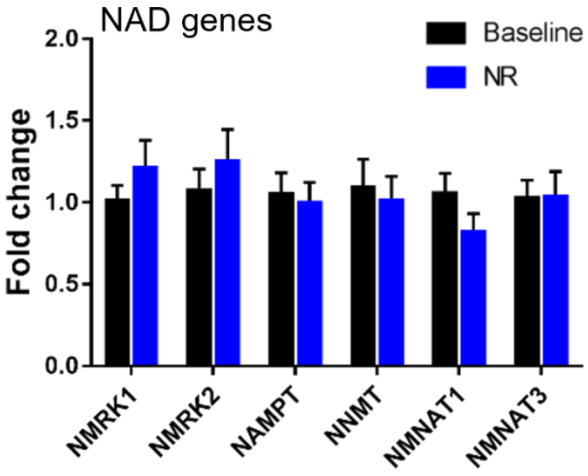

Figure 4.8: A qPCR analysis of a selected panel of NAD+ pathway-related genes comparing before and after NR supplementation. GAPDH was used as housekeeping gene.

We also validated some of the upregulated targets by qPCR and were also able to successfully perform immunoblotting validation (Figure 4.9).

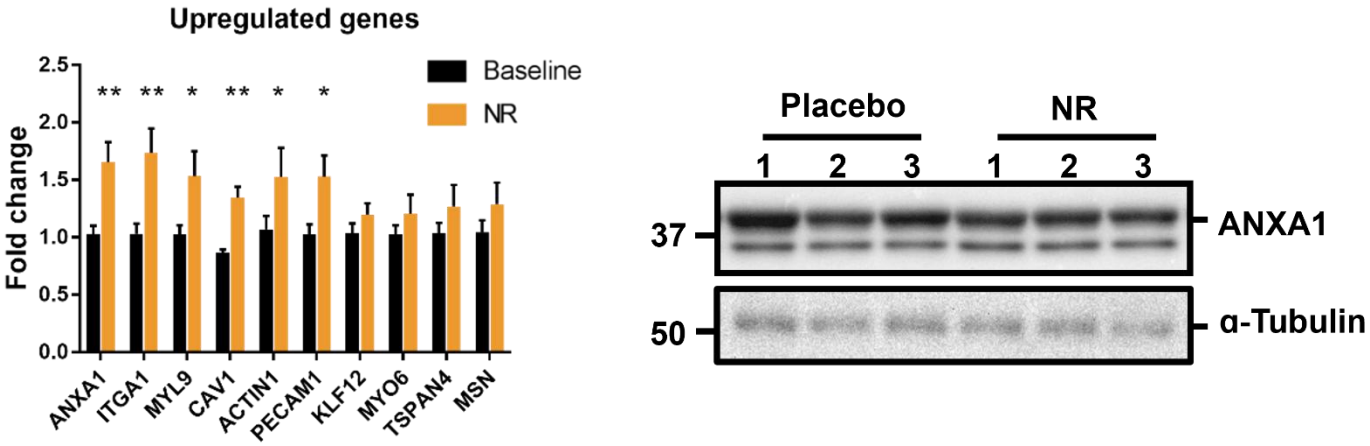

Figures 4.9: qPCR analysis of a selected panel of NR-induced upregulated genes from the actin filament process and cell adhesion gene sets identified through differential gene expression analysis. The immunoblotting assay showed Annexin A1 (ANXA1) protein. Tubulin was used as a loading control.

Due to the report that NR increases glycolysis in mouse cardiac cells (402), and whilst our data do not suggest an NR-mediated upregulation of glycolysis related genes, we investigated the protein expression levels of key enzymes involved in glycolysis in skeletal muscle biopsies and found they were unchanged following NR supplementation (Figure 4.10).

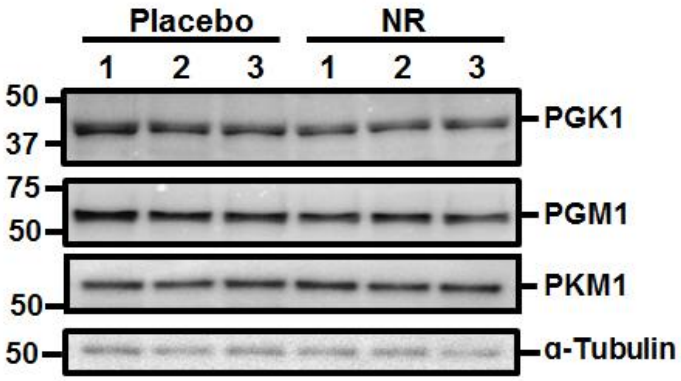

Figure 4.10: Quantification of phosphoglycerate kinase 1 (PGK1), phosphoglucomutase 1 (PGM1), and pyruvate kinase M1 (PKM1) proteins using immunoblotting assay.

4.1.3. Hand-grip strength assessment

After NR supplementation for 3 weeks, we could not detect any differences in the peak hand-grip strength (NR 32.5 kg vs. placebo 34.7 kg; p = 0.96) or body weight adjusted relative strength (NR 2.4 vs. placebo 2.3; p = 0.96) between NR and placebo (Figure 4.11).

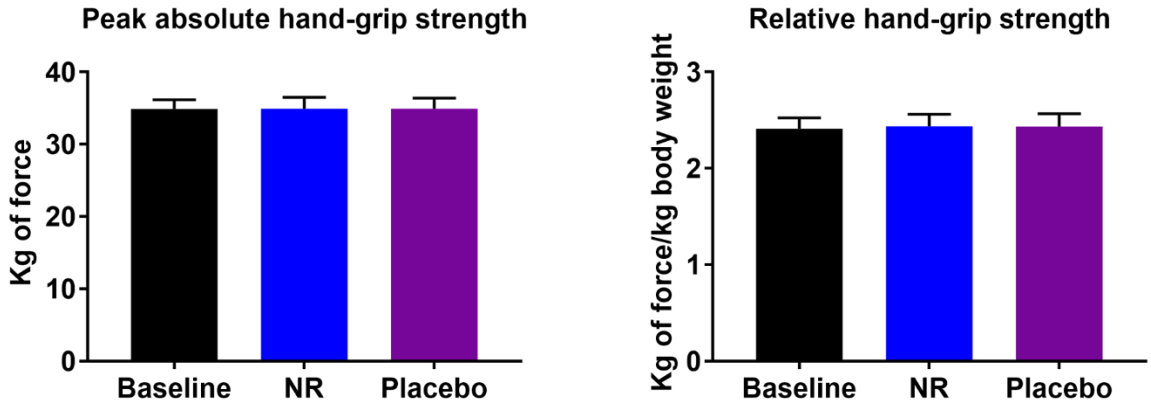

Figure 4.11: Peak hand-grip strength at baseline and after each of the NR placebo phases. For the relative strength, data are adjusted for the body weight. The absence of significance symbols indicates that there is no statistical significance.

4.1.4. The effect of NR supplementation on muscle blood flow

We employed venous occlusive plethysmography to assess the forearm muscle blood flow in a non-invasive manner (385). At fasting, no NR-mediated differences were detected in muscle blood. Similarly, following the oral glucose load, muscle blood flow gradually increased, but without a discernible difference between NR and placebo (Figure 4.12).

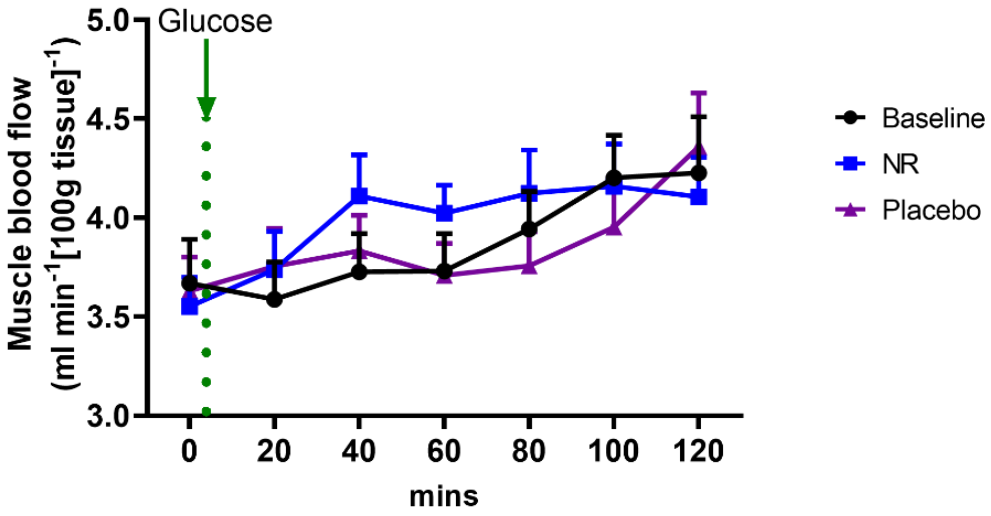

Figure 4.12: Venous occlusive plethysmography. Muscle blood flow using venous occlusive plethysmography at baseline and after NR and placebo. The green line represents the administration of the 75 g of oral glucose load. The absence of significance symbols indicates that there is no statistical significance.

4.1.5. The effect of NR supplementation on muscle substrate utilisation

We employed the arteriovenous difference technique to compare substrate utilisation across the forearm muscle (between arterial blood supplying the muscle and venous blood drained from the muscle), with muscle blood flow taken into account as measure of the substrate flux (412). No differences were detected in O_2 consumption and CO_2 production between NR and placebo at the fasting state and in response to oral glucose (Figure 4.13).

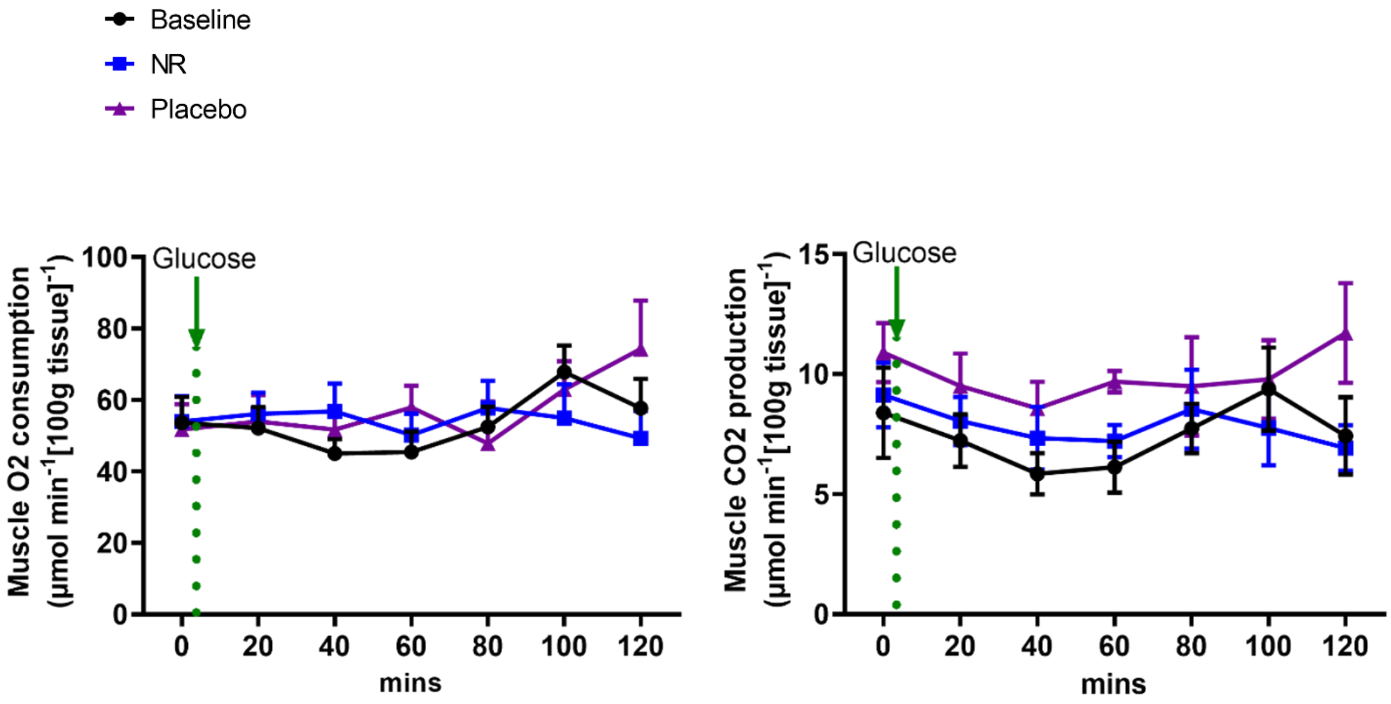

Figure 4.13: Muscle O2 consumption and CO2 production at baseline and after NR and placebo. The green line represents the administration of the 75 g of oral glucose load. The absence of significance symbols indicates that there is no statistical significance.

We then assessed the forearm muscle glucose uptake and lactate release. As physiologically expected, muscle glucose uptake was increased following the administration of oral glucose before gradual decline. No changes in muscle glucose handling were demonstrated before and after NR. Oral glucose reduced lactate production from muscle, again without a discernible difference in response between NR and placebo (Figure 4.14).

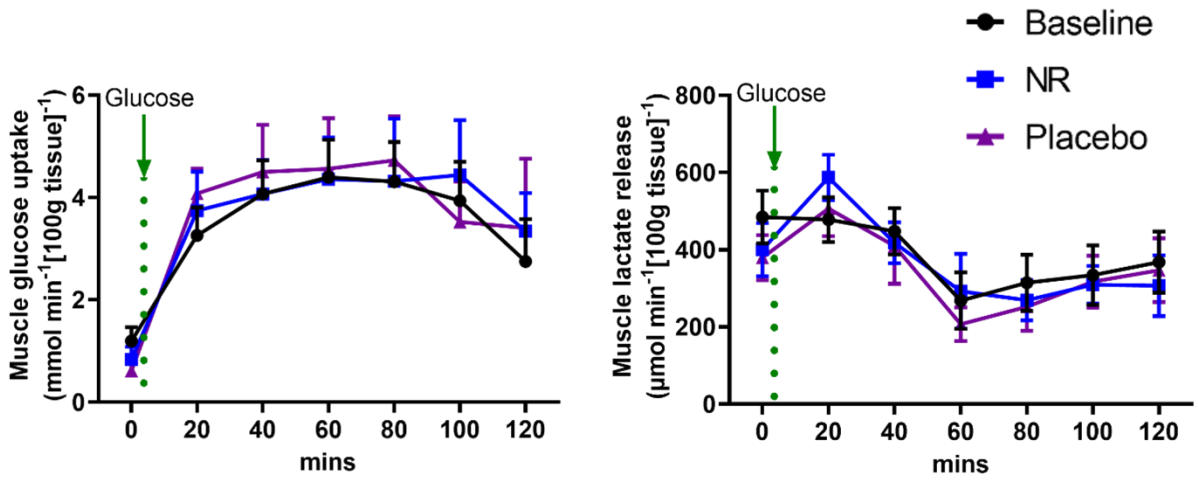

Figure 4.14: Muscle substrate utilisation. Muscle glucose uptake and lactate release at baseline and after NR and placebo. The green line represents the administration of the 75 g of oral glucose load. The absence of significance symbols indicates that there is no statistical significance.

4.2. Discussion

Several preclinical reports highlighted that NR enhanced mitochondrial energy pathways and dynamics in skeletal muscle (56,146) through mechanisms that likely predominantly involve redox and sirtuins activation. High resolution respirometry represents the gold-standard methods for the ex-vivo assessment of mitochondrial function (413). Using this start of the art method, we did not detect any changes in mitochondrial respiration after 3-weeks of NR supplementation in aged men. Mitochondrial content within skeletal muscle is a major quantitative indicator of oxidative capacity; using to readouts, citrate synthase activity and mitochondrial copy number (mtDNA), we also did not detect any NR-mediated differences.

The downregulation of genes linked to energy metabolism (glycolysis, TCA cycle, and mitochondria) is consistent with the report that oral NR depresses mitochondrial membrane potential while improving blood stem cell production in mice (414). The finding of NR-mediated upregulation of the gene ontology categories of cell adhesion, actin cytoskeleton organisation, and cell motility may support a previously reported function for the NAD+-generating enzyme nicotinamide riboside kinase 2b (Nrk2b) in supporting zebrafish skeletal muscle cell adhesion (415).

As the studies in rodents suggested that NAD^+ supplementation can enhance the skeletal muscle physical function (56,146,400), we utilised hand-drip strength as a surrogate marker for improved muscle physical function. Hand-grip strength correlates with leg strength and is a tool in diagnosing sarcopenia and frailty. Hand-grip strength also appears to be a better predictor for clinical outcomes than low muscle mass per se (416). A drop in hand-grip strength starts to be noted in the fourth decade in life when the median peak strength in men is 51 kg of force (417). Of note, a grip strength of less than 30 kg of force in men is considered among the diagnostic criteria of sarcopenia (418). We detected a median hand-grip strength in our participants of 33.8 kg of force, which is consistent with muscle ageing for men in their eighth decade.

We were not able to detect differences in hand-grip strength before and after 3 weeks of NR supplementation. However, it is possible that concomitant training exercise was required to stimulate an improvement in muscle function and increase strength. This was not considered in this study due to the invasive intervention at each clinic visit.

Rodent data reported that NR increased angiogenesis and muscle blood flow (419). Using venous occlusive plethysmography, we could not detect a similar finding in our human cohort. Again, one may argue that a 3-week intervention is not sufficiently long to detect an increase in muscle blood flow.

The forearm muscle substrate utilisation data suggest that the skeletal muscle transcriptomic signature of downregulated mitochondrial and glycolysis genes did not result in functional changes in O2 consumption or CO2 production, or in the glucose uptake or lactate release. One can argue that this could be perceived as reflective of more efficient mitochondria.

Chapter 5: The Effects of Oral NAD+ Supplementation on Human Systemic Metabolic Readouts and Inflammatory Cytokines

Parts of this chapter have been published as:

Nicotinamide Riboside Augments the Aged Human Skeletal Muscle NAD+ Metabolome and Induces Transcriptomic and Anti-inflammatory Signatures

Elhassan YS et al.

Cell Reports. 2019 Aug 13;28(7):1717-1728.e6

DOI: 10.1016/j.celrep.2019.07.043

5.1. Introduction

The previous chapter focussed on skeletal muscle readouts and in this chapter the focus is on the systemic impact of NR supplementation in the clinical study. Preclinical studies have associated NAD+ supplementation with resistance to weight gain, amelioration of cardiometabolic risk, and improvement in metabolic flexibility (420). As NR increased the whole blood NAD+ metabolome, we argued that there was increased NAD+ metabolism in central tissues and aimed to assess for consequent cardiometabolic changes. Two studies—one of 12 weeks of NR supplementation at 2 g/day in subjects with obesity (406), and one of 6 weeks of NR supplementation at 1 g/day in older adults (405) suggested potential benefits with respect to fatty liver and blood pressure, respectively.

5.1.1. Effects of NR on systemic glucose handling

We detected no NR-mediated changes in fasting glucose and insulin and HOMA-IR with or without NR supplementation. Systemic glucose handling was then assessed using an oral glucose tolerance test with no effect of NR measured in glucose levels during the 2-hour test (Figure 5.1).

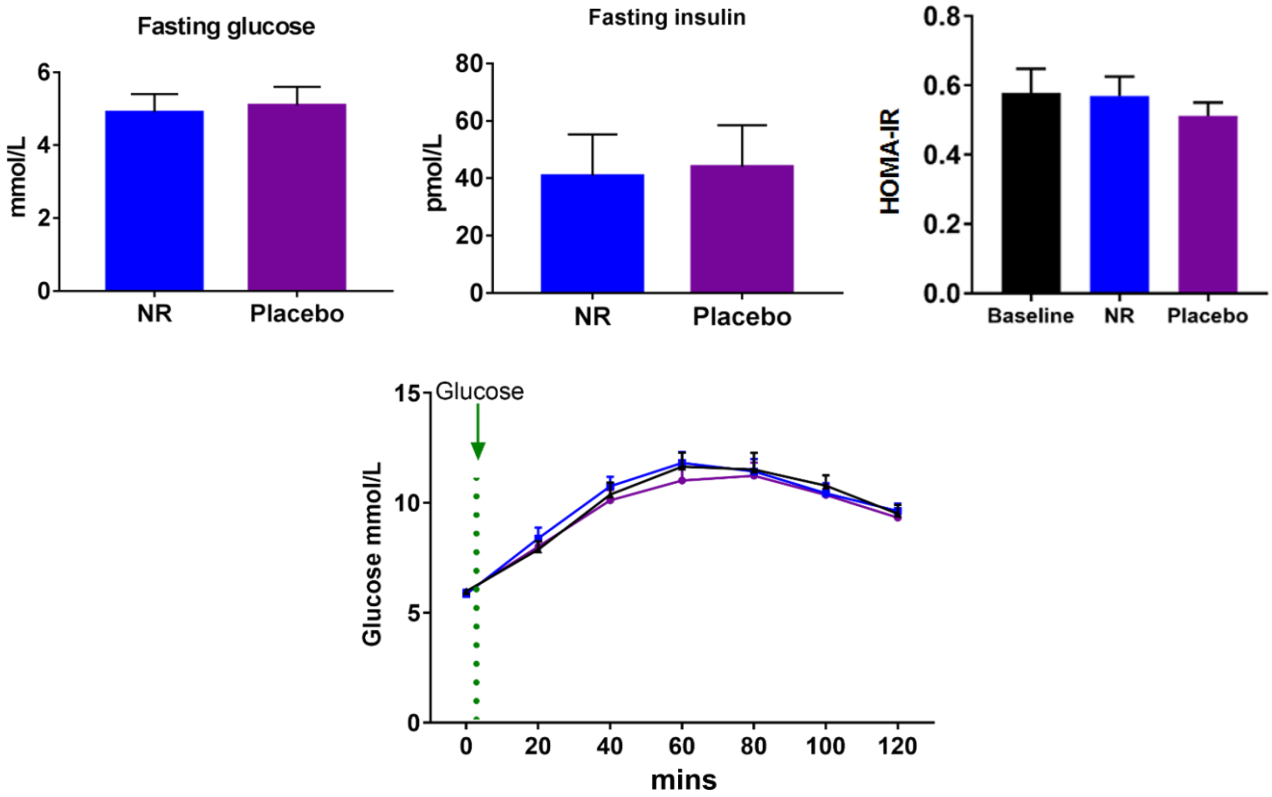

Figure 5.1: Fasting glucose and insulin and HOMA-IR at baseline and after NR and placebo. Glucose tolerance test showing the glucose response at baseline and after NR and placebo. The green dotted line represents when 75 g of oral glucose load was taken. The green line represents the administration of the 75 g of oral glucose load. The absence of significance symbols indicates that there is no statistical significance.

5.1.2. Effects of NR on fatty acid handling

We detected no NR-mediated changes in fasting NEFA levels with or without NR supplementation. Following the oral glucose load and the consequent insulin stimulation, NEFA levels were appropriately suppressed, and we detected no difference in this response between the NR and placebo phases (Figure 5.2).

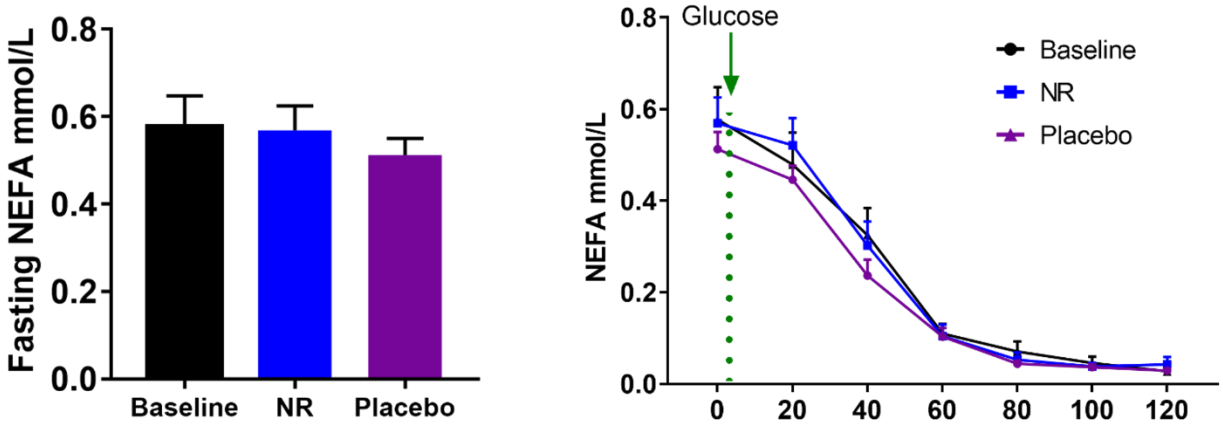

Figure 5.2: Fasting NEFA at baseline and after NR and placebo. Plasma NEFA response in a glucose tolerance test at baseline and after NR and placebo. The green line represents the administration of the 75 g of oral glucose load. The absence of significance symbols indicates a lack of statistical significance.

5.1.3. Effects of NR on metabolic flexibility using indirect calorimetry

We then assessed metabolic flexibility using the gold-standard *in vivo* method, indirect calorimetry. The method was used to derive respiratory exchange ratios (RER; calculated as VCO_2 expired/ VO_2 consumed) as a measure of whole-body metabolic substrate utilisation. Measurements were initiated whilst fasted and then readings were captured during the response to 75 g oral glucose load. The Median fasting RER was appropriate at 0.72 and 0.73 for the NR and placebo periods, respectively ($p = 0.68$). In response to the oral glucose load, the RER values significantly increased indicating an appropriate switch from lipids (during fasting) towards carbohydrates utilisation (fed state); no differences in this response were detected after 3 weeks of NR supplementation observed at baseline and throughout the 2 hours (RER 0.83 and 0.84 for NR and placebo, respectively) (Figure 5.3).

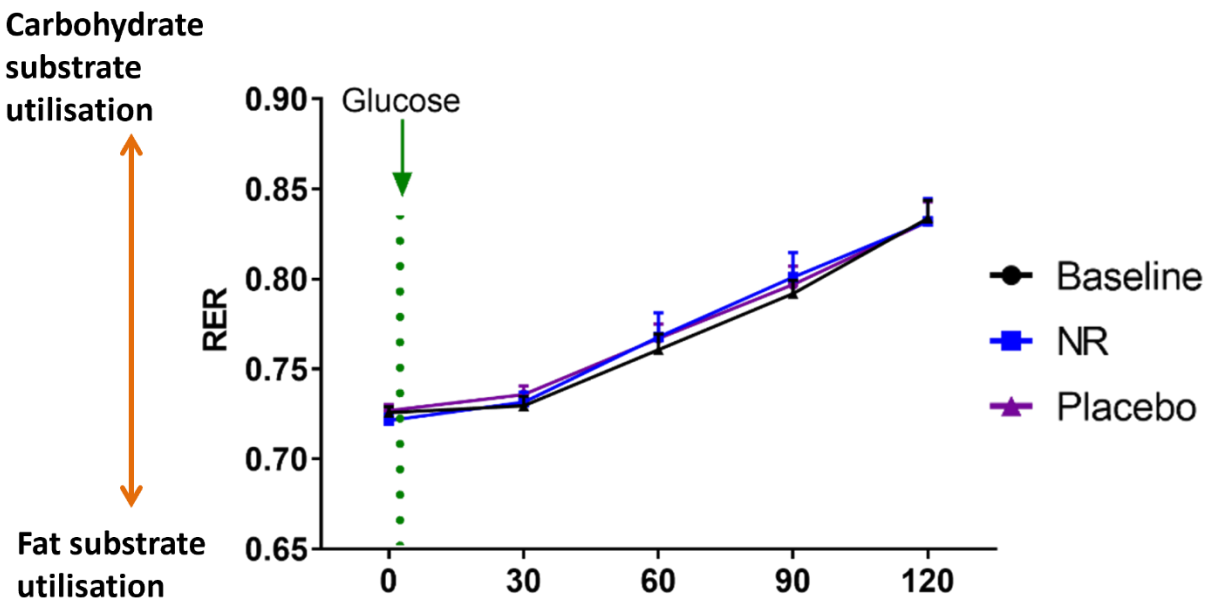

Figure 5.3: Respiratory exchange ratio (RER) at baseline and after NR and the placebo. The green dotted line indicates when 75 g of oral glucose was taken. The green line represents the administration of the 75 g of oral glucose load. The absence of significance symbols indicates that there is no statistical significance.

5.1.4. Effects of NR supplementation on the systemic inflammatory cytokines

We measured multiple inflammatory cytokines ten of which were detectable, i.e. within the assay detection range. NR statistically significantly decreased the levels of the interleukins IL-6, IL-5, and IL-2, and tumour necrosis factor-alpha (TNF-α) compared to baseline. We also found a statistically significant difference in the levels of IL-2 between baseline and placebo, and a lack of a difference in levels of TNF-α between NR and placebo despite the established difference between NR and baseline (Figure 5.4)

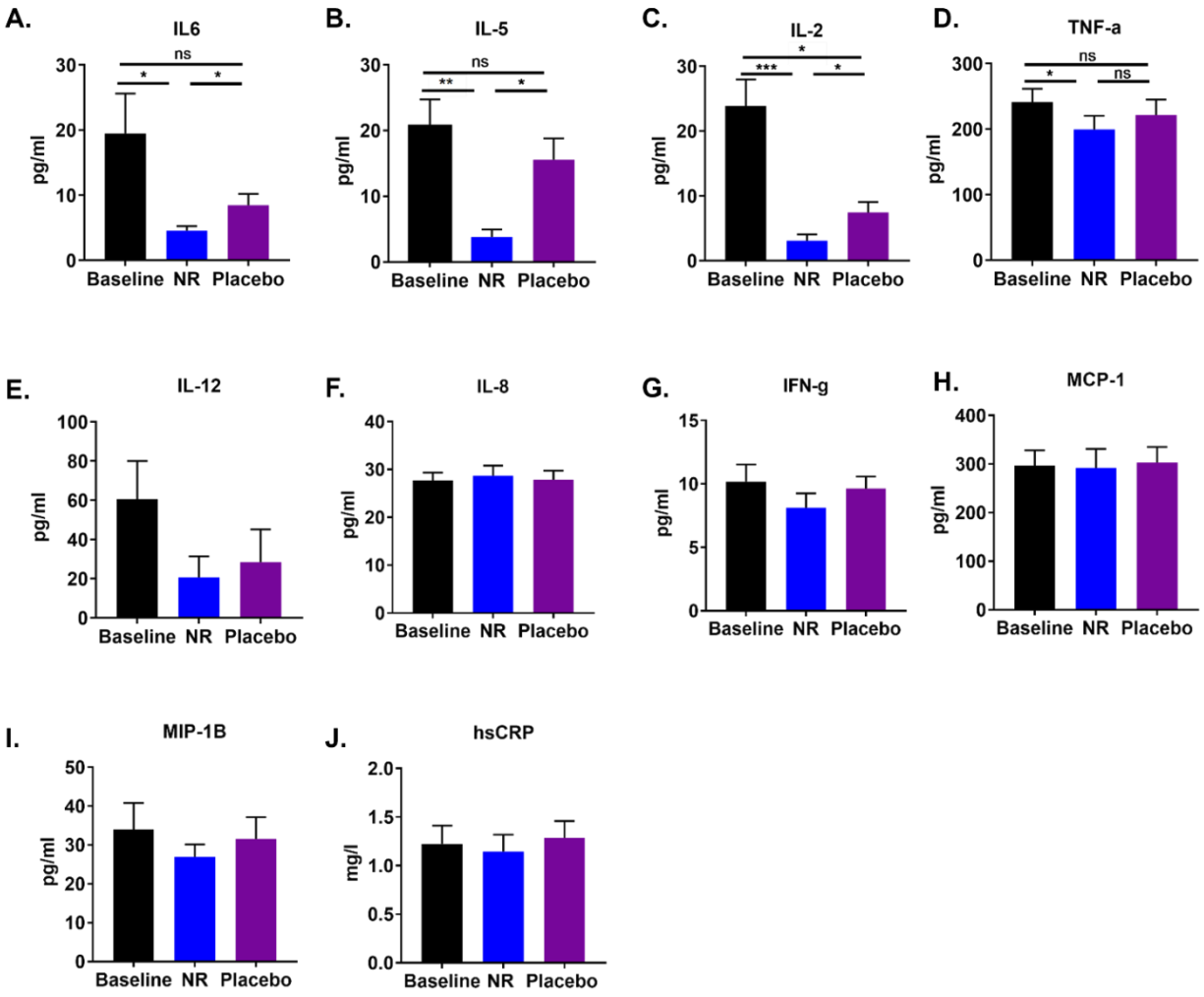

Figure 5.4: NR Supplementation suppresses the circulating levels of inflammatory cytokines. The absence of significance symbols indicates a lack of statistical significance. Significance was set at p <0.05 with * <0.05; ** <0.01; *** <0.001.

To further explore the statistical difference between baseline and placebo in IL-2 and the lack of a difference TNF-α between NR and placebo despite the difference between NR and baseline, we questioned the possibility of a drug carryover effect between the NR and placebo phases. We undertook a period effect analysis in which data where sub-analysed by those who received NR first and then placebo first. We confirmed that the cohort randomised to receive placebo first had no difference in IL-2 between baseline and placebo and there was a detectable difference in TNF-α between NR and placebo (Figure 5.5).

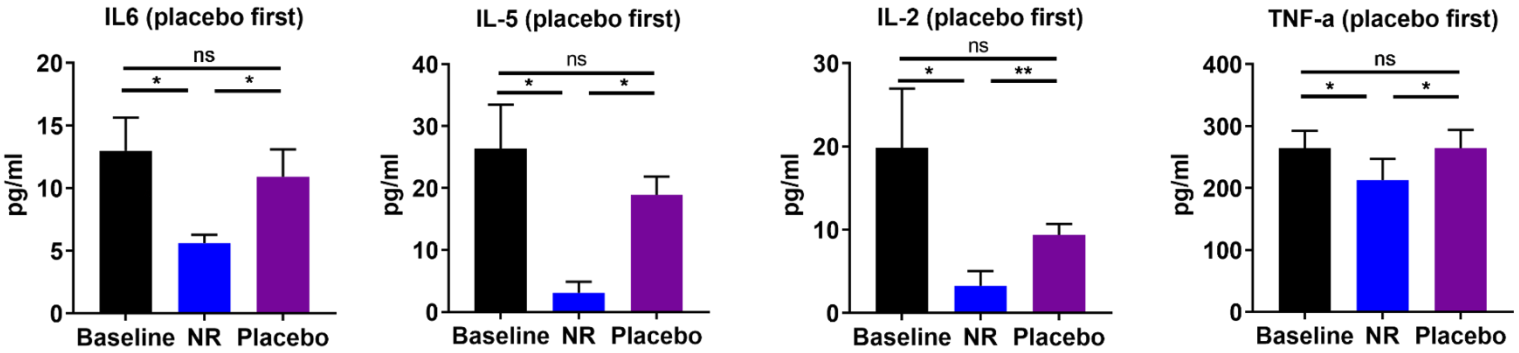

Figure 5.5: Levels of serum inflammatory cytokines at baseline and after each of the NR and placebo phases. Here the period effect analysis is shown, and each panel is produced from only the 6 subjects that were randomised to placebo first as a demonstration of the NR carryover effect, evident in IL-2 and TNF-α. Significance was set at $p < 0.05$ with * <0.05; ** <0.01.

5.2. Discussion

Prior to our study, two studies found potential beneficial effects of NR supplementation on fatty liver (12 weeks of NR 2 g/day in participants with obesity) (406) and blood pressure (6 weeks of NR 1 g/day in older individuals) (405). This led us to assess several cardiometabolic endpoints. Ideally, a hyperinsulinaemic euglycaemic clamp study before and after NR supplementation would have been the more ideal way of assessing for systemic insulin resistance, however, the already highly invasive protocol (involving muscle biopsy, arterial catheterisation and deep venous cannulation) has led to exclude this measure.

A rebound increase in NEFA has previously been reported with the nicotinic acid analogue, acipimox (332), which resulted in decreased insulin sensitivity. However, NR supplementation did not produce a similar outcome in our study.

In the previous chapter, we reported that there was no difference in the muscle-specific O2 consumption or CO2 production with or without NR supplementation. In this chapter, we assessed this at a systemic level using indirect calorimetry which is considered the gold standard method to determine energy expenditure. We combined this method with assessment during fasting and on OGTT to assess the metabolic flexibility, which is the ability of the mitochondrial machinery to switch freely between alternative fuels (glucose or fat) depending on the physiological and nutritional circumstances (295). Our data demonstrated a normal physiological response with the RER rising after the glucose load (indicating a switch from fatty oxidation to glucose oxidation (glycolysis). No changes in RER were detected during fasting or OGTT with or without NR supplementation which mirrors the muscle specific readout of tissue substrate utilisation.

Chronic inflammation has consistently been regarded as a common feature in human ageing, even in those subjects who are apparently healthy (273). This has been strongly linked to the age-related disturbance in metabolic homeostasis (274). As an exploratory outcome in the NADMet study, we hypothesised that NR supplementation may suppress the circulating levels of

inflammatory cytokines. Indeed, for the first time in humans, we established that key inflammatory cytokines, such as IL-6, were suppressed following NR supplementation. It is worthwhile highlighting that IL-6 is a skeletal muscle myokine secreted in response to exercise and metabolic alterations (421). Therefore, it is reasonable to question whether the NR-mediated IL-6 suppression is beneficial. This exploratory assessment in the study paves the path for future studies to validate the finding in larger cohorts and explore mechanistic insights by employing in vitro and in vivo studies addressing the interaction between NAD+ and key inflammatory cells, such as macrophages. It will be interesting to further investigate depressed IL-6, IL-5, IL-2 and TNF-α as biomarkers and/or mediators of oral NR in rodent models and humans. Of note, some preclinical studies have suggested that NR reduced macrophage infiltration in diseased muscle (399,422) and supressed plasma TNF-alpha in fatty liver disease (356). Another point to consider is that the expression of the NAD+-consuming enzyme CD38 increases in inflammatory cells during inflammation (423), as well as in the blood of aged humans (424). Supplementing NAD+ in this context may be a mechanism mediating the NR-induced anti-inflammatory effects.

Chapter 6: NAD+ Availability and 11β-Hydroxysteroid Dehydrogenase type-1 Mediated Glucocorticoid Regeneration in Skeletal Muscle Cells

6.1. Introduction

This chapter studied a fundamental aspect of NAD+ biology that is poorly understood, namely the existence of ER-cytosol pyridine nucleotide cross talk. Firstly, I investigated the capacity of FK866 and NR to modulate the level of NAD+ and NADH in the cytosol. Secondly, I examined the impact of NAD+ and NADH manipulation on the oxoreductase activity of 11β-HSD1 enzyme as a readout of ER pyridine nucleotide availability. Thirdly, I examined the effect of NAD+ manipulation on the 11β-HSD1 dehydrogenase activity in the cell model of H6PDH Knock out. Finally, I examined the generalisability of 11β-HSD1 modulation by FK866 and NR in C2C12 cell and primary mouse myotubes.

The NADP/H-H6PDH-11β-HSD1 pathway links nutrients and hormones together and the relevance of this work is two-fold. First, 11β-HSD1 can be purely regarded as a readout for the SR pyridine nucleotide status. Second, this pathway raises the possibility whether lowering NAD+ results in biological implications akin to those observed in H6PD KO mice (374).

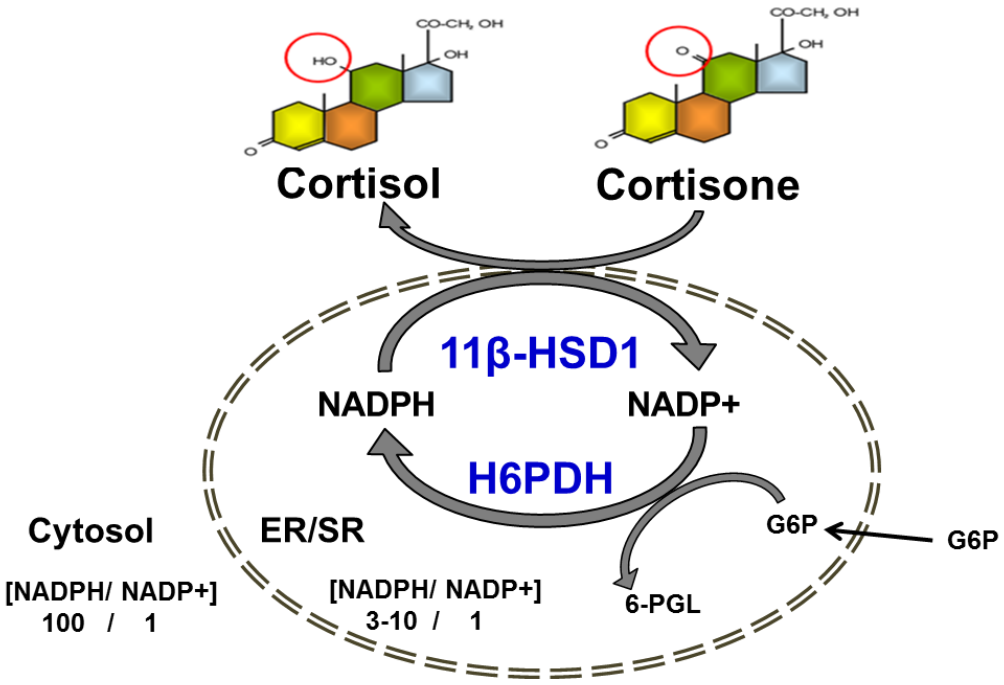

1 Figure 6.1: Schematic representation of the interaction between H6PDH and 11β-HSD1 within the SR. H6PDH generates NADPH by conversion of glucose-6-phosphate (G6P) to 6-phosphogluconate (6PG) within the ER. 11β-HSD1 uses the NADPH as cofactor, allowing the conversion of cortisone to cortisol.

6.2. Hypothesis, Aims and Objectives

Hypothesis: Modulating skeletal muscle cytosolic NAD(P)(H) impacts upon the SR nucleotide pool and 11β-HSD1 activity can be used as a read-out.

Aim: Determine the maintenance of the SR pyridine nucleotide pool that support the 11β-HSD1 activity in skeletal muscle.

Objective: 11β-HSD1 is a key enzyme in the development of Cushing's syndrome phenotype and is implicated in the pathogenesis of obesity, insulin resistance, and type II diabetes(377,425). Defining the redox level of the regulation of 11β-HSD1 in skeletal muscle will help us investigate whether there is crosstalk between the SR and cytosolic NAD(P)(H) pools.

The methods used in this chapter, including cell culture, NR and FK866 treatment, cell viability assessment, and enzymatic activity assays are detailed in Chapter 2.

6.3. Results

6.3.1. Effects of NR and FK866 on NAD+ content in C2C12 cells

As expected, the NAD/H content in C2C12 myotubes was increased after 48 hours treatment with the NAD+ precursor, NR. Conversely, NAMPT inhibition with FK866 for 48 hours markedly decreased the NAD+ level. Co-administration of NR with FK866 rescued the NAD+ levels by bypassing the NAMPT inhibition (Figure 6.2).

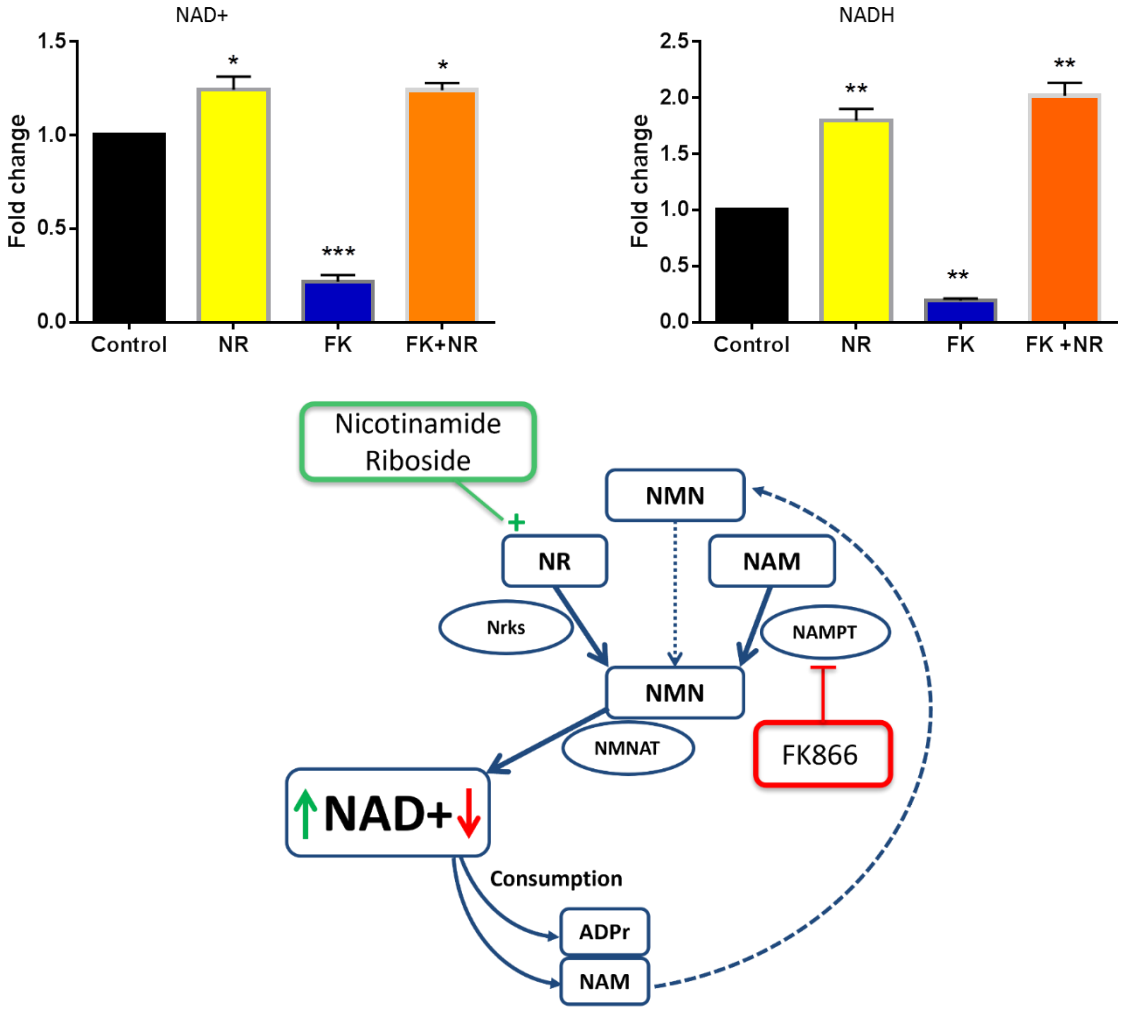

Figure 6.2: Manipulating NAD+ using NR and FK866. NAD+ and NADH levels in differentiated C2C12 myotubes. Control (untreated), NR (Nicotinamide Riboside (NR); 0.5mM; 48hours), FK866 (NAMPT inhibitor; 100nmol; 48hours) and FK866+NR (48hours). Significance was set at $p < 0.05$ with * <0.05; ** <0.01. Bottom figure is a reminder of the NAD+ biosynthesis salvage pathways showing the effects of FK866 and NR.

I then assessed the effects of FK866 and NR on the gene expression of key enzymes in the NAD+ synthesis pathway and demonstrated upregulation of NAMPT with downregulation of the Nrks 1 and 2 (Figure 6.3).

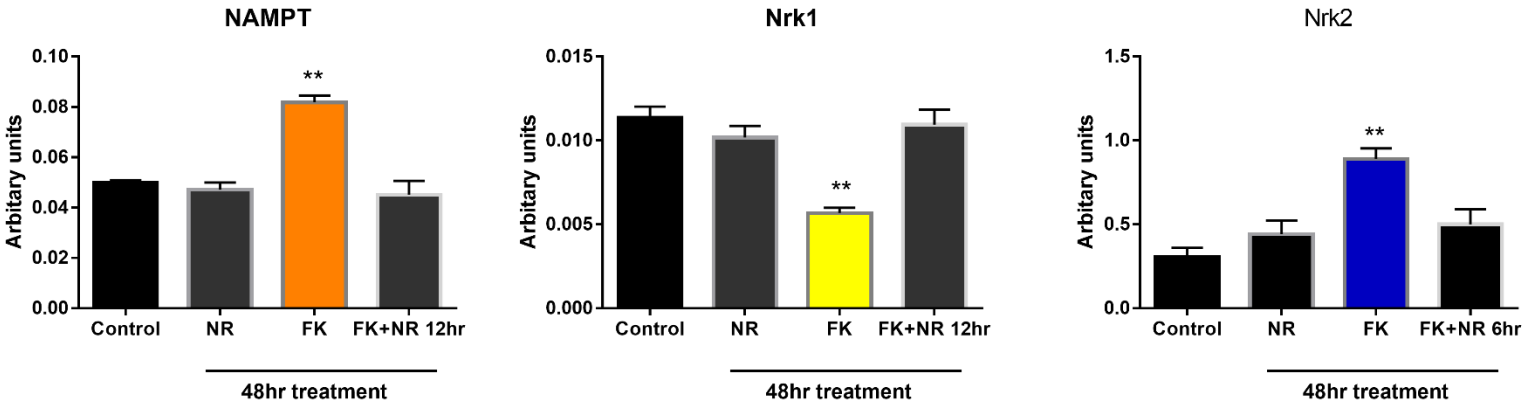

Figure 6.3: Effects of NAD+ modulation on the expression levels of NAMPT (rate-limiting enzyme in NAD+-biosynthesis) and Nrk1 and Nrk2 of the NRK salvage pathway. Significance was set at $p < 0.05$ with * <0.05; ** <0.01.

6.3.2. Effects of FK866 inhibition on C2C12 cell viability and apoptosis

As NAD+ is a cofactor for cellular reactions and a consumed substrate for essential cell signalling reaction, the question was whether limiting NAD+ causes cell death. Therefore, I assessed cell viability and apoptosis at different durations of NAD+ depletion. The data show that cells are viable at 48hours of FK866 treatment, but beyond that, viability is reduced with increased apoptosis enzymes. Therefore, no experiments included more than 48 hours of FK866 treatment (Figure 6.4).

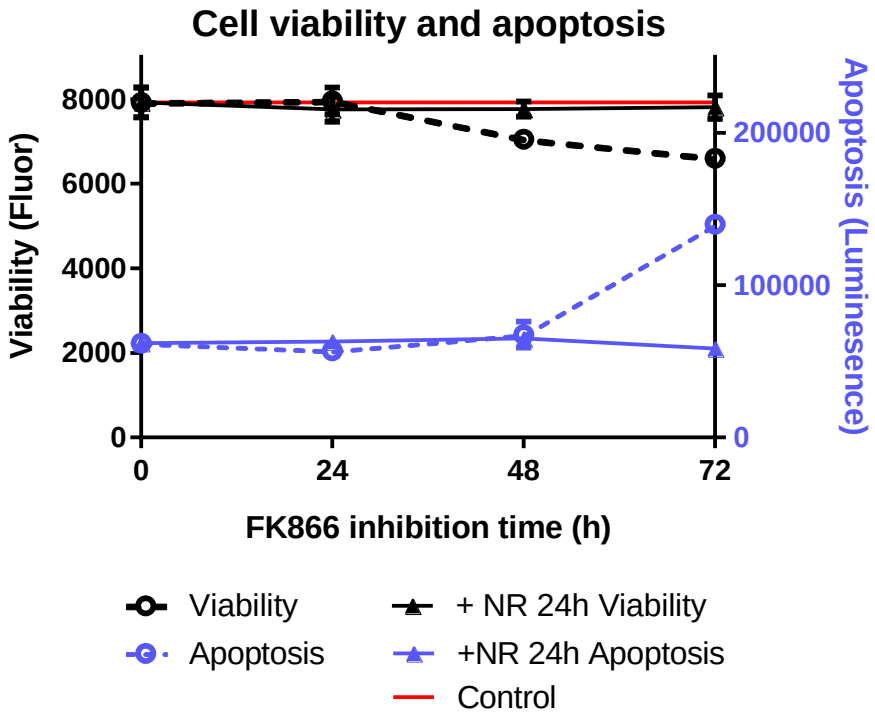

Figure 6.4: C2C12 viability and apoptosis with FK866 and NR. Viability and apoptosis in differentiated C2C12 myotubes. Red solid line: control (untreated), Dotted lines (black is viability; blue is apoptosis): FK866 100nmol for 24, 48 and 72hours, and Solid lines (black is viability; blue is apoptosis): NR 0.5nmol for 24, 48 and 72hours.

Although C2C12 cells were viable at 48hours, clearly NAD+ depletion enhanced the expression of genes implicated in muscle cell stress response and atrophy and decreased the expression of muscle differentiation genes. All effects were reversed with the administration of NR (Figure 6.5).

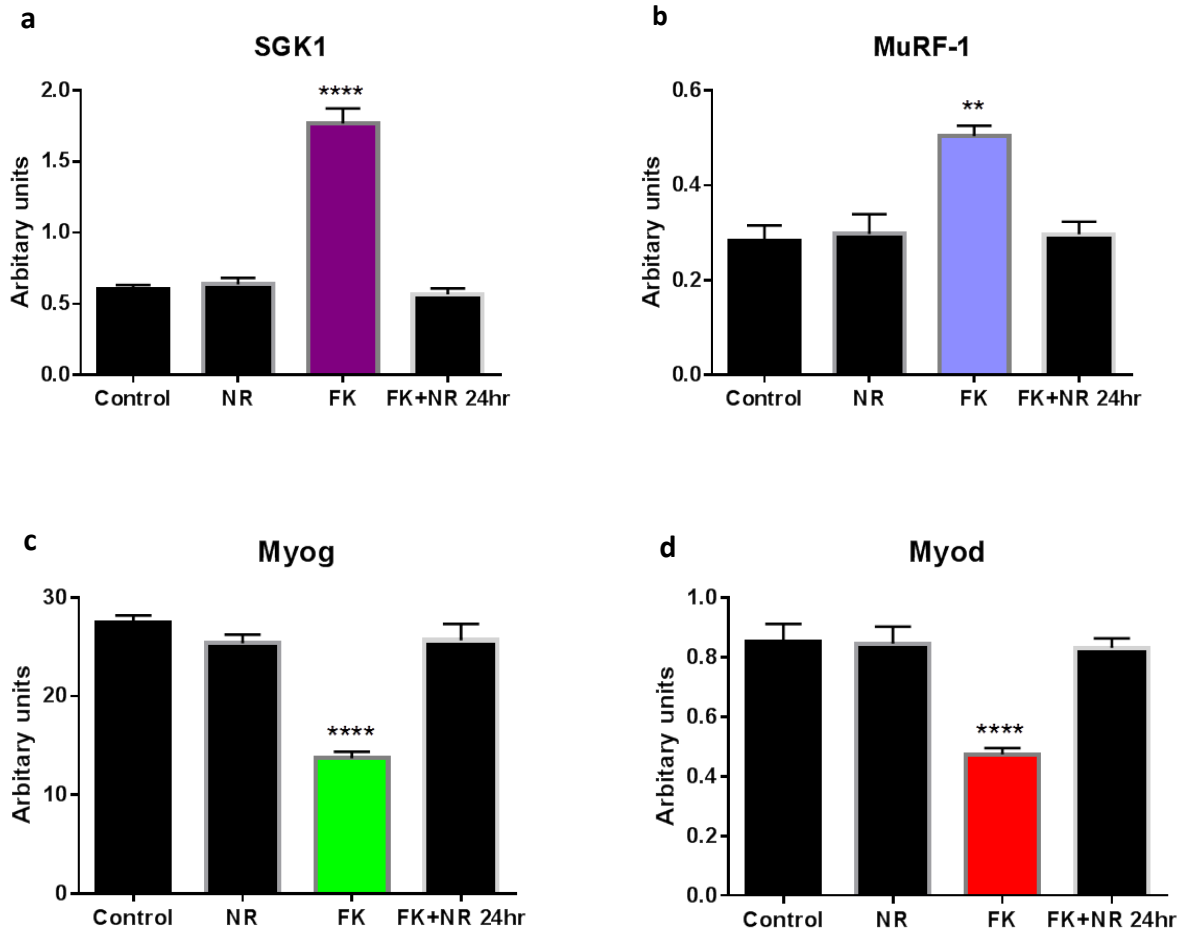

Figure 6.5: Effects of NAD+ modulation on cell stress response, atrophy, and differentiation. Gene expression in differentiated C2C12 myotubes expressed as arbitrary units. Control (untreated), NR (0.5mM; 48hours), FK866 (100nmol; 48hours) and FK866+NR (48hours). a) SGK1 plays an important role in cellular stress response and is involved in the regulation of cell survival, b) MuRF-1 plays an important role in the atrophy of skeletal muscle, are c) Myog and d) Myod play important roles in muscle cell differentiation. Significance was set at $p < 0.05$ with * <0.05; ** <0.01; *** <0.001; **** <0.0001.

6.3.3. Effects of NAD+ modulation on 11β-HSD1 activity in C2C12 myotubes

I then tested the hypothesis that NAD+ manipulation impacts upon 11β-HSD1 activity. No changes were observed with 24hours treatment; however, 48hours of FK866 treatment markedly

decreased 11β-HSD1 activity. Interestingly NR co-administered with FK866 rescued the 11β-HSD1 activity. NR treatment did not increase 11β-HSD1 activity above control cells (Figure 6.6).

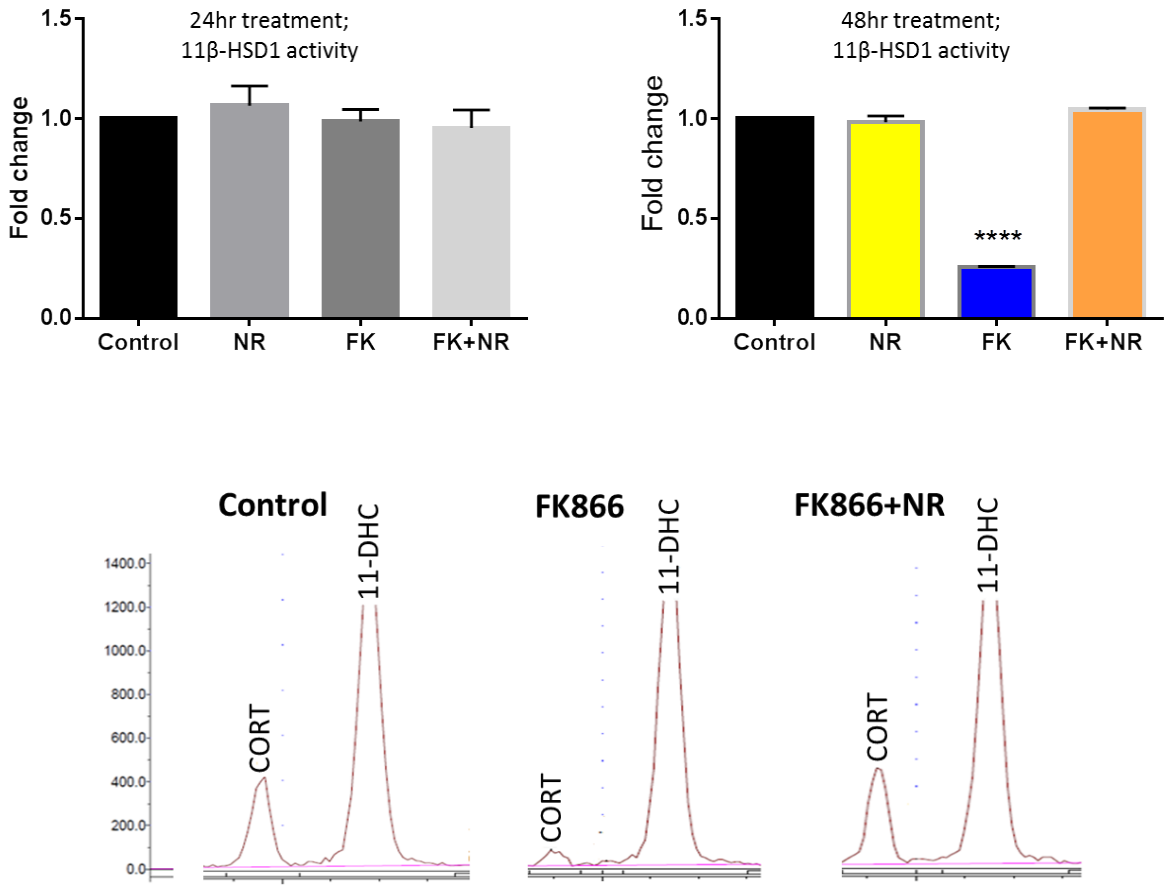

Figure 6.6: Effects of NAD+ modulation on 11β-HSD1 activity. 11β-HSD1 activity in differentiated C2C12 myotubes expressed as fold change. Control (untreated), FK866 (100nmol; a) 24hours, b) 48hours) and FK866+NR (48hours; a) 24hours, b) 48hours). Significance was set at p <0.05 with * <0.05; ** <0.01; *** <0.001; **** <0.0001. c) Representative Bioscan tracers of tritiated steroids for the 48hours experiment.

As it took >24hours of FK866 treatment (NAD+ depletion) to impact upon 11β-HSD1 activity, I went to ascertain the time required to rescue the enzymatic activity following NR treatment (NAD+ repletion). Interestingly as short as 30min NR treatment was sufficient to rescue the 11β-HSD1

activity, with full restoration of the enzymatic activity by 24hours. This corresponded to the rescue of NAD+ levels (Figure 6.7).

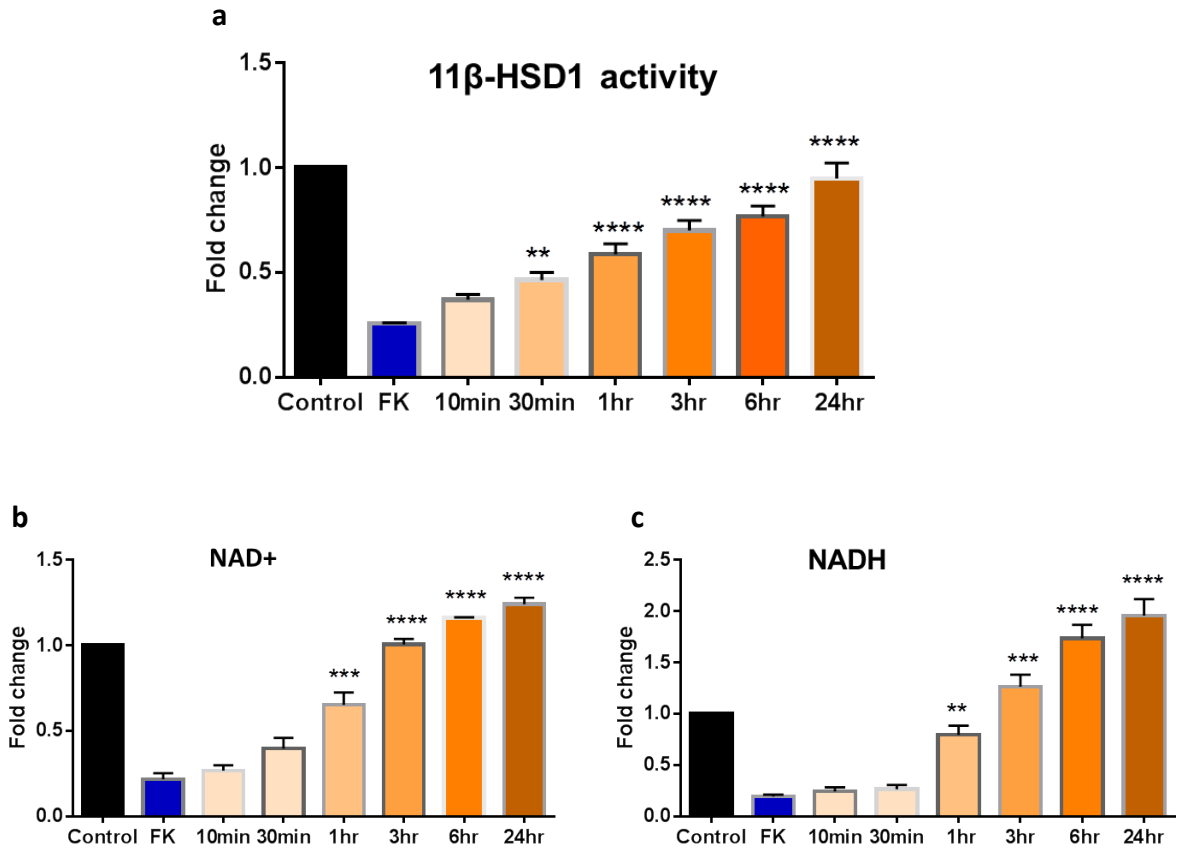

Figure 6.7: Time course of 11β-HSD1 activity and NAD+ levels rescue. a) 11β-HSD1 activity, b) NAD+ levels and c) NADH levels in differentiated C2C12 myotubes expressed as fold change. Control (untreated), FK866 (100nmol; 48hours) and FK866 (100nmol; 48 hours) + NR (0.5mM; added last 10min, 30min, 1hour, 3hr, 6hr and 24hr of the 48hour experiment). Significance was set at $p < 0.05$ with * <0.05; ** <0.01; *** <0.001; **** <0.0001

I then assessed the effects of NR and FK866 on the gene expression and protein level of 11β-HSD1 and H6PDH (Figure 6.8).

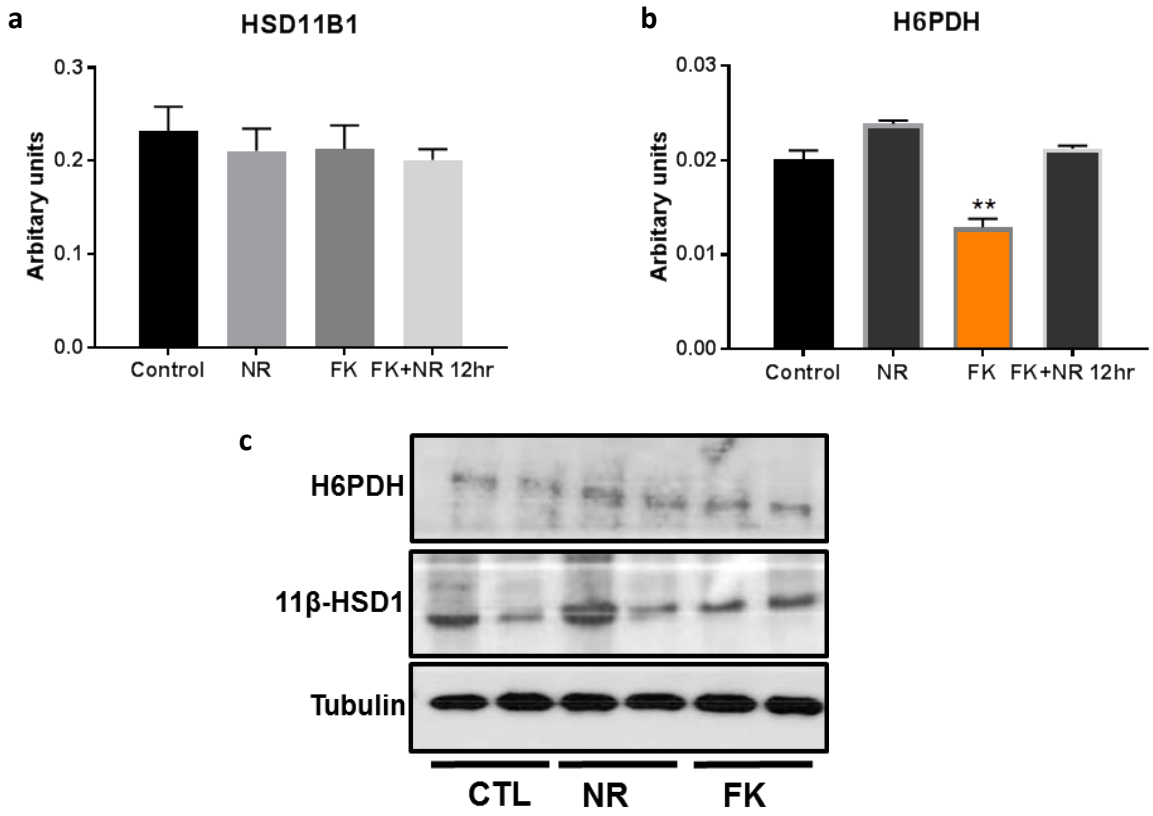

Figure 6.8: Enzymatic gene expression and immunoblotting. a) HS11B1 and b) H6PDH gene expression in differentiated C2C12 myotubes expressed as arbitrary units. Control (untreated), NR (0.5mM; 48hours), FK866 (100nmol; 48hours) and FK866 (100nmol; 48hours) + NR (0.5Mm; added the last 12 hours of the 48hour experiment). Significance was set at $p < 0.05$ with * <0.05; ** <0.01. c) H6PDH and 11β-HSD1 Western Blots in differentiated C2C12 myotubes. Control (untreated), NR (0.5mM; 48hours) and FK866 (100nmol; 48hours).

6.3.4. Effects of NAD+ modulation on 11β-HSD1 activity in primary mouse skeletal muscle cells

NR and FK866 treatments were added to primary wild type mouse myotubes. As in C2C12 myotubes, 48 hours of FK866 treatment markedly decreased 11β-HSD1 activity which was rescued by the concomitant administration of NR. As short as 30 minutes of NR supplementation was sufficient to rescue the 11β-HSD1 activity (Figure 6.9).

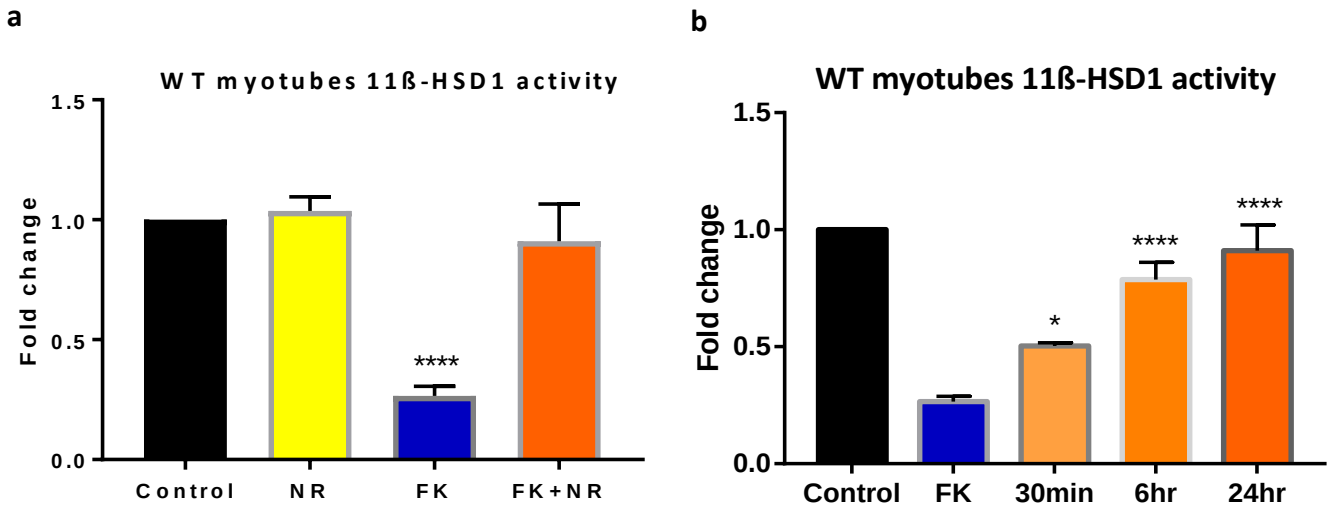

Figure 6.9: Effects of FK866 and NR on 11β-HSD1 activity WT mouse myotubes. a) 11β-HSD1 activity expressed as fold change. Control (untreated), NR (0.5Mm; 48hrs), FK866 (100nmol; 48hours) and FK866+NR (48hours). b) 11β-HSD1 activity expressed as fold change. Control (untreated), FK866 (100nmol; 48hours) and FK866 (100nmol; 48hours) + NR (0.5mM; added last 30min, 6hr and 24hr of the 48hour experiment). Significance was set at p <0.05 *with * <0.05; ** <0.01; *** <0.001; **** <0.0001.*

6.3.5. Effects of NAD+ modulation on 11β-HSD1 activity in H6PDH knock out mouse model

I then turned to the H6PDH KO mouse model. In this model, I confirmed that 11β-HSD1 assumes a dehydrogenase activity inactivating glucocorticoids; a process that is NADP+ dependant i.e. independent of G6P (Figure 6.10).

a b

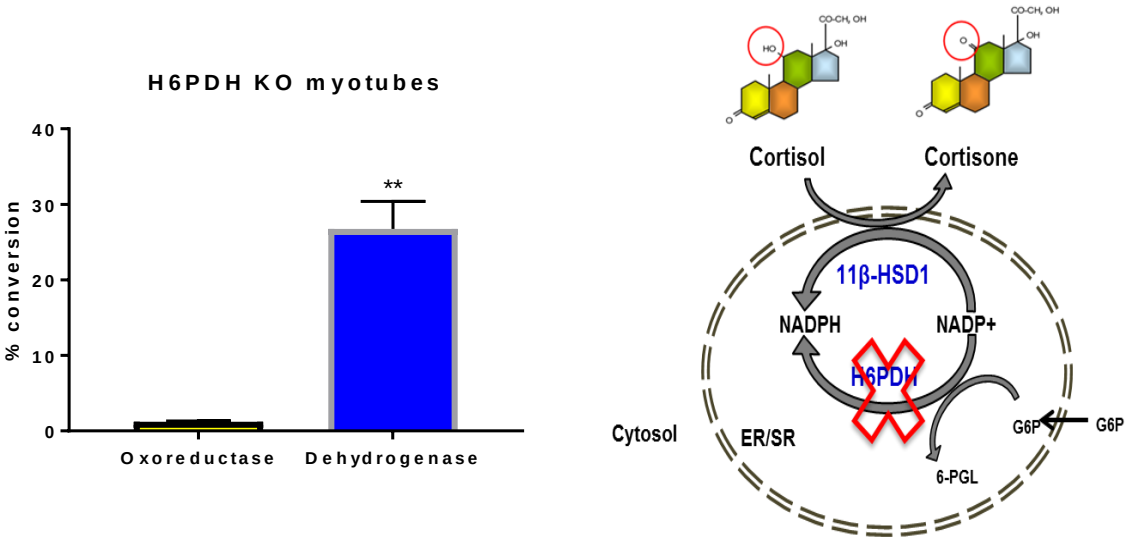

Figure 6.10: 11β-HSD1 activity in H6PDH KO mouse myotubes. a) 11β-HSD1 assumes a dehydrogenase activity inactivating corticosterone (cortisol in humans) to 11-dehydrocortiscosterone (cortisone in humans). b) Diagram explaining the 11β-HSD1 dehydrogenase activity in H6PDH KO mouse myotubes. Steroids inactivation is NADP+ dependant i.e. independent of G6P. Significance was set at $p < 0.05$ with * <0.05; ** <0.01.

NAD+ modulation using FK866 and NR also affected 11β-HSD1 dehydrogenase activity as before, reflecting the changes in the ER NADP+ pool (Figure 6.11).

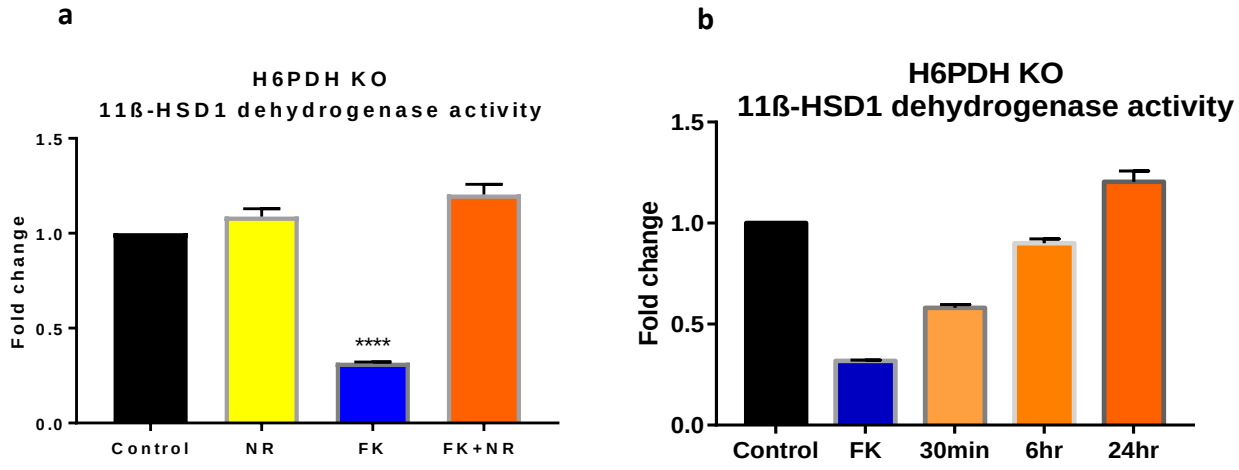

Figure 6.11: Effects of FK866 and NR on 11β-HSD1 dehydrogenase activity in H6PDH KO mouse myotubes. a) 11β-HSD1 dehydrogenase activity expressed as fold change. Control (untreated), NR (0.5Mm; 48hrs), FK866 (100nmol; 48hours) and FK866+NR (48hours). b) 11β-HSD1 activity expressed as fold change. Control (untreated), FK866 (100nmol; 48hours) and FK866 (100nmol; 48hours) + NR (0.5mM; added last 30min, 6hr and 24hr of the 48hour experiment). Significance was set at p <0.05 with * <0.05; ** <0.01; *** <0.001; **** <0.0001.

6.4. Discussion

These data suggest a novel level of regulated glucocorticoid metabolism in skeletal muscle whereby 11β-HSD1 activity can be influenced by cellular redox status and NAD+ levels beyond the SR.

The existence of a crosstalk between the cytosolic and SR pyridine nucleotide pools has been a subject of long debate. These data show that reducing cytosolic NAD+ (using FK866), markedly reduces 11β-HSD1 activity, whereas NAD+ repletion (using NR) rescues 11β-HSD1 activity. This supports that there is crosstalk between the SR and cytosolic NAD(P)(H) pools.

In contrast to other cellular organelles, very little is known about the maintenance of SR pyridine nucleotide pool. The nuclear nucleotide content is similar to that in the cytosolic compartment due to the nuclear membrane permeability to the pyridine nucleotides (426). The mitochondrial pyridine nucleotide pool is distinct from the cytosol (427) but there are biochemical shuttling systems, such as the malate-aspartate shuttle, that supply NADH to the mitochondria(361).

When liver microsomes with intact membranes were incubated with NADPH for 60mins, this led to a significant increase in the activity of intraluminal 11β-HSD1 activity(373). This suggests that the microsomal membrane is not completely impermeable to the pyridine nucleotides. Furthermore in the same study, inhibition of the cytosolic pentose phosphate pathway in intact rodent adipocytes [using Dehydroepiandrostenedione (DHEA) and Norepinephrine (NE)] inhibited the 11β-HSD1 activity(373). Interestingly the same observation could not be replicated in liver microsomes. Conversely, G6P did not stimulate 11β-HSD1 activity in intact adipocytes but this was achieved in liver microsomes(373). These puzzling data suggest that the cytosolic pentose phosphate pathway modifies 11β-HSD1 activity in intact cells. However, in liver microsomes, it appears that G6P modifies the 11β-HSD1 activity and in addition, somehow, NADPH enters the SR and supports 11β-HSD1 activity. Lavery et al have shown that the SR NADPH level is primarily sustained by the coordinated action of the G6P and the luminal H6PDH. This is

supported by their report that in H6PDH knockout mice, 11β-HSD1 oxoreductase activity is lost and the enzyme confers dehydrogenase activity(382).

The data in mouse skeletal muscle cells show that limiting cytosolic NAD+ via FK866 reduced 11β-HSD1 activity. Tan et al showed that NAMPT inhibition, using FK866, attenuated glycolysis at the level of glyceraldehyde 3-phosphate dehydrogenase and promoted carbon overflow into the pentose phosphate pathway with accumulation of G6P(58). Applying this to my data, the supposed increase in G6P did not prevent 11β-HSD1 inhibition.

Upon the deletion of H6PDH, mice were unable to convert 11-DHC to CORT but rather assumed a dehydrogenase activity inactivating CORT to 11-DHC in liver microsomes(428). Despite the abolished 11β-HSD1 oxoreductase activity by limiting NAD+, no dehydrogenase activity was detected suggesting that 11β-HSD1 still had access to nucleotides that maintained the directionality of the enzyme. This contrast to the report that not only H6PDH knock out lose 11β-HSD1 reductase activity

Treatment with FK866 for 24 hours did not impact upon 11β-HSD1 activity. However more chronic NAD+ depletion with 48hours FK866 was required to decrease 11β-HSD1 activity. Our laboratory data showed that 24 hours FK866 significantly reduces NAD+, but it appears it takes more time for this depleted NAD+ to reflect upon 11β-HSD1 activity. Despite a reduced expression of H6PDH, the level of protein is unchanged with 48hours FK866 treatment. The FK866 dose used was relatively high, however, I was able to confirm that the FK866-treated cells remained viable at 48 hours of treatment. The NR dose used, 0.5Mm, in the mouse models cannot be directly compared to the NR dose used in the human study (Chapters 3-5). However, this dose increased NAD+ in myotubes and induced clear transcriptomic changes.

Regarding how exactly this cytosol-SR nucleotide communication occurs, it is possible that there is a nucleotide shuttling system, similar to the mitochondrial malate-aspartate shuttle, which

provides NADPH for the 11β-HSD1 activity. Another possibility is whether there is a luminal NAD+ kinase that provides NADP+ to the SR. As lowering NAD+ inhibits the NADP-dependant 11β-HSD1 dehydrogenase activity, this suggests a G6P-independent process and supports nucleotide entry into the ER either directly or via a nucleotide transport shuttle.

Chapter 7: Final Conclusions and Future Directions

NR has garnered significant interest in recent years due to its potential to increase cellular NAD+ levels and promote the concept of healthy ageing. Numerous preclinical studies have assessed the impact of NAD+ supplementation via NR on animal and cell line models. These studies showed promise, with NR improving various metabolic parameters and preventing skeletal muscle decline (429). Leading to the study undertaken in this thesis, the NR supplementation studies in humans have focused on cardiovascular (405), systemic metabolic (406), exercise (430), and safety (407) parameters. Martens NR found that 6 weeks of NR supplementation in middle-aged adults reduced blood pressure and the carotid-femoral pulse wave velocity as surrogate of aortic stiffness (405). Dollerup et al reported that 12 weeks of NR supplementation did not not improve insulin sensitivity (assessed using hyperinsulinaemic euglycaemic clamp studies) and whole-body glucose metabolism individuals with obesity (406). None of these studies focussed on ageing, metabolomic changes in tissues, or skeletal muscle responses in terms of metabolism and function. Specifically, research was lacking in key areas including how well NR reaches human skeletal muscle after being orally ingested, and whether NR induces any favourable changes in skeletal muscle and systemic metabolism.

This experimental medicine study investigated the safety and effects of NR supplements in older men. The healthy aged men tolerated oral NR very well over 21 days, and led to increased levels of NAD+ metabolome in whole blood, confirming findings from previous studies (204,405).

For the first time, we showed that oral NR increases the skeletal muscle NAD+ metabolome (NAAD, MeNAM, Me-4-py, and Me-2-py), without increasing NAD+ or NAM. Previously it was reported that NAAD is a more sensitive marker of increased NAD+ metabolism than NAD per se (204). This contrasts to previous mouse studies showing that oral NR increases NAD+ in cardiac and skeletal muscle (56,402), with a suggestion that the beneficial effects of NR are mediated via increased NAM (404). Of note, genetic mouse model studies have established that oral NR is able to restore NAD+ in muscle despite loss of NAM salvage (56,402).

Previous studies including by our research group clearly showed that in mouse skeletal muscle, NR requires Nrk acitivity (189,190). It remains unknown whether this is also the case in human skeletal muscle.

The marked NR-mediated increase in MeNAM in this study is interesting as it has previously been associated with dysglycaemia and insulin resistance (431,432). We have not detected any unfavourable metabolic readouts as a result of NR supplementation in this study.

Considering that MeNAM, Me-4-py, and Me-2-py are NAM excretory products, one can speculate that their abundance as a result of NR supplementation reflects an underlying NAD+ sufficiency and may also explain the unchanged mitochondrial, physiological, and cardiometabolic readouts. This challenges the notion that low NAD+ is prevalent in ageing and strongly contributes to the ageing phenotype (271,346,433,434). However, recruited participants were very healthy for age and they may not be a true representation of this cohort. It is also possible that a second hit during ageing may explain the association between ageing and disturbed NAD+ metabolism. This second hit may be physical inactivity leading to metabolic stress, presence of pre-existing cardiometabolic illness, or chronic inflammation all of which may contribute to NAMPT downregulation (274,398), and activation of the NAD+ consumer CD38 (128,435). The lack of beneficial NR mediated effects suggest that more studies are needed to better understand the NAD+ metabolism in human ageing.

We aimed to assess functional skeletal muscle readouts before and after NR supplementation. Given the invasiveness and the complex interventions during each study visit, we were only able to assess the hand-grip strength. No increase in the grip strength was detected after NR. However, it is important to consider that an increase in muscle strength would not be spontaneous without associated muscle training alongside NR supplementation.

Our data showed downregulation of gene sets relevant in glycolysis and mitochondrial function. However, we did not detect any changes in mitochondrial respiration, citrate synthase activity, and mitochondrial copy number. One can speculate that that unaltered mitochondrial functional

readouts despite the transcriptomic downregulation could be perceived as evidence of more efficient mitochondria and stress-resilience. Indeed, the downregulation of mitochondrial energy-generating processes has been observed with caloric restriction (436–438).

These data also raise the possibility a potential role of NAD+ in the maintenance of skeletal muscle architecture. The signal comes from our finding of NR-induced upregulation of genes involved in actin filament-based process, cell motility, and biological cell adhesion. This is further supported by preclinical studies showing a beneficial effect of increased NAD+ on muscle structural proteins (56,399,422). The potential for NAD+-mediated ADP-ribosylation of integrin receptors within muscle cell membranes has been implicated in facilitating integrin-laminin binding and inducing paxillin mobilisation to adhesion complexes (415,439).

Our work is the first to show in humans that NR supplementation supressed the levels of key inflammatory cytokines in the blood. As chronic inflammation appears to be a hallmark feature of ageing (273), the use of NR in various chronic inflammatory conditions is an interesting avenue for further future investigation.

Despite the encouraging preclinical data, the research on NR in humans is still in its early stages. Future studies should focus on robust clinical trials with specific disease endpoints and larger participant numbers. These trials should meticulously control for confounding variables like diet and lifestyle to delineate the NR-specific effects. The longest reported NR supplementation study period in humans to-date is 3 months (406). Long term safety profile data of NR supplementation are still required. Of note, some ongoing clinical trials are pursing 6-12 months NR supplementation strategies (clinicaltrials.gov as NCT05561738). Exploring NR's efficacy in combination with lifestyle modifications (e.g. exercise) could also be valuable. The future studies should more specifically address the following areas:

- Baseline NAD+ Levels: perhaps before jumping into supplementing NAD+ in humans, it is likely that NR's effectiveness hinges on a person's baseline NAD+ levels. Individuals with severely depleted NAD+ stores might exhibit a better response to NR

supplementation compared to those with relatively “healthy” NAD+ levels. Future research could explore personalised dosing strategies based on individual NAD+ status. More data are needed to define optimal NAD+ levels in humans including in the various tissues.

- Underlying health conditions: the presence of underlying specific health conditions could influence the response to NR supplementation. NR might be more effective in specific disease contexts, requiring stratified clinical trials to tease out these potential interactions.
- Variations in NR dosing: the optimal dosage of NR for specific health benefits could be a moving target. Studies employing inadequate NR intake might not achieve the threshold necessary to trigger significant cellular changes. Conversely, excessively high doses could lead to unintended consequences requiring further investigation.
- Duration of supplementation: one can also speculate that the window of opportunity for NR's effects could be time sensitive. Studies with short supplementation periods might miss the long-term benefits that require sustained NAD+ elevation.

Regarding the in vitro studies assessing the possibility of a crosstalk between the cytosol and SR pyridine nucleotide pool, the data clearly show that decreasing NAD+ in the cytosol through NAMPT inhibition led an inhibition of the 11β-HSD1 activity in the SR. Conversely, increasing NAD+ in the cytosol using the NAD+ precursor, NR, rescued the 11β-HSD1 activity. Future studies could aim to lower NAD+ in the SR through a different mechanism to FK866, such as PARP overexpression to increase NAD+ consumption in the SR. One should expect effects 11β-HSD1 activity similar to FK866 which may also be rescuable with NR. Furthermore, future studies could utilise a NAD+ biosensor which may illuminate the level of the cytosol-SR pyridine nucleotide crosstalk.

Overall Conclusions

We found that the oral intake of NR boosted the skeletal muscle NAD+ metabolome in aged men and provoked a transcriptomic signature. However, the mitochondrial function and systemic cardiometabolic readouts remained unaltered. The NAD+ metabolome analysis showed abundance of NAM clearance products suggesting a preexisting NAD+ sufficiency. Our data support the notion that, in contrast to aged laboratory rodents, chronological age per se may not be a major factor in altering muscle NAD+. A potential limitation of this study could be the relatively small number of individuals. Additionally, the duration of NR administration may not be sufficiently long, albeit the sample size and duration of NR supplementation were sufficient to detect NR-mediated changes in the NAD+ metabolome, muscle transcriptional signature, and inflammatory profile. Further studies are needed to further explore some of the NR-induced changes in this experimental medicine study.

References

1. Mukund K, Subramaniam S. Skeletal muscle: A review of molecular structure and function, in health and disease. Wiley Interdiscip Rev Syst Biol Med. 2020;12(1):1–46.

2. Frontera WR, Ochala J. Skeletal Muscle: A Brief Review of Structure and Function. Behav Genet. 2015;45(2):183–95.

3. Argilés JM, Campos N, Lopez-Pedrosa JM, Rueda R, Rodriguez-Mañas L. Skeletal Muscle Regulates Metabolism via Interorgan Crosstalk: Roles in Health and Disease. J Am Med Dir Assoc. 2016;17(9):789–96.

4. Guridi M, Kupr B, Romanino K, Lin S, Falcetta D, Tintignac L, et al. Alterations to mTORC1 signaling in the skeletal muscle differentially affect whole-body metabolism. Skelet Muscle. 2016;6(1):1–14.

5. Guridi M, Tintignac LA, Lin S, Kupr B, Castets P, Rüegg MA. Activation of mTORC1 in skeletal muscle regulates whole-body metabolism through FGF21. Sci Signal. 2015;8(402):ra113–ra113.

6. Cantó C, Jiang LQ, Deshmukh AS, Mataki C, Coste A, Lagouge M, et al. Interdependence of AMPK and SIRT1 for Metabolic Adaptation to Fasting and Exercise in Skeletal Muscle. Cell Metab [Internet]. 2010;11(3):213–9. Available from: http://dx.doi.org/10.1016/j.cmet.2010.02.006

7. Hawley JA, Burke LM, Phillips SM, Spriet LL. Nutritional modulation of training-induced skeletal muscle adaptations. Vol. 110, Journal of Applied Physiology. 2011. p. 834–45.

8. Röckl KSC, Hirshman MF, Brandauer J, Fujii N, Witters LA, Goodyear LJ. Skeletal muscle adaptation to exercise training: AMP-activated protein kinase mediates muscle fiber type shift. Diabetes. 2007;56(8):2062–9.

9. White AT, Schenk S. NAD(+)/NADH and skeletal muscle mitochondrial adaptations to exercise. AJP Endocrinol Metab [Internet]. 2012;303(3):E308-21. Available from: http://eutils.ncbi.nlm.nih.gov/entrez/eutils/elink.fcgi?dbfrom=pubmed&id=22436696&retmode=ref&cmd=prlinks%5Cnpapers2://publication/doi/10.1152/ajpendo.00054.2012

10. Ponticos M, Lu QL, Morgan JE, Hardie DG, Partridge TA, Carling D. Dual regulation of the AMP-activated protein kinase provides a novel mechanism for the control of creatine kinase in skeletal muscle. EMBO J. 1998;17(6):1688–99.

11. Hultman E. Fuel selection, muscle fibre. Proc Nutr Soc. 1995;54(1):107–21.

12. Burton DA, Stokes K, Hall GM. Physiological effects of exercise. Contin Educ Anaesthesia, Crit Care Pain. 2004;4(6):185–8.

13. Conley KE. Mitochondria to motion: Optimizing oxidative phosphorylation to improve exercise performance. J Exp Biol. 2016;219(2):243–9.

14. van Hall G. The Physiological Regulation of Skeletal Muscle Fatty Acid Supply and Oxidation During Moderate-Intensity Exercise. Vol. 45, Sports Medicine. 2015. p. 23–32.

15. Holeček M. Branched-chain amino acids in health and disease: Metabolism, alterations in blood plasma, and as supplements. Vol. 15, Nutrition and Metabolism. 2018.

16. Milan G, Romanello V, Pescatore F, Armani A, Paik JH, Frasson L, et al. Regulation of autophagy and the ubiquitin-proteasome system by the FoxO transcriptional network during muscle atrophy. Nat Commun. 2015;6(1):1–14.

17. Copeland WC, Longley MJ. Mitochondrial genome maintenance in health and disease. DNA Repair (Amst). 2014;19:190–8.

18. Gnaiger E. Capacity of oxidative phosphorylation in human skeletal muscle. New perspectives of mitochondrial physiology. Vol. 41, International Journal of Biochemistry

and Cell Biology. 2009. p. 1837–45.

19. Gureev AP, Shaforostova EA, Popov VN. Regulation of mitochondrial biogenesis as a way for active longevity: Interaction between the Nrf2 and PGC-1α signaling pathways. Vol. 10, Frontiers in Genetics. 2019. p. 435.

20. Irrcher I, Adhihetty PJ, Sheehan T, Joseph AM, Hood DA. PPARγ coactivator-1α expression during thyroid hormone- and contractile activity-induced mitochondrial adaptations. Am J Physiol - Cell Physiol. 2003;284(6 53-6).

21. Wu Z, Puigserver P, Andersson U, Zhang C, Adelmant G, Mootha V, et al. Mechanisms controlling mitochondrial biogenesis and respiration through the thermogenic coactivator PGC-1. Cell. 1999;98(1):115–24.

22. Reznick RM, Zong H, Li J, Morino K, Moore IK, Yu HJ, et al. Aging-Associated Reductions in AMP-Activated Protein Kinase Activity and Mitochondrial Biogenesis. Cell Metab. 2007;5(2):151–6.

23. Hardie DG, Ross F a., Hawley S a. AMPK: a nutrient and energy sensor that maintains energy homeostasis. Nat Rev Mol Cell Biol [Internet]. 2012;13(4):251–62. Available from: http://dx.doi.org/10.1038/nrm3311

24. Zong H, Ren JM, Young LH, Pypaert M, Mu J, Birnbaum MJ, et al. AMP kinase is required for mitochondrial biogenesis in skeletal muscle in response to chronic energy deprivation. Proc Natl Acad Sci U S A [Internet]. 2002;99(25):15983–7. Available from: http://www.ncbi.nlm.nih.gov/entrez/query.fcgi?cmd=Retrieve&db=PubMed&dopt=Citation&list_uids=12444247%5Cnhttp://www.pubmedcentral.nih.gov/articlerender.fcgi?artid=138551&tool=pmcentrez&rendertype=abstract

25. Srivastava S, Diaz F, Iommarini L, Aure K, Lombes A, Moraes CT. PGC-1α/β induced expression partially compensates for respiratory chain defects in cells from patients with mitochondrial disorders. Hum Mol Genet. 2009;18(10):1805–12.

26. Lin J, Handschin C, Spiegelman BM. Metabolic control through the PGC-1 family of transcription coactivators. Cell Metab. 2005;1(6):361–70.

27. Boyman L, Karbowski M, Lederer WJ. Regulation of Mitochondrial ATP Production: Ca2+ Signaling and Quality Control. Trends Mol Med. 2020;26(1):21–39.

28. Nath S. Integration of demand and supply sides in the ATP energy economics of cells. Biophys Chem. 2019;252:106208.

29. Matlin KS. The Heuristic of Form: Mitochondrial Morphology and the Explanation of Oxidative Phosphorylation. J Hist Biol. 2016;49(1):37–94.

30. Miranda-Quintana RA, Martínez González M, Ayers PW. Electronegativity and redox reactions. Phys Chem Chem Phys. 2016;18(32):22235–43.

31. Hirst J. Mitochondrial complex i. Annu Rev Biochem. 2013;82:551–75.

32. Brandt U. Energy converting NADH:quinone oxidoreductase (complex I). Annu Rev Biochem. 2006;75:69–92.

33. Yankovskaya V, Horsefield R, Törnroth S, Luna-Chavez C, Miyoshi H, Léger C, et al. Architecture of succinate dehydrogenase and reactive oxygen species generation. Science (80-). 2003;299(5607):700–4.

34. Cecchini G. Function and structure of complex II of the respiratory chain. Annu Rev Biochem. 2003;72:77–109.

35. Crofts AR. The cytochrome bc1 complex: Function in the context of structure. Annu Rev

Physiol. 2004;66:689–733.

36. Wikström M, Sharma V. Proton pumping by cytochrome c oxidase – A 40 year anniversary. Biochim Biophys Acta - Bioenerg. 2018;1859(9):692–8.

37. Tsukihara T, Aoyama H, Yamashita E, Tomizaki T, Yamaguchi H, Shinzawa-Itoh K, et al. The Whole Structure of the 13-Subunit Oxidized Cytochrome c Oxidase at 2.8 Å. Science (80-). 1996;272(5265):1136–44.

38. Boyer PD. The ATP synthase - A splendid molecular machine. Annu Rev Biochem. 1997;66:717–49.

39. Abrahams JP, Leslie AGW, Lutter R, Walker JE. Structure at 2.8 Â resolution of F1-ATPase from bovine heart mitochondria. Nature. 1994;370(6491):621–8.

40. Scialò F, Fernández-Ayala DJ, Sanz A. Role of mitochondrial reverse electron transport in ROS signaling: Potential roles in health and disease. Front Physiol. 2017;8(JUN):273331.

41. Sauve A a. NAD + and Vitamin B 3 : From Metabolism to Therapies. J Pharmacol Exp Ther. 2008;324(3):883–93.

42. Belenky P, Bogan KL, Brenner C. NAD+ metabolism in health and disease. Trends Biochem Sci. 2007;32(1):12–9.

43. Berger F. The new life of a centenarian: signalling functions of NAD(P). Trends Biochem Sci. 2004;29(3):111–8.

44. Houtkooper RH, Cantó C, Wanders RJ, Auwerx J. The secret life of NAD+: An old metabolite controlling new metabolic signaling pathways. Endocr Rev. 2010;31(2):194–223.

45. Baker BY, Shi W, Wang B, Palczewski K. High-resolution crystal structures of the photoreceptor glyceraldehyde 3-phosphate dehydrogenase (GAPDH) with three and four-bound NAD molecules. Protein Sci. 2014;23(11):1629–39.

46. Kerbey AL, Radcliffe PM, Randle PJ. Diabetes and the control of pyruvate dehydrogenase in rat heart mitochondria by concentration ratios of adenosine triphosphate/adenosine diphosphate, of reduced/oxidized nicotinamide-adenine dinucleotide and of acetyl-coenzyme A/coenzymeA. Biochem J. 1977;164(3):509–19.

47. Rindler PM, Crewe CL, Fernandes J, Kinter M, Szweda LI. Redox regulation of insulin sensitivity due to enhanced fatty acid utilization in the mitochondria. Am J Physiol Circ Physiol. 2013;305(5):H634–43.

48. Aubert G, Martin OJ, Horton JL, Lai L, Vega RB, Leone TC, et al. The Failing Heart Relies on Ketone Bodies as a Fuel. Circulation. 2016;133(8):698–705.

49. Chen JQ, Russo J. Dysregulation of glucose transport, glycolysis, TCA cycle and glutaminolysis by oncogenes and tumor suppressors in cancer cells. Vol. 1826, Biochimica et Biophysica Acta - Reviews on Cancer. 2012. p. 370–84.

50. Pollak N, Dölle C, Ziegler M. The power to reduce: pyridine nucleotides-small molecules with a multitude of functions. Biochem J. 2007;402(2):205–18.

51. Tedeschi PM, Bansal N, Kerrigan JE, Abali EE, Scotto KW, Bertino JR. NAD+ kinase as a therapeutic target in cancer. Vol. 22, Clinical Cancer Research. 2016. p. 5189–95.

52. Magni G, Amici a., Emanuelli M, Orsomando G, Raffaelli N, Ruggieri S. Enzymology of NAD+ homeostasis in man. Cell Mol Life Sci. 2004;61(1):19–34.

53. Di Stefano M, Conforti L. Diversification of NAD biological role : the importance of location. FEBS J. 2013;280(19):4711–28.

54. Kurosawa K, Shibata H, Hayashi N, Sato N, Kamada T, Tagawa K. Kinetics of Hydroperoxide Degradation by NADP-Glutathione System in Mitochondria 1. Vol. 108, J. Biochem. 1990.

55. Agledal L, Niere M, Ziegler M. The phosphate makes a difference: cellular functions of NADP. Redox Rep. 2010;15(1):2–10.

56. Frederick DW, Loro E, Liu L, Davila A, Chellappa K, Silverman IM, et al. Loss of NAD Homeostasis Leads to Progressive and Reversible Degeneration of Skeletal Muscle. Cell Metab. 2016;24(2):269–82.

57. Ju HQ, Zhuang ZN, Li H, Tian T, Lu YX, Fan XQ, et al. Regulation of the Nampt-mediated NAD salvage pathway and its therapeutic implications in pancreatic cancer. Cancer Lett. 2016;379(1):1–11.

58. Tan B, Young DA, Lu ZH, Wang T, Meier TI, Shepard RL, et al. Pharmacological inhibition of nicotinamide phosphoribosyltransferase (NAMPT), an enzyme essential for NAD+ biosynthesis, in human cancer cells: Metabolic basis and potential clinical implications. J Biol Chem. 2013;288(5):3500–11.

59. Easlon E, Tsang F, Skinner C, Wang C, Lin S. Erin Easlon, Felicia Tsang, Craig Skinner, Chen Wang, and Su-Ju Lin 1. Genes Dev. 2008;931–44.

60. Gregoretti I, Lee Y-M, Goodson H V. Molecular Evolution of the Histone Deacetylase Family: Functional Implications of Phylogenetic Analysis. J Mol Biol. 2004;338(1):17–31.

61. Grozinger CM, Schreiber SL. Deacetylase enzymes: Biological functions and the use of small-molecule inhibitors. Chem Biol. 2002;9(1):3–16.

62. Su X, Wellen KE, Rabinowitz JD. Metabolic control of methylation and acetylation. Curr Opin Chem Biol. 2016;30:52–60.

63. Martin C, Zhang Y. The diverse functions of histone lysine methylation. Nat Rev Mol Cell Biol. 2005;6(11):838–49.

64. Bannister AJ, Kouzarides T. Regulation of chromatin by histone modifications. Cell Res. 2011;21(3):381–95.

65. Ashamu GA, Sethi JK, Galione A, Potter BVL. Roles for Adenosine Ribose Hydroxyl Groups in Cyclic Adenosine 5‘-Diphosphate Ribose-Mediated Ca 2+ Release †. Biochemistry. 1997 Aug;36(31):9509–17.

66. Kim MY, Zhang T, Kraus WL. Poly(ADP-ribosyl)ation by PARP-1: “PAR-laying” NAD+ into a nuclear signal. Genes Dev. 2005;19(17):1951–67.

67. Khan J a, Forouhar F, Tao X, Tong L. Nicotinamide adenine dinucleotide metabolism as an attractive target for drug discovery. Expert Opin Ther Targets [Internet]. 2007;11(5):695–705. Available from: http://www.ncbi.nlm.nih.gov/pubmed/17465726

68. Mellert HS, McMahon SB. Biochemical pathways that regulate acetyltransferase and deacetylase activity in mammalian cells. Trends Biochem Sci. 2009;34(11):571–8.

69. Yang X-J, Seto E. HATs and HDACs: from structure, function and regulation to novel strategies for therapy and prevention. Oncogene [Internet]. 2007;26(37):5310–8. Available from: ifinder/10.1038/sj.onc.1210599

70. Haberland M, Montgomery RL, Olson EN. The many roles of histone deacetylases in development and physiology: implications for disease and therapy. Nat Rev Genet. 2009;10(1):32–42.

71. Gray SG, Ekström TJ. The Human Histone Deacetylase Family. Exp Cell Res. 2001;262(2):75–83.

72. Brachmann CB, Sherman JM, Devine SE, Cameron EE, Pillus L, Boeke JD. The SIR2

gene family, conserved \nfrom bacteria to humans, functions in \nsilencing, cell cycle progiression, and \nchromosome stability. Genes Dev. 1995;9:2888-2902.

73. Imai S, Armstrong CM, Kaeberlein M, Guarente L. Transcriptional silencing and longevity protein Sir2 is an NAD-dependent histone deacetylase. Nature. 2000;403(6771):795–800.

74. Tanner KG, Landry J, Sternglanz R, Denu JM. Silent information regulator 2 family of NAD- dependent histone/protein deacetylases generates a unique product, 1-O-acetyl-ADP-ribose. Proc Natl Acad Sci U S A. 2000;97(26):14178–82.

75. Landry J, Slama JT, Sternglanz R. Role of NAD(+) in the deacetylase activity of the SIR2-like proteins. Biochem Biophys Res Commun. 2000;278(3):685–90.

76. Sebastian C, Satterstrom FK, Haigis MC, Mostoslavsky R. From Sirtuin Biology to Human Diseases: An Update. J Biol Chem [Internet]. 2012;287(51):42444–52. Available from: http://www.jbc.org/cgi/doi/10.1074/jbc.R112.402768

77. Langley B, Sauve A. Sirtuin Deacetylases as Therapeutic Targets in the Nervous System. Neurotherapeutics. 2013;10(4):605–20.

78. Lin SJ, Defossez P a, Guarente L. Requirement of NAD and SIR2 for life-span extension by calorie restriction in Saccharomyces cerevisiae. Science. 2000;289(5487):2126–8.

79. Burnett C, Valentini S, Cabreiro F, Goss M, Somogyvári M, Piper MD, et al. Absence of effects of Sir2 overexpression on lifespan in C. elegans and Drosophila. Nature. 2011;477(7365):482–5.

80. Frye RA. Phylogenetic classification of prokaryotic and eukaryotic Sir2-like proteins. Biochem Biophys Res Commun. 2000;273(2):793–8.

81. Michan S, Sinclair D. Sirtuins in mammals: insights into their biological function. Biochem

J. 2007;404(1):1–13.

82. Michishita E, Park JY, Burneskis JM, Barrett JC, Horikawa I. Evolutionarily conserved and nonconserved cellular localizations and functions of human SIRT proteins. Mol Biol Cell. 2005;16(10):4623–35.

83. Tanno M, Sakamoto J, Miura T, Shimamoto K, Horio Y. Nucleocytoplasmic Shuttling of the NAD+-dependent Histone Deacetylase SIRT1. J Biol Chem. 2006;282(9):6823–32.

84. Houtkooper RH, Pirinen E, Auwerx J. Sirtuins as regulators of metabolism and healthspan. Nat Rev Mol Cell Biol [Internet]. 2012;13(4):225–38. Available from: http://dx.doi.org/10.1038/nrm3293

85. Hallows WC, Albaugh BN, Denu JM. Where in the cell is SIRT3?--functional localization of an NAD+-dependent protein deacetylase. Vol. 411, The Biochemical journal. 2008. p. e11–3.

86. North BJ, Marshall BL, Borra MT, Denu JM, Verdin E. The human Sir2 ortholog, SIRT2, is an NAD+-dependent tubulin deacetylase. Mol Cell. 2003;11(2):437–44.

87. Nogueiras R, Habegger KM, Chaudhary N, Finan B, Banks AS, Dietrich MO, et al. Sirtuin 1 and sirtuin 3: Physiological modulators of metabolism. Physiol Rev. 2012;92(3):1479–514.

88. Brunet A. Stress-Dependent Regulation of FOXO Transcription Factors by the SIRT1 Deacetylase. Science (80-). 2004;303(5666):2011–5.

89. Motta MC, Divecha N, Lemieux M, Kamel C, Chen D, Gu W, et al. Mammalian SIRT1 represses forkhead transcription factors. Cell. 2004;116(4):551–63.

90. Rodgers JT, Lerin C, Haas W, Gygi SP, Spiegelman BM, Puigserver P. Nutrient control of glucose homeostasis through a complex of PGC-1α and SIRT1. Nature.

2005;434(7029):113–8.

91. Vaziri H, Dessain SK, Eaton EN, Imai SI, Frye R a., Pandita TK, et al. hSIR2SIRT1 functions as an NAD-dependent p53 deacetylase. Cell. 2001;107(2):149–59.

92. Bouras T, Fu M, Sauve AA, Wang F, Quong AA, Perkins ND, et al. SIRT1 Deacetylation and Repression of p300 Involves Lysine Residues 1020 / 1024 within the Cell Cycle Regulatory Domain 1 *. J Biol Chem. 2005;280(11):10264–76.

93. Kauppinen A, Suuronen T, Ojala J, Kaarniranta K, Salminen A. Antagonistic crosstalk between NF-kappaB and SIRT1 in the regulation of inflammation and metabolic disorders. Cell Signal. 2013;25(10):1939–48.

94. Lim J-H, Lee Y-M, Chun Y-S, Chen J, Kim J-E, Park J-W. Sirtuin 1 Modulates Cellular Responses to Hypoxia by Deacetylating Hypoxia-Inducible Factor 1α. Mol Cell. 2010;38(6):864–78.

95. Cantó C, Gerhart-Hines Z, Feige JN, Lagouge M, Noriega L, Milne JC, et al. AMPK regulates energy expenditure by modulating NAD+ metabolism and SIRT1 activity. Nature. 2009;458(7241):1056–60.

96. Wang P, Xu TY, Guan YF, Tian WW, Viollet B, Rui YC, et al. Nicotinamide phosphoribosyltransferase protects against ischemic stroke through SIRT1-dependent adenosine monophosphate-activated kinase pathway. Ann Neurol. 2011;69(2):360–74.

97. van der Horst A, Tertoolen LGJ, de Vries-Smits LMM, Frye RA, Medema RH, Burgering BMT. FOXO4 is acetylated upon peroxide stress and deacetylated by the longevity protein hSir2(SIRT1). J Biol Chem [Internet]. 2004;279(28):28873–9. Available from: http://www.jbc.org/content/279/28/28873.long

98. Verdin E, Hirschey MD, Finley LWS, Haigis MC. Sirtuin regulation of mitochondria:

Energy production, apoptosis, and signaling. Vol. 35, Trends in Biochemical Sciences. 2010. p. 669–75.

99. Lombard DB, Alt FW, Cheng H-L, Bunkenborg J, Streeper RS, Mostoslavsky R, et al. Mammalian Sir2 Homolog SIRT3 Regulates Global Mitochondrial Lysine Acetylation. Mol Cell Biol. 2007;27(24):8807–14.

100. Ahn B-H, Kim H-S, Song S, Lee IH, Liu J, Vassilopoulos A, et al. A role for the mitochondrial deacetylase Sirt3 in regulating energy homeostasis. Proc Natl Acad Sci U S A. 2008;105(38):14447–52.

101. Hirschey MD, Shimazu T, Goetzman E, Jing E, Schwer B, Lombard DB, et al. SIRT3 regulates mitochondrial fatty-acid oxidation by reversible enzyme deacetylation. Nature. 2010;464(7285):121–5.

102. Shimazu T, Hirschey MD, Hua L, Dittenhafer-Reed KE, Schwer B, Lombard DB, et al. SIRT3 deacetylates mitochondrial 3-hydroxy-3-methylglutaryl CoA synthase 2 and regulates ketone body production. Cell Metab. 2010;12(6):654–61.

103. Schlicker C, Gertz M, Papatheodorou P, Kachholz B, Becker CFW, Steegborn C. Substrates and Regulation Mechanisms for the Human Mitochondrial Sirtuins Sirt3 and Sirt5. J Mol Biol. 2008;382(3):790–801.

104. Qiu X, Brown K, Hirschey MD, Verdin E, Chen D. Calorie restriction reduces oxidative stress by SIRT3-mediated SOD2 activation. Cell Metab. 2010;12(6):662–7.

105. Yu W, Dittenhafer-Reed KE, Denu JM. SIRT3 protein deacetylates isocitrate dehydrogenase 2 (IDH2) and regulates mitochondrial redox status. J Biol Chem. 2012;287(17):14078–86.

106. Jing E, O'Neill BT, Rardin MJ, Kleinridders A, Ilkeyeva OR, Ussar S, et al. Sirt3 regulates

metabolic flexibility of skeletal muscle through reversible enzymatic deacetylation. Diabetes. 2013;62(10):3404–17.

107. Mishra S, Cosentino C, Tamta AK, Khan D, Srinivasan S, Ravi V, et al. Sirtuin 6 inhibition protects against glucocorticoid-induced skeletal muscle atrophy by regulating IGF/PI3K/AKT signaling. Nat Commun. 2022;13(1):1–22.

108. Krishnakumar R, Kraus WL. The PARP side of the nucleus: molecular actions, physiological outcomes, and clinical targets. Mol Cell. 2010;39(1):8–24.

109. Hassa PO, Hottiger MO. The diverse biological roles of mammalian PARPS, a small but powerful family of poly-ADP-ribose polymerases. Front Biosci. 2008;13:3046–82.

110. Gibson BA, Kraus WL. New insights into the molecular and cellular functions of poly(ADP-ribose) and PARPs. Nat Rev Mol Cell Biol. 2012;13(7):411–24.

111. Ruggieri S, Orsomando G, Sorci L, Raffaelli N. Regulation of NAD biosynthetic enzymes modulates NAD-sensing processes to shape mammalian cell physiology under varying biological cues. Biochim Biophys Acta - Proteins Proteomics. 2015;1854(9):1138–49.

112. Tallis M, Morra R, Barkauskaite E, Ahel I. Poly(ADP-ribosyl)ation in regulation of chromatin structure and the DNA damage response. Vol. 123, Chromosoma. 2014. p. 79–90.

113. Durkacz BW, Omidiji O, Gray DA, Shall S. (ADP-Ribose)n participates in DNA excision repair. Vol. 283, Nature. 1980. p. 593–6.

114. Malanga M, Althaus FR. The role of poly(ADP-ribose) in the DNA damage signaling network. Biochem Cell Biol [Internet]. 2005;83(3):354–64. Available from: http://www.nrcresearchpress.com/doi/abs/10.1139/o05-038?url_ver=Z39.88-2003&rfr_id=ori:rid:crossref.org&rfr_dat=cr_pub=pubmed#.VajdT5OYphE

115. Schreiber V, Dantzer F, Ame J-C, de Murcia G. Poly(ADP-ribose): novel functions for an old molecule. Nat Rev Mol Cell Biol [Internet]. 2006;7(7):517–28. Available from: http://www.nature.com/doifinder/10.1038/nrm1963

116. Langelier M-F, Riccio AA, Pascal JM. PARP-2 and PARP-3 are selectively activated by 5′ phosphorylated DNA breaks through an allosteric regulatory mechanism shared with PARP-1. Nucleic Acids Res. 2014;42(12):7762–75.

117. El-Khamisy SF, Masutani M, Suzuki H, Caldecott KW. A requirement for PARP-1 for the assembly or stability of XRCC1 nuclear foci at sites of oxidative DNA damage. Nucleic Acids Res. 2003;31(19):5526–33.

118. Imai S ichiro, Guarente L. NAD+ and sirtuins in aging and disease. Trends Cell Biol [Internet]. 2014;24(8):464–71. Available from: http://dx.doi.org/10.1016/j.tcb.2014.04.002

119. Mohamed JS, Hajira A, Pardo PS, Boriek AM. MicroRNA-149 inhibits PARP-2 and promotes mitochondrial biogenesis via SIRT-1/PGC-1α network in skeletal muscle. Diabetes. 2014;63(5):1546–59.

120. Mouchiroud L, Houtkooper RH, Moullan N, Katsyuba E, Ryu D, Canto C, et al. The NAD(+)/Sirtuin Pathway Modulates Longevity through Activation of Mitochondrial UPR and FOXO Signaling. Cell. 2013;154(2):430–41.

121. Bai P, Cantó C, Oudart H, Brunyánszki A, Cen Y, Thomas C, et al. PARP-1 Inhibition Increases Mitochondrial Metabolism through SIRT1 Activation. Cell Metab [Internet]. 2011;13(4):461–8. Available from: http://linkinghub.elsevier.com/retrieve/pii/S155041311100091X

122. Bai P, Canto C, Brunyánszki A, Huber A, Szántó M, Cen Y, et al. PARP-2 Regulates SIRT1 Expression and Whole-Body Energy Expenditure. Cell Metab [Internet].

2011;13(4):450–60. Available from: http://linkinghub.elsevier.com/retrieve/pii/S1550413111001008

123. Asher G, Reinke H, Altmeyer M, Gutierrez-Arcelus M, Hottiger MO, Schibler U. Poly(ADP-ribose) polymerase 1 participates in the phase entrainment of circadian clocks to feeding. Cell [Internet]. 2010;142(6):943–53. Available from: http://www.ncbi.nlm.nih.gov/pubmed/20832105

124. Lee HC. Cyclic ADP-ribose and nicotinic acid adenine dinucleotide phosphate (NAADP) as messengers for calcium mobilization. J Biol Chem. 2012;287(38):31633–40.

125. Aksoy P, White TA, Thompson M, Chini EN. Regulation of intracellular levels of NAD: A novel role for CD38. Biochem Biophys Res Commun. 2006;345(4):1386–92.

126. Graeff R, Liu Q, Kriksunov I a., Hao Q, Hon CL. Acidic residues at the active sites of CD38 and ADP-ribosylt cyclase determine nicotinic acid adenine dinucleotide phosphate (NAADP) synthesis and hydrolysis activities. J Biol Chem. 2006;281(39):28951–7.

127. Aarhus R, Graeff RM, Dickey DM, Walseth TF, Lee HC. ADP-ribosyl cyclase and CD38 catalyze the synthesis of a calcium-mobilizing metabolite from NADP. J Biol Chem. 1995;270(51):30327–33.

128. Camacho-Pereira J, Tarragó MG, Chini CCS, Nin V, Escande C, Warner GM, et al. CD38 Dictates Age-Related NAD Decline and Mitochondrial Dysfunction through an SIRT3-Dependent Mechanism. Cell Metab. 2016;23(6):1127–39.

129. De Flora A, Guida L, Franco L, Zocchi E, Bruzzone S, Benatti U, et al. CD38 and ADP-ribosyl cyclase catalyze the synthesis of a dimeric ADP- ribose that potentiates the calcium-mobilizing activity of cyclic ADP-ribose. J Biol Chem. 1997;272(20):12945–51.

130. Aksoy P, Escande C, White T a., Thompson M, Soares S, Benech JC, et al. Regulation of

SIRT 1 mediated NAD dependent deacetylation: A novel role for the multifunctional enzyme CD38. Biochem Biophys Res Commun. 2006;349:353–9.

131. Barbosa MTP, Soares SM, Novak CM, Sinclair D, Levine J a., Aksoy P, et al. The enzyme CD38 (a NAD glycohydrolase, EC 3.2.2.5) is necessary for the development of diet-induced obesity. FASEB J. 2007;21(13):3629–39.

132. Dali-Youcef N, Lagouge M, Froelich S, Koehl C, Schoonjans K, Auwerx J. Sirtuins: the “magnificent seven”, function, metabolism and longevity. Ann Med. 2007;39(5):335–45.

133. Houtkooper RH, Auwerx J. Exploring the therapeutic space around NAD+. J Cell Biol. 2012;199(2):205–9.

134. Imai SI. A possibility of nutriceuticals as an anti-aging intervention: Activation of sirtuins by promoting mammalian NAD biosynthesis. Pharmacol Res [Internet]. 2010;62(1):42–7. Available from: http://dx.doi.org/10.1016/j.phrs.2010.01.006

135. Lanska DJ. Historical aspects of the major neurological vitamin deficiency disorders: the water-soluble B vitamins. Vol. 95, Handbook of Clinical Neurology. 2009. 445–476 p.

136. Rajakumar K. Pellagra in the United States: A Historical Perspective. South Med J [Internet]. 2000;93(3):272–7. Available from: http://www.jmcgowan.com/pellagra.pdf

137. Koehn CJ, Elvehjem CA. Further studies on the concentration of the antipellagra factor. J Biol Chem. 1937;118:693–9.

138. Elvehjem CA, Madden RJ, Strong FM, Woolley DW. Relation of nicotinic acid and nicotinic acid amide to canine black tongue. J Am Chem Soc [Internet]. 1937 Sep [cited 2017 Feb 14];59(9):1767–8. Available from: http://pubs.acs.org/doi/abs/10.1021/ja01288a509

139. Revollo JR, Grimm AA, Imai S -i. The NAD Biosynthesis Pathway Mediated by

Nicotinamide Phosphoribosyltransferase Regulates Sir2 Activity in Mammalian Cells. J Biol Chem. 2004;279(49):50754–63.

140. Opitz CA, Heiland I. Dynamics of NAD-metabolism: everything but constant. Biochem Soc Trans [Internet]. 2015;43(6):1127–32. Available from: http://biochemsoctrans.org/cgi/doi/10.1042/BST20150133

141. Alano C, Tran A, Tao R, Ying W, JS K, Swanson RA. Differences among Cell Types in NAD1 Compartmentalization: A Comparison of Neurons, Astrocytes, and Cardiac Myocytes. J Neurosci Res. 2007;85:3378–85.

142. Fulco M, Cen Y, Zhao P, Hoffman EP, McBurney MW, Sauve AA, et al. Glucose Restriction Inhibits Skeletal Myoblast Differentiation by Activating SIRT1 through AMPK-Mediated Regulation of Nampt. Dev Cell. 2008;14(5):661–73.

143. Song J, Ke SF, Zhou CC, Zhang SL, Guan YF, Xu TY, et al. Nicotinamide phosphoribosyltransferase is required for the calorie restriction-mediated improvements in oxidative stress, mitochondrial biogenesis, and metabolic adaptation. Journals Gerontol - Ser A Biol Sci Med Sci. 2014;69(1):44–57.

144. Koltai E, Szabo Z, Atalay M, Boldogh I, Naito H, Goto S, et al. Exercise alters SIRT1, SIRT6, NAD and NAMPT levels in skeletal muscle of aged rats. Mech Ageing Dev. 2010;131(1):21–8.

145. Yoshino J, Mills KF, Yoon MJ, Imai S. Nicotinamide mononucleotide, a key NAD(+) intermediate, treats the pathophysiology of diet- and age-induced diabetes in mice. Cell Metab [Internet]. 2011;14(4):528–36. Available from: http://www.pubmedcentral.nih.gov/articlerender.fcgi?artid=3204926&tool=pmcentrez&rendertype=abstract

146. Cantó C, Houtkooper RH, Pirinen E, Youn DY, Oosterveer MH, Cen Y, et al. The NAD+ precursor nicotinamide riboside enhances oxidative metabolism and protects against high-fat diet-induced obesity. Cell Metab. 2012;15(6):838–47.

147. Gomes AP, Price NL, Ling AJY, Moslehi JJ, Montgomery MK, Rajman L, et al. Declining NAD+ induces a pseudohypoxic state disrupting nuclear-mitochondrial communication during aging. Cell. 2013;155(7):1624–38.

148. Yang H, Yang T, Baur JA, Perez E, Matsui T, Carmona JJ, et al. Nutrient-Sensitive Mitochondrial NAD+ Levels Dictate Cell Survival. Cell. 2007;130(6):1095–107.

149. Nishizuka Y, Hayaishi O. Studies on the Biosynthesis of Nicotinamide Adenine Dinucleotide. J Biol Chem. 1963;238(10):3369–77.

150. Dölle C, Skoge RH, Vanlinden MR, Ziegler M. NAD biosynthesis in humans--enzymes, metabolites and therapeutic aspects. Curr Top Med Chem. 2013;13(23):2907–17.

151. Hara N, Yamada K, Terashima M, Osago H, Shimoyama M, Tsuchiya M. Molecular identification of human glutamine- and ammonia-dependent NAD synthetases: Carbon-nitrogen hydrolase domain confers glutamine dependency. J Biol Chem. 2003;278(13):10914–21.

152. Rongvaux A, Andris F, Van Gool F, Leo O. Reconstructing eukaryotic NAD metabolism. BioEssays [Internet]. 2003;25(7):683–90. Available from: http://doi.wiley.com/10.1002/bies.10297

153. Ikeda M, Tsuji H, Nakamura S, Ichiyama A, Nishizuka Y, Hayaishi O. Studies on the Biosynthesis of Nicotinamide Adenine Dinucleotide. II. A Role OF Picolinic Carboxylase In The Biosynthesis Of Nicotinamide Adenine Dinucleotide From Tryptophan In Mammals. J Biol Chem. 1965;240(3):1395–401.

154. Watson M, Roulston A, Belec L, Billot X, Marcellus R, Bedard D, et al. The small molecule GMX1778 is a potent inhibitor of NAD+ biosynthesis: strategy for enhanced therapy in nicotinic acid phosphoribosyltransferase 1-deficient tumors. Mol Cell Biol [Internet]. 2009;29(21):5872–88. Available from: http://www.ncbi.nlm.nih.gov/pubmed/19703994

155. Nikiforov A, Dölle C, Niere M, Ziegler M. Pathways and subcellular compartmentation of NAD biosynthesis in human cells: From entry of extracellular precursors to mitochondrial NAD generation. J Biol Chem. 2011;286(24):21767–78.

156. Stein LR, Imai S. The dynamic regulation of NAD metabolism in mitochondria. Trends Endocrinol Metab [Internet]. 2012;23(9):420–8. Available from: http://www.pubmedcentral.nih.gov/articlerender.fcgi?artid=3683958&tool=pmcentrez&rendertype=abstract

157. Chi Y, Sauve A a. Nicotinamide riboside, a trace nutrient in foods, is a vitamin B3 with effects on energy metabolism and neuroprotection. Curr Opin Clin Nutr Metab Care [Internet]. 2013;16(6):657–61. Available from: http://www.ncbi.nlm.nih.gov/pubmed/24071780

158. Preiss J, Handler P. Biosynthesis of Diphosphopyridine Nucleotide I. IDENTIFICATION OF INTERMEDIATES. J Biol Chem. 1958;233:488–92.

159. Preiss J, Handler P. Biosynthesis of Diphosphopyridine Nucleotide II. ENZYMATIC ASPECTS. J Biol Chem. 1958;233:493–500.

160. Mori V, Amici A, Mazzola F, Di Stefano M, Conforti L, Magni G, et al. Metabolic profiling of alternative NAD biosynthetic routes in mouse tissues. PLoS One. 2014;9(11):1–27.

161. Garten A, Petzold S, Körner A, Imai SI, Kiess W. Nampt: linking NAD biology, metabolism

and cancer. Trends Endocrinol Metab. 2009;20(3):130–8.

162. Zhang LQ, Heruth DP, Ye SQ. Nicotinamide phosphoribosyltransferase in human diseases. J Bioanal Biomed. 2011;3(1):13–25.

163. Preiss J, Handler P. Intermediates in the synthesis of diphosphopyridine nucleotide from nicotinic acid. 1957;1514(3).

164. Martin PR, Shea RJ, Mulks MH. Identification of a Plasmid-Encoded Gene from Haemophilus ducreyi Which Confers NAD Independence. J Bacteriol. 2001;183:1168–74.

165. Rongvaux A, She RJ, Mulks MH, Gigot D, Urbain J, Leo O, et al. Pre-B-cell colony-enhancing factor, whose expression is up-regulated in activated lymphocytes, is a nicotinamide phosphoribosyltransferase, a cytosolic enzyme involved in NAF biosynthesis. Eur J Immunol. 2002;32(11):3225–34.

166. Samal B, Sun Y, Stearns G, Xie C, Suggs S, McNiece I. Cloning and Characterization of the cDNA Encoding a Novel Human Pre-B-Cell Colony-Enhancing Factor. Mol Cell Biol. 1994;14(2):1431–7.

167. Chen MP, Chung FM, Chang DM, Tsai JCR, Huang HF, Shin SJ, et al. Elevated plasma level of visfatin/pre-B cell colony-enhancing factor in patients with type 2 diabetes mellitus. J Clin Endocrinol Metab. 2006;91(1):295–9.

168. Haider DG, Schindler K, Schaller G, Prager G, Wolzt M, Ludvik B. Increased plasma visfatin concentrations in morbidly obese subjects are reduced after gastric banding. J Clin Endocrinol Metab. 2006;91(4):1578–81.

169. Sandeep S, Velmurugan K, Deepa R, Mohan V. Serum visfatin in relation to visceral fat, obesity, and type 2 diabetes mellitus in Asian Indians. Metabolism. 2007 Apr;56(4):565–70.

170. Harasim E, Chabowski A, Górski J. Lack of downstream insulin-mimetic effects of visfatin/eNAMPT on glucose and fatty acid metabolism in skeletal muscles. Acta Physiol. 2011;202(1):21–8.

171. Kitani T, Okuno S, Fujisawa H. Growth phase-dependent changes in the subcellular localization of pre-B-cell colony-enhancing factor. FEBS Lett. 2003;544(1–3):74–8.

172. Revollo JR, Körner A, Mills KF, Satoh A, Wang T, Garten A, et al. Nampt/PBEF/Visfatin Regulates Insulin Secretion in β Cells as a Systemic NAD Biosynthetic Enzyme. Cell Metab. 2007;6(5):363–75.

173. Hasmann M, Schemainda I. FK866, a highly specific noncompetitive inhibitor of nicotinamide phosphoribosyltransferase, represents a novel mechanism for induction of tumor cell apoptosis. Cancer Res [Internet]. 2003 Nov 1 [cited 2019 Jun 19];63(21):7436–42. Available from: http://www.ncbi.nlm.nih.gov/pubmed/14612543

174. Wang P, Miao CY. NAMPT as a Therapeutic Target against Stroke. Trends Pharmacol Sci [Internet]. 2015;36(12):891–905. Available from: http://dx.doi.org/10.1016/j.tips.2015.08.012

175. Hara N, Yamada K, Shibata T, Osago H, Tsuchiya M. Nicotinamide phosphoribosyltransferase/visfatin does not catalyze nicotinamide mononucleotide formation in blood plasma. PLoS One. 2011;6(8):e22781.

176. Yoshida M, Satoh A, Lin JB, Mills KF, Sasaki Y, Rensing N, et al. Extracellular Vesicle-Contained eNAMPT Delays Aging and Extends Lifespan in Mice. Cell Metab. 2019;30(2):329-342.e5.

177. Audrito V, Managò A, Zamporlini F, Rulli E, Gaudino F, Madonna G, et al. Extracellular nicotinamide phosphoribosyltransferase (eNAMPT) is a novel marker for patients with

BRAF-mutated metastatic melanoma. Oncotarget. 2018;9(27):18997–9005.

178. Bi T, Che X. Nampt/PBEF/visfatin and cancer. Cancer Biol Ther [Internet]. 2010;10(2):119–25. Available from: http://www.tandfonline.com/doi/abs/10.4161/cbt.10.2.12581

179. Ramsey KM, Yoshino J, Brace CS, Abrassart D, Kobayashi Y, Marcheva B, et al. Circadian clock feedback cycle through NAMPT-Mediated NAD+ biosynthesis. Science (80-). 2009;324(5927):651–4.

180. Masri S. Sirtuin-dependent clock control. Curr Opin Clin Nutr Metab Care [Internet]. 2015;1. Available from: http://content.wkhealth.com/linkback/openurl?sid=WKPTLP:landingpage&an=00075197-900000000-99425

181. Imai SI. “Clocks” in the NAD World: NAD as a metabolic oscillator for the regulation of metabolism and aging. Biochim Biophys Acta - Proteins Proteomics. 2010;1804(8):1584–90.

182. Bieganowski P, Brenner C. Discoveries of nicotinamide riboside as a nutrient and conserved NRK genes establish a preiss-handler independent route to NAD+ in fungi and humans. Cell. 2004;117(4):495–502.

183. Shifrine M, Biberstein E. A growth factor for Haemophilus species secreted by a Pseudomonad. Nature. 1960;187(4737):623.

184. Gingrich W, Schlenk F. Codehydrogenase I and Other Pyridinium Compounds as V-Factor for Hemophilus Influenzae and H. Parainfluenzae. J Bacteriol. 1944;47(6):535–50.

185. Bogan KL, Brenner C. Nicotinic acid, nicotinamide, and nicotinamide riboside: a molecular evaluation of NAD+ precursor vitamins in human nutrition. Annu Rev Nutr.

2008;28:115–30.

186. Kulikova V, Shabalin K, Nerinovski K, Dölle C, Niere M, Yakimov A, et al. Generation, Release, and Uptake of the NAD Precursor Nicotinic Acid Riboside by Human Cells. J Biol Chem. 2015;290(45):27124–37.

187. Tempel W, Rabeh WM, Bogan KL, Belenky P, Wojcik M, Seidle HF, et al. Nicotinamide riboside kinase structures reveal new pathways to NAD +. PLoS Biol. 2007;5(10):2220–30.

188. Dölle C, Ziegler M. Application of a coupled enzyme assay to characterize nicotinamide riboside kinases. Anal Biochem. 2009;385(2):377–9.

189. Fletcher RS, Ratajczak J, Doig CL, Oakey LA, Callingham R, Da Silva Xavier G, et al. Nicotinamide riboside kinases display redundancy in mediating nicotinamide mononucleotide and nicotinamide riboside metabolism in skeletal muscle cells. Mol Metab. 2017;6(8):819–32.

190. Ratajczak J, Joffraud M, Trammell SAJ, Ras R, Canela N, Boutant M, et al. NRK1 controls nicotinamide mononucleotide and nicotinamide riboside metabolism in mammalian cells. Nat Commun. 2016;7:13103.

191. Sasaki Y, Araki T, Milbrandt J. Stimulation of nicotinamide adenine dinucleotide biosynthetic pathways delays axonal degeneration after axotomy. J Neurosci. 2006;26(33):8484–91.

192. Aguilar CA, Shcherbina A, Ricke DO, Pop R, Carrigan CT, Gifford CA, et al. In vivo monitoring of transcriptional dynamics after lower-limb muscle injury enables quantitative classification of healing. Sci Rep. 2015;5(1):1–17.

193. Xu W, Barrientos T, Mao L, Rockman HA, Sauve AA, Andrews NC. Lethal

Cardiomyopathy in Mice Lacking Transferrin Receptor in the Heart. Cell Rep [Internet]. 2015;13(3):533–45. Available from: http://dx.doi.org/10.1016/j.celrep.2015.09.023

194. Bogan KL, Evans C, Belenky P, Song P, Burant CF, Kennedy R, et al. Identification of Isn1 and Sdt1 as glucose- and vitamin-regulated nicotinamide mononucleotide and nicotinic acid ddenine dinucleotide 5′-nucleotidases responsible for production of nicotinamide riboside and nicotinic acid riboside. J Biol Chem. 2009;284(50):34861–9.

195. Grozio A, Mills KF, Yoshino J, Bruzzone S, Sociali G, Tokizane K, et al. Slc12a8 is a nicotinamide mononucleotide transporter. Nat Metab. 2019;1(1):47–57.

196. Yang Y, Sauve AA. NAD+ metabolism: Bioenergetics, signaling and manipulation for therapy. Biochim Biophys Acta - Proteins Proteomics [Internet]. 2016; Available from: http://linkinghub.elsevier.com/retrieve/pii/S1570963916301236

197. Williams GT, Lau KENMK, Johnstone AP, Coote M. NAD Metabolism and Mitogen Stimulation of Human Lymphocytes. 1985;160:419–26.

198. Rechsteiner M, Hillyard D, Olivera BM. Turnover of nicotinamide adenine dinucleotide in cultures of human cells. J Cell Physiol. 1976;88(2):207–17.

199. Elliott G, Rechsteiner M. Pyridine nucleotide metabolism in mitotic cells. J Cell Physiol. 1975 Dec;86 Suppl 2(3 Pt 2):641–51.

200. Finglas PM. Dietary Reference intakes for thiamin, riboflavin, niacin, vitamin B6, folate, vitamin B12, pantothenic acid, biotin and choline. Vol. 11, Trends in Food Science & Technology. 2000. 296–297 p.

201. Henderson LM. Niacin. Annu Rev Nutr. 1983;3(1):289–307.

202. Gross CJ, Henderson LM. Digestion and absorption of NAD by the small intestine of the rat. J Nutr. 1983;113(2):412–20.

203. Žák A. Niacin in the Treatment of Hyperlipidemias in Light of New Clinical Trials: Has Niacin Lost its Place? Med Sci Monit [Internet]. 2015;21:2156–62. Available from: http://www.medscimonit.com/abstract/index/idArt/893619

204. Trammell SA, Schmidt MS, Weidemann BJ, Redpath P, Jaksch F, Dellinger RW, et al. Nicotinamide riboside is uniquely and orally bioavailable in mice and humans. Nat Commun. 2016;7:12948.

205. Li J, Dou X, Li S, Zhang X, Zeng Y, Song Z. Nicotinamide ameliorates palmitate-induced ER stress in hepatocytes via cAMP/PKA/CREB pathway-dependent Sirt1 upregulation. Biochim Biophys Acta - Mol Cell Res [Internet]. 2015;1853(11):2929–36. Available from: http://dx.doi.org/10.1016/j.bbamcr.2015.09.003

206. Belenky P, Racette FG, Bogan KL, McClure JM, Smith JS, Brenner C. Nicotinamide Riboside Promotes Sir2 Silencing and Extends Lifespan via Nrk and Urh1/Pnp1/Meu1 Pathways to NAD+. Cell. 2007;129(3):473–84.

207. To C, Kim EH, Royce DB, Williams CR, Collins RM, Risingsong R, et al. The PARP inhibitors, veliparib and olaparib, are effective chemopreventive agents for delaying mammary tumor development in BRCA1-deficient mice. Cancer Prev Res. 2014;7(7):698–707.

208. Pirinen E, Cantó C, Jo YS, Morato L, Zhang H, Menzies KJ, et al. Pharmacological inhibition of poly(ADP-ribose) polymerases improves fitness and mitochondrial function in skeletal muscle. Cell Metab. 2014;19(6):1034–41.

209. Bender DA, Olufunwa R. Utilization of tryptophan, nicotinamide and nicotinic acid as precursors for nicotinamide nucleotide synthesis in isolated rat liver cells. Br J Nutr. 1988 Mar;59(2):279–87.

210. Trammell SA, Yu L, Redpath P, Migaud ME, Brenner C. Nicotinamide Riboside Is a Major NAD+ Precursor Vitamin in Cow Milk. J Nutr. 2016;3(11):3–9.

211. Hara N, Yamada K, Shibata T, Osago H, Hashimoto T, Tsuchiya M. Elevation of cellular NAD levels by nicotinic acid and involvement of nicotinic acid phosphoribosyltransferase in human cells. J Biol Chem. 2007;282(34):24574–82.

212. Taskinen MR, Nikkilä EA. Effects of acipimox on serum lipids, lipoproteins and lipolytic enzymes in hypertriglyceridemia. Atherosclerosis. 1988;69(2–3):249–55.

213. Digby JE, Ruparelia N, Choudhury RP. Niacin in cardiovascular disease: Recent preclinical and clinical developments. Arterioscler Thromb Vasc Biol. 2012;32(3):582–8.

214. Altschul R, Hoffer A, Stephen JD. Influence of Nicotinic Acid on Serum Cholesterol in Man. Arch Biochem Biophys. 1955;54(2):558–9.

215. Benyó Z, Gille A, Bennett CL, Clausen BE, Offermanns S. Nicotinic acid-induced flushing is mediated by activation of epidermal langerhans cells. Mol Pharmacol. 2006;70(6):1844–9.

216. Benyó Z, Gille A, Kero J, Csiky M, Suchánková MC, Nüsing RM, et al. GPR109A (PUMA-G / HM74A) mediates nicotinic acid – induced flushing. J Clin Invest. 2005;115(12):3634–40.

217. NICE guidelines. Cardio Cardiovascular disease: risk assessment vascular disease: risk assessment and reduction, including lipid and reduction, including lipid modification modification. 2014;(January).

218. Stone NJ, Robinson JG, Lichtenstein AH, Bairey Merz CN, Blum CB, Eckel RH, et al. 2013 ACC/AHA guideline on the treatment of blood cholesterol to reduce atherosclerotic cardiovascular risk in adults: A report of the American college of cardiology/American

heart association task force on practice guidelines. J Am Coll Cardiol. 2014;63(25 PART B):2889–934.

219. Ferrell M, Wang Z, Anderson JT, Li XS, Witkowski M, DiDonato JA, et al. A terminal metabolite of niacin promotes vascular inflammation and contributes to cardiovascular disease risk. Nat Med. 2024;30(2):424–34.

220. Knip M, Douek IF, Moore WP, Gillmor HA, McLean AE, Bingley PJ, et al. Safety of high-dose nicotinamide: a review. Diabetologia [Internet]. 2000;43(11):1337–45. Available from: http://www.scopus.com/inward/record.url?eid=2-s2.0-0033752240&partnerID=tZOtx3y1

221. Avalos JL, Bever KM, Wolberger C. Mechanism of sirtuin nhibition by nicotinamide: Altering the NAD + cosubstrate specificity of a Sir2 enzyme. Mol Cell. 2005;17(6):855–68.

222. Bitterman KJ, Anderson RM, Cohen HY, Latorre-Esteves M, Sinclair DA. Inhibition of silencing and accelerated aging by nicotinamide, a putative negative regulator of yeast Sir2 and human SIRT1. J Biol Chem. 2002;277(47):45099–107.

223. Collins PB, Chaykin S. The Management of Nicotinamide and Nicotinic Acid in the Mouse. J Biol Chem. 1972;247:778–83.

224. Yang SJ, Choi JM, Kim L, Park SE, Rhee EJ, Lee WY, et al. Nicotinamide improves glucose metabolism and affects the hepatic NAD-sirtuin pathway in a rodent model of obesity and type 2 diabetes. J Nutr Biochem [Internet]. 2014;25(1):66–72. Available from: http://dx.doi.org/10.1016/j.jnutbio.2013.09.004

225. Pike NB. Flushing out the role of GPR109A (HM74A) in the clinical efficacy of nicotinic acid. J Clin Invest. 2005;115(12):3400–3.

226. Felici R, Lapucci A, Cavone L, Pratesi S, Berlinguer-palmini R, Chiarugi A.

Pharmacological NAD-Boosting Strategies Improve Mitochondrial Homeostasis in Human Complex I – Mutant Fibroblasts s. Mol Pharmacol. 2015;87(6):965–71.

227. Yang T, Chan NYK, Sauve A a. Syntheses of nicotinamide riboside and derivatives: Effective agents for increasing nicotinamide adenine dinucleotide concentrations in mammalian cells. J Med Chem. 2007;50(26):6458–61.

228. Harlan BA, Pehar M, Sharma DR, Beeson G, Beeson CC, Vargas MR. Enhancing NAD+ salvage pathway reverts the toxicity of primary astrocytes expressing amyotrophic lateral sclerosislinked mutant superoxide dismutase 1 (SOD1). J Biol Chem. 2016;291(20):10836–46.

229. Stromsdorfer KL, Yamaguchi S, Yoon MJ, Moseley AC, Franczyk MP, Kelly SC, et al. NAMPT-Mediated NAD+ Biosynthesis in Adipocytes Regulates Adipose Tissue Function and Multi-organ Insulin Sensitivity in Mice. Cell Rep [Internet]. 2016;1–10. Available from: http://linkinghub.elsevier.com/retrieve/pii/S2211124716309457

230. Uddin GM, Youngson NA, Sinclair DA, Morris MJ. Head to Head Comparison of Short-Term Treatment with the NAD+ Precursor Nicotinamide Mononucleotide (NMN) and 6 Weeks of Exercise in Obese Female Mice. Front Pharmacol [Internet]. 2016;7(August):1–11. Available from: http://journal.frontiersin.org/article/10.3389/fphar.2016.00258

231. Yang Y, Mohammed FS, Zhang N, Sauve AA. Dihydronicotinamide riboside is a potent NAD concentration enhancer in vitro and in vivo. J Biol Chem. 2019;294(23):9295–307.

232. Riches Z, Liu Y, Berman JM, Walia G, Collier AC. The ontogeny and population variability of human hepatic dihydronicotinamide riboside:quinone oxidoreductase (NQO2). J Biochem Mol Toxicol. 2017;31(8):e21921.

233. Megarity CF, Gill JRE, Clare Caraher M, Stratford IJ, Nolan KA, Timson DJ. The two

common polymorphic forms of human NRH-quinone oxidoreductase 2 (NQO2) have different biochemical properties. FEBS Lett. 2014;588(9):1666–72.

234. Timmers S, Auwerx J, Schrauwen P. The journey of resveratrol from yeast to human. Aging (Albany NY). 2012;4(3):146–58.

235. Baur JA. Resveratrol, sirtuins, and the promise of a DR mimetic. Mech Ageing Dev [Internet]. 2010;131(4):261–9. Available from: http://dx.doi.org/10.1016/j.mad.2010.02.007

236. Timmers S, Konings E, Bilet L, Houtkooper RH, Van De Weijer T, Goossens GH, et al. Calorie restriction-like effects of 30 days of resveratrol supplementation on energy metabolism and metabolic profile in obese humans. Cell Metab [Internet]. 2011;14(5):612–22. Available from: http://dx.doi.org/10.1016/j.cmet.2011.10.002

237. Crandall JP, Oram V, Trandafirescu G, Reid M, Kishore P, Hawkins M, et al. Pilot study of resveratrol in older adults with impaired glucose tolerance. J Gerontol A Biol Sci Med Sci [Internet]. 2012;67(12):1307–12. Available from: http://biomedgerontology.oxfordjournals.org/content/early/2012/01/04/gerona.glr235.short

238. Vang O, Ahmad N, Baile CA, Baur JA, Brown K, Csiszar A, et al. What is new for an old molecule? systematic review and recommendations on the use of resveratrol. PLoS One. 2011;6(6).

239. Fullerton MD, Galic S, Marcinko K, Sikkema S, Pulinilkunnil T, Chen ZP, et al. Single phosphorylation sites in Acc1 and Acc2 regulate lipid homeostasis and the insulin-sensitizing effects of metformin. Nat Med [Internet]. 2013;19(12):1649–54. Available from: http://www.ncbi.nlm.nih.gov/pubmed/24185692

240. Pieper AA, Xie S, Capota E, Estill SJ, Zhong J, Long JM, et al. Discovery of a

Proneurogenic, Neuroprotective Chemical. Cell [Internet]. 2010;142(1):39–51. Available from: http://dx.doi.org/10.1016/j.cell.2010.06.018

241. Yin TC, Britt JK, De Jesús-Cortés H, Lu Y, Genova RM, Khan MZ, et al. P7C3 neuroprotective chemicals block axonal degeneration and preserve function after traumatic brain injury. Cell Rep. 2014;8(6):1731–40.

242. Wang G, Han T, Nijhawan D, Theodoropoulos P, Naidoo J, Yadavalli S, et al. P7C3 neuroprotective chemicals function by activating the rate-limiting enzyme in NAD salvage. Cell [Internet]. 2014;158(6):1324–34. Available from: http://dx.doi.org/10.1016/j.cell.2014.07.040%5Cnhttp://www.ncbi.nlm.nih.gov/pubmed/25215490%5Cnhttp://www.pubmedcentral.nih.gov/articlerender.fcgi?artid=PMC4163014

243. Zhang ZF, Fan SH, Zheng YL, Lu J, Wu DM, Shan Q, et al. Troxerutin improves hepatic lipid homeostasis by restoring NAD +-depletion-mediated dysfunction of lipin 1 signaling in high-fat diet-treated mice. Biochem Pharmacol [Internet]. 2014;91(1):74–86. Available from: http://dx.doi.org/10.1016/j.bcp.2014.07.002

244. Aragonès G, Suárez M, Ardid-Ruiz A, Vinaixa M, Rodríguez MA, Correig X, et al. Dietary proanthocyanidins boost hepatic NAD(+) metabolism and SIRT1 expression and activity in a dose-dependent manner in healthy rats. Sci Rep. 2016;6:24977.

245. Ribas-Latre A, Baselga-Escudero L, Casanova E, Arola-Arnal A, Salvadó M-J, Bladé C, et al. Dietary proanthocyanidins modulate BMAL1 acetylation, Nampt expression and NAD levels in rat liver. Sci Rep. 2015;5:10954.

246. Li H, Xu M, Lee J, He C, Xie Z. Leucine supplementation increases SIRT1 expression and prevents mitochondrial dysfunction and metabolic disorders in high-fat diet-induced obese mice. Am J Physiol Endocrinol Metab [Internet]. 2012;303(10):E1234-44. Available from: http://www.ncbi.nlm.nih.gov/pubmed/22967499

247. Rupaimoole R, Slack FJ. MicroRNA therapeutics: Towards a new era for the management of cancer and other diseases. Vol. 16, Nature Reviews Drug Discovery. 2017. p. 203–21.

248. Choi SE, Fu T, Seok S, Kim DH, Yu E, Lee KW, et al. Elevated microRNA-34a in obesity reduces NAD+ levels and SIRT1 activity by directly targeting NAMPT. Aging Cell. 2013;12(6):1062–72.

249. Haffner CD, Becherer JD, Boros EE, Cadilla R, Carpenter T, Cowan D, et al. Discovery, synthesis, and biological evaluation of thiazoloquin(az)olin(on)es as potent CD38 inhibitors. J Med Chem. 2015;58(8):3548–71.

250. Fang EF, Scheibye-Knudsen M, Brace LE, Kassahun H, Sengupta T, Nilsen H, et al. Defective mitophagy in XPA via PARP-1 hyperactivation and NAD +/SIRT1 reduction. Cell. 2014;157(4):882–96.

251. Zha S, Li Z, Cao Q, Wang F, Liu F. PARP1 inhibitor (PJ34) improves the function of aging-induced endothelial progenitor cells by preserving intracellular NAD + levels and increasing SIRT1 activity. Stem Cell Res Ther. 2018;9(1):224.

252. Chiang S-H, Harrington WW, Luo G, Milliken NO, Ulrich JC, Chen J, et al. Genetic Ablation of CD38 Protects against Western Diet-Induced Exercise Intolerance and Metabolic Inflexibility. PLoS One. 2015;10(8):e0134927.

253. Rouleau M, Patel A, Hendzel MJ, Kaufmann SH, Poirier GG. PARP inhibition: PARP1 and beyond. Nat Rev Cancer [Internet]. 2010;10(4):293–301. Available from: http://www.pubmedcentral.nih.gov/articlerender.fcgi?artid=2910902&tool=pmcentrez&rendertype=abstract

254. Yuan Y, Liao Y-M, Hsueh C-T, Mirshahidi HR. Novel targeted therapeutics: inhibitors of

MDM2, ALK and PARP. J Hematol Oncol. 2011;4:16.

255. Feng FY, de Bono JS, Rubin MA, Knudsen KE. Chromatin to Clinic: The Molecular Rationale for PARP1 Inhibitor Function. Mol Cell [Internet]. 2015;58(6):925–34. Available from: http://www.sciencedirect.com/science/article/pii/S1097276515002725

256. Connell NJ, Houtkooper RH, Schrauwen P. NAD + metabolism as a target for metabolic health: have we found the silver bullet? Diabetologia. 2019;62(6):888–99.

257. Elhassan YS, Philp AA, Lavery GG. Targeting NAD+ in Metabolic Disease: New Insights Into an Old Molecule. J Endocr Soc. 2017;1(7):816–35.

258. Chung HY, Kim HJ, Kim JW, Yu BP. The Inflammation Hypothesis of Aging. Ann N Y Acad Sci. 2006;928(1):327–35.

259. FRANCESCHI C, BONAFÈ M, VALENSIN S, OLIVIERI F, DE LUCA M, OTTAVIANI E, et al. Inflamm-aging: An Evolutionary Perspective on Immunosenescence. Ann N Y Acad Sci. 2006;908(1):244–54.

260. Cadenas E, Davies KJA. Mitochondrial free radical generation, oxidative stress, and aging. Free Radic Biol Med. 2000;29(3–4):222–30.

261. ONS. Population Ageing in the United Kingdom, its Constituent Countries and the European Union. Off Natl Stat. 2012;(March):1–12.

262. Ortman JM, Velkoff VA, Hogan H. An Aging Nation: The Older Population in the United States Current Population Reports. 2014;

263. Kim TN, Choi KM. Sarcopenia: definition, epidemiology, and pathophysiology. J Bone Metab. 2013;20(1):1–10.

264. Sousa AS, Guerra RS, Fonseca I, Pichel F, Ferreira S, Amaral TF. Financial impact of

sarcopenia on hospitalization costs. Eur J Clin Nutr. 2016;70(9):1046–51.

265. Chini CCS, Tarrag MG, Chini EN. NAD and the aging process: Role in life, death and everything in between. Mol Cell Endocrinol. 2016;1–13.

266. Imai SI. Dissecting systemic control of metabolism and aging in the NAD World: The importance of SIRT1 and NAMPT-mediated NAD biosynthesis. FEBS Lett [Internet]. 2011;585(11):1657–62. Available from: http://dx.doi.org/10.1016/j.febslet.2011.04.060

267. Satoh A, Brace CS, Rensing N, Cliften P, Wozniak DF, Herzog ED, et al. Sirt1 extends life span and delays aging in mice through the regulation of Nk2 Homeobox 1 in the DMH and LH. Cell Metab. 2013;18(3):416–30.

268. Kanfi Y, Naiman S, Amir G, Peshti V, Zinman G, Nahum L, et al. The sirtuin SIRT6 regulates lifespan in male mice. Nature. 2012;483(7388):218–21.

269. Schmeisser K, Mansfeld J, Kuhlow D, Weimer S, Priebe S, Heiland I, et al. Role of sirtuins in lifespan regulation is linked to methylation of nicotinamide. Nat Chem Biol. 2013;9(11):693–700.

270. López-Otín C, Blasco MA, Partridge L, Serrano M, Kroemer G. The hallmarks of aging. Cell. 2013;153(6):1194–1217.

271. Massudi H, Grant R, Braidy N, Guest J, Farnsworth B, Guillemin GJ. Age-associated changes in oxidative stress and NAD+ metabolism in human tissue. PLoS One. 2012;7(7):1–9.

272. Veith S, Mangerich A. RecQ helicases and PARP1 team up in maintaining genome integrity. Ageing Res Rev [Internet]. 2015;23(PA):12–28. Available from: http://dx.doi.org/10.1016/j.arr.2014.12.006

273. Singh T, Newman AB. Inflammatory markers in population studies of aging. Ageing Res

Rev. 2011;10(3):319–29.

274. Imai S, Yoshino J. The importance of NAMPT/NAD/SIRT1 in the systemic regulation of metabolism and ageing. Diabetes, Obes Metab. 2013;15(S3):26–33.

275. Herranz D, Muñoz-Martin M, Cañamero M, Mulero F, Martinez-Pastor B, Fernandez-Capetillo O, et al. Sirt1 improves healthy ageing and protects from metabolic syndrome-associated cancer. Nat Commun. 2010;1:3.

276. Gong B, Pan Y, Vempati P, Zhao W, Knable L, Ho L, et al. Nicotinamide riboside restores cognition through an upregulation of proliferator-activated receptor-γ coactivator 1α regulated β-secretase 1 degradation and mitochondrial gene expression in Alzheimer's mouse models. Neurobiol Aging [Internet]. 2013;34(6):1581–8. Available from: http://dx.doi.org/10.1016/j.neurobiolaging.2012.12.005

277. Jaacks LM, Siegel KR, Gujral UP, Narayan KMV. Type 2 diabetes: A 21st century epidemic. Best Pract Res Clin Endocrinol Metab [Internet]. 2016;30(3):331–43. Available from: http://dx.doi.org/10.1016/j.beem.2016.05.003

278. Kelley DE, He J, Menshikova E V., Ritov VB. Dysfunction of mitochondria in human skeletal muscle in type 2 diabetes. Diabetes. 2002;51(10):2944–50.

279. Parish R, Petersen KF. Mitochondrial dysfunction and type 2 diabetes. Curr Diab Rep [Internet]. 2005;5(3):177–83. Available from: http://www.pubmedcentral.nih.gov/articlerender.fcgi?artid=2995500&tool=pmcentrez&rendertype=abstract

280. Petersen KF, Dufour S, Befroy D, Garcia R, Shulman GI. Impaired Mitochondrial Activity in the Insulin-Resistant Offspring of Patients with Type 2 Diabetes. N Engl J Med [Internet]. 2004 [cited 2017 May 6];3507350:664–71. Available from:

http://www.nejm.org/doi/pdf/10.1056/NEJMoa031314

281. Petersen KF, Dufour S, Shulman GI. Decreased insulin-stimulated ATP synthesis and phosphate transport in muscle of insulin-resistant offspring of type 2 diabetic parents. PLoS Med. 2005;2(9):0879–84.

282. Phielix E, Schrauwen-hinderling VB, Mensink M, Lenaers E, Meex R, Hoeks J, et al. Lower intrinsic ADP stimulated mitochondrial respirationin underlies in vivo mitochondrial dysfunction in muscle of male type 2 diabetic patients. Diabetes. 2008;57(11):2943–9.

283. Patti ME, Corvera S. The role of mitochondria in the pathogenesis of type 2 diabetes. Endocr Rev. 2010;31(3):364–95.

284. Ritov VB, Menshikova E V., He J, Ferrell RE, Goodpaster BH, Kelley DE. Deficiency of subsarcolemmal mitochondria in obesity and type 2 diabetes. Diabetes. 2005;54(1):8–14.

285. Evans JL, Goldfine ID, Maddux BA, Grodsky GM. Are Oxidative Stress−Activated Signaling Pathways Mediators of Insulin Resistance and β-Cell Dysfunction? Diabetes. 2003;52(1):1–8.

286. Leloup C, Tourrel-Cuzin C, Magnan C, Karaca M, Castel J, Carneiro L, et al. Mitochondrial reactive oxygen species are obligatory signals for glucose-induced insulin secretion. Diabetes [Internet]. 2009;58(March):673–81. Available from: http://diabetes.diabetesjournals.org/content/58/3/673.short

287. Savage DB, Petersen KF, Shulman GI. Disordered lipid metabolism and the pathogenesis of insulin resistance. Physiol Rev [Internet]. 2007;87(2):507–20. Available from: http://www.pubmedcentral.nih.gov/articlerender.fcgi?artid=2995548&tool=pmcentrez&rendertype=abstract

288. Koves TR, Ussher JR, Noland RC, Slentz D, Mosedale M, Ilkayeva O, et al. Mitochondrial Overload and Incomplete Fatty Acid Oxidation Contribute to Skeletal Muscle Insulin Resistance. Cell Metab. 2008;7(1):45–56.

289. Holland WL, Brozinick JT, Wang LP, Hawkins ED, Sargent KM, Liu Y, et al. Inhibition of Ceramide Synthesis Ameliorates Glucocorticoid-, Saturated-Fat-, and Obesity-Induced Insulin Resistance. Cell Metab. 2007;5(3):167–79.

290. Chibalin A V., Leng Y, Vieira E, Krook A, Bj??rnholm M, Long YC, et al. Downregulation of Diacylglycerol Kinase Delta Contributes to Hyperglycemia-Induced Insulin Resistance. Cell. 2008;132(3):375–86.

291. Houstis N, Rosen ED, Lander ES. Reactive oxygen species have a causal role in multiple forms of insulin resistance. Nature [Internet]. 2006;440(7086):944–8. Available from: http://www.ncbi.nlm.nih.gov/entrez/query.fcgi?cmd=Retrieve&db=PubMed&dopt=Citation&list_uids=16612386

292. Gerbitz KD, Gempel K, Brdiczka D. Mitochondria and diabetes. Genetic, biochemical, and clinical implications of the cellular energy circuit. Diabetes [Internet]. 1996 Feb [cited 2017 Feb 13];45(2):113–26. Available from: http://www.ncbi.nlm.nih.gov/pubmed/8549853

293. Simoneau JA, Colberg SR, Thaete FL, Kelley DE. Skeletal muscle glycolytic and oxidative enzyme capacities are determinants of insulin sensitivity and muscle composition in obese women. FASEB J. 1995;9(2):273–8.

294. Simoneau J, Bouchard C. Skeletal Muscle Metabolism and Body Fat Content in Men and Women. Obes Res. 1995;3(1):23–9.

295. Muoio DM. Metabolic inflexibility: When mitochondrial indecision leads to metabolic gridlock. Cell [Internet]. 2014;159(6):1253–62. Available from:

http://dx.doi.org/10.1016/j.cell.2014.11.034

296. Prior SJ, Ryan AS, Stevenson TG, Goldberg AP. Metabolic inflexibility during submaximal aerobic exercise is associated with glucose intolerance in obese older adults. Obesity. 2014;22(2):451–7.

297. Kelley DE, Goodpaster B, Wing RR, Simoneau J-A. Skeletal muscle fatty acid metabolism in association with insulin resistance, obesity, and weight loss. Am J Physiol - Endocrinol Metab. 1999;277(6).

298. Sinha R, Dufour S, Petersen KF, Lebon V, Enoksson S, Ma Y, et al. Assessment of skeletal muscle triglyceride content by (1)H Nuclear nuclear magnetic resonance spectroscopy in lean and obese adolescents: relationships to insulin sensitivity, total body fat, and central adiposity. Diabetes. 2002;51(4):1022–7.

299. Kotronen A, Seppälä-Lindroos A, Bergholm R, Yki-Järvinen H. Tissue specificity of insulin resistance in humans: Fat in the liver rather than muscle is associated with features of the metabolic syndrome. Diabetologia. 2008;51(1):130–8.

300. Wang R, Kim H, Xiao C, Xu X. Hepatic Sirt1 deficiency in mice impairs mTorc2 / Akt signaling and results in hyperglycemia , oxidative damage , and insulin resistance. 2011;121(11).

301. Liang F, Chen R, Nakagawa A, Nishizawa M, Tsuda S, Wang H, et al. Low-frequency electroacupuncture improves insulin sensitivity in obese diabetic mice through activation of SIRT1/PGC-1α in skeletal muscle. Evidence-based Complement Altern Med. 2011;2011.

302. Zhang H-H, Ma X-J, Wu L-N, Zhao Y-Y, Zhang P-Y, Zhang Y-H, et al. SIRT1 attenuates high glucose-induced insulin resistance via reducing mitochondrial dysfunction in skeletal

muscle cells. Exp Biol Med. 2015;240(5):557–65.

303. Fröjdö S, Durand C, Molin L, Carey AL, El-Osta A, Kingwell BA, et al. Phosphoinositide 3-kinase as a novel functional target for the regulation of the insulin signaling pathway by SIRT1. Mol Cell Endocrinol. 2011;335(2):166–76.

304. Chalkiadaki A, Guarente L. High-fat diet triggers inflammation-induced cleavage of SIRT1 in adipose tissue to promote metabolic dysfunction. Cell Metab [Internet]. 2012;16(2):180–8. Available from: http://dx.doi.org/10.1016/j.cmet.2012.07.003

305. Rutanen J, Yaluri N, Modi S. SIRT1 mRNA expression may be associated with energy expenditure and insulin sensitivity. Diabetes [Internet]. 2010;59(April):829–35. Available from: http://diabetes.diabetesjournals.org/content/59/4/829.short

306. Xu C, Bai B, Fan P, Cai Y, Huang B, Law IKM, et al. Selective overexpression of human SIRT1 in adipose tissue enhances energy homeostasis and prevents the deterioration of insulin sensitivity with ageing in mice. Am J Transl Res. 2013;5(4):412–26.

307. Caton PW, Nayuni NK, Kieswich J, Khan NQ, Yaqoob MM, Corder R. Metformin suppresses hepatic gluconeogenesis through induction of SIRT1 and GCN5. J Endocrinol. 2010;205(1):97–106.

308. Zhou B, Zhang Y, Zhang F, Xia Y, Liu J, Huang R, et al. CLOCK/BMAL1 regulates circadian change of mouse hepatic insulin sensitivity by SIRT1. Hepatology. 2014;59(6):2196–206.

309. Rodgers JT, Puigserver P. Fasting-dependent glucose and lipid metabolic response through hepatic sirtuin 1. Proc Natl Acad Sci. 2007;104(31):12861–6.

310. Meex RCR, Schrauwen-Hinderling VB, Moonen-Kornips E, Schaart G, Mensink M, Phielix E, et al. Restoration of muscle mitochondrial function and metabolic flexibility in

type 2 diabetes by exercise training is paralleled by increased myocellular fat storage and improved insulin sensitivity. Diabetes. 2010;59(3):572–9.

311. Phielix E, Meex R, Moonen-Kornips E, Hesselink MKC, Schrauwen P. Exercise training increases mitochondrial content and ex vivo mitochondrial function similarly in patients with type 2 diabetes and in control individuals. Diabetologia. 2010;53(8):1714–21.

312. Kover K, Tong PY, Watkins D, Clements M, Stehno-Bittel L, Novikova L, et al. Expression and Regulation of Nampt in Human Islets. PLoS One. 2013;8(3):1–11.

313. Moynihan KA, Grimm AA, Plueger MM, Bernal-Mizrachi E, Ford E, Cras-M??neur C, et al. Increased dosage of mammalian Sir2 in pancreatic β cells enhances glucose-stimulated insulin secretion in mice. Cell Metab. 2005;2(2):105–17.

314. Luu L, Dai FF, Prentice KJ, Huang X, Hardy AB, Hansen JB, et al. The loss of Sirt1 in mouse pancreatic beta cells impairs insulin secretion by disrupting glucose sensing. Diabetologia. 2013;56(9):2010–20.

315. Ramachandran D, Roy U, Garg S, Ghosh S, Pathak S, Kolthur-Seetharam U. Sirt1 and mir-9 expression is regulated during glucose-stimulated insulin secretion in pancreatic β-islets. FEBS J. 2011;278(7):1167–74.

316. Do Amaral MEC, Ueno M, Oliveira CAM, Borsonello NC, Vanzela EC, Ribeiro RA, et al. Reduced expression of SIRT1 is associated with diminished glucose-induced insulin secretion in islets from calorie-restricted rats. J Nutr Biochem [Internet]. 2011;22(6):554–9. Available from: http://dx.doi.org/10.1016/j.jnutbio.2010.04.010

317. Ramsey KM, Mills KF, Satoh A, Imai SI. Age-associated loss of Sirt1-mediated enhancement of glucose-stimulated insulin secretion in beta cell-specific Sirt1-overexpressing (BESTO) mice. Aging Cell. 2008;7(1):78–88.

318. Nakahata Y, Kaluzova M, Grimaldi B, Sahar S, Hirayama J, Chen D, et al. The NAD+-Dependent Deacetylase SIRT1 Modulates CLOCK-Mediated Chromatin Remodeling and Circadian Control. Cell. 2008;134(2):329–40.

319. Asher G, Gatfield D, Stratmann M, Reinke H, Dibner C, Kreppel F, et al. SIRT1 Regulates Circadian Clock Gene Expression through PER2 Deacetylation. Cell. 2008;134(2):317–28.

320. Song MY, Wang J, Ka SO, Bae EJ, Park BH. Insulin secretion impairment in Sirt6 knockout pancreatic β cells is mediated by suppression of the FoxO1-Pdx1-Glut2 pathway. Sci Rep. 2016;6(1):1–9.

321. Ming X, Chung ACK, Mao D, Cao H, Fan B, Wong WKK, et al. Pancreatic Sirtuin 3 Deficiency Promotes Hepatic Steatosis by Enhancing 5-Hydroxytryptamine Synthesis in Mice With Diet-Induced Obesity. Diabetes. 2021;70(1):119–31.

322. Trammell SAJ, Weidemann BJ, Chadda A, Yorek MS, Holmes A, Coppey LJ, et al. Nicotinamide Riboside Opposes Type 2 Diabetes and Neuropathy in Mice. Sci Rep. 2016;6(May):26933.

323. Daniele G, Eldor R, Merovci A, Clarke GD, Xiong J, Tripathy D, et al. Chronic reduction of plasma free fatty acid improves mitochondrial function and whole-body insulin sensitivity in obese and type 2 diabetic individuals. Diabetes. 2014;63(8):2812–20.

324. Bajaj M, Suraamornkul S, Romanelli A, Cline GW, Mandarino LJ, Shulman GI, et al. Effect of a sustained reduction in plasma free fatty acid concentration on intramuscular long-chain fatty Acyl-CoAs and insulin action in type 2 diabetic patients. Diabetes. 2005;54(0012-1797 (Print)):3148–53.

325. Dorte W, Henriksen JE, Vaag A, Thye-Rønn P, Melander A, Beck-Nielsen H. Pronounced

Blood Glucose Effect of the Antilipolytic Drug Acipimox in Noninsulin-Dependent Diabetes Mellitus Patients during a 3-Day Intensified Treatment Period. J Clin Endocrinol Metab. 1994;78(3):717–21.

326. Santomauro AT, Boden G, Silva ME, Rocha DM, Santos RF, Ursich MJ, et al. Overnight lowering of free fatty acids with Acipimox improves insulin resistance and glucose tolerance in obese diabetic and nondiabetic subjects. Diabetes. 1999;48(9):1836–41.

327. Liang H, Tantiwong P, Sriwijitkamol A, Shanmugasundaram K, Mohan S, Espinoza S, et al. Effect of a sustained reduction in plasma free fatty acid concentration on insulin signalling and inflammation in skeletal muscle from human subjects. J Physiol [Internet]. 2013;591(Pt 11):2897–909. Available from: http://www.pubmedcentral.nih.gov/articlerender.fcgi?artid=3690693&tool=pmcentrez&rendertype=abstract

328. Vaag A, Skott P, Damsbo P, Gall M-A, Richter EA, Beck-Nielsen H. Effect of the antilipolytic nicotinic acid analogue acipimox on whole-body and skeletal muscle glucose metabolism in patients with non-insulin-dependent diabetes mellitus. J Clin Invest. 1991;88(4):1282–90.

329. Fulcher GR, Catalano C, Walker M, Farrer M, Thow J, Whately-Smith CR, et al. A Double Blind Study of the Effect of Acipimox on Serum Lipids, Blood Glucose Control and Insulin Action in Non-obese Patients with Type 2 Diabetes Mellitus. Diabet Med. 1992;9:908–14.

330. Merovci A, Abdul-Ghani M, Mari A, Herrera CS, Xiong J, Daniele G, et al. Effect of Dapagliflozin With and Without Acipimox on Insulin Sensitivity and Insulin Secretion in T2DM Males 1. 2016;101(March):1249–56.

331. Makimura H, Stanley TL, Suresh C, Luisa De Sousa-Coelho A, Frontera WR, Syu S, et al. Metabolic Effects of Long-term Reduction in Free Fatty Acids with Acipimox in

Obesity: A Randomized Trial. J Clin Endocrinol Metab. 2015;101(March):jc20153696.

332. van de Weijer T, Phielix E, Bilet L, Williams EG, Ropelle ER, Bierwagen A, et al. Evidence for a direct effect of the NAD+ precursor acipimox on muscle mitochondrial function in humans. Diabetes. 2015;64(4):1193–201.

333. Saloranta C, Taskinen MR, Widen E, Harkonen M, Melander A, Groop L. Metabolic consequences of sustained suppression of free fatty acids by acipimox in patients with NIDDM. Diabetes. 1993;42(11):1559–66.

334. Espino-Gonzalez E, Dalbram E, Mounier R, Gondin J, Farup J, Jessen N, et al. Impaired skeletal muscle regeneration in diabetes: From cellular and molecular mechanisms to novel treatments. Cell Metab. 2024;36(6):1204–36.

335. Younossi ZM, Stepanova M, Afendy M, Fang Y, Younossi Y, Mir H, et al. Changes in the Prevalence of the Most Common Causes of Chronic Liver Diseases in the United States From 1988 to 2008. Clin Gastroenterol Hepatol [Internet]. 2011;9(6):524-530.e1. Available from: http://dx.doi.org/10.1016/j.cgh.2011.03.020

336. Leamy AK, Egnatchik R a, Shiota M, Ivanova PT, Myers DS, Brown HA, et al. Enhanced synthesis of saturated phospholipids is associated with ER stress and lipotoxicity in palmitate treated hepatic cells. J Lipid Res [Internet]. 2014;55(7):1478–88. Available from: http://www.ncbi.nlm.nih.gov/pubmed/24859739

337. Schuppan D, Schattenberg JM. Non-alcoholic steatohepatitis: pathogenesis and novel therapeutic approaches. J Gastroenterol Hepatol [Internet]. 2013;28 Suppl 1:68–76. Available from: http://www.ncbi.nlm.nih.gov/pubmed/23855299

338. Cohen JC, Horton JD, Hobbs HH. Human Fatty Liver Disease: Old Questions and New Insights. Science (80-). 2011;332(6037):1519–23.

339. Koliaki C, Szendroedi J, Kaul K, Jelenik T, Nowotny P, Jankowiak F, et al. Adaptation of hepatic mitochondrial function in humans with non-alcoholic fatty liver is lost in steatohepatitis. Cell Metab [Internet]. 2015;21(5):739–46. Available from: http://dx.doi.org/10.1016/j.cmet.2015.04.004

340. Serviddio G, Bellanti F, Tamborra R, Rollo T, Romano AD, Giudetti AM, et al. Alterations of hepatic ATP homeostasis and respiratory chain during development of non-alcoholic steatohepatitis in a rodent model. Eur J Clin Invest. 2008;38(4):245–52.

341. Pérez-Carreras M, Del Hoyo P, Martín M a, Rubio JC, Martín A, Castellano G, et al. Defective hepatic mitochondrial respiratory chain in patients with nonalcoholic steatohepatitis. Hepatology. 2003;38(4):999–1007.

342. Lee S, Rivera-Vega M, Alsayed HMAA, Boesch C, Libman I. Metabolic inflexibility and insulin resistance in obese adolescents with non-alcoholic fatty liver disease. Pediatr Diabetes. 2015;16(3):211–8.

343. Hwang JH, Kim DW, Jo EJ, Kim YK, Jo YS, Park JH, et al. Pharmacological stimulation of NADH oxidation ameliorates obesity and related phenotypes in mice. Diabetes. 2009;58(4):965–74.

344. Cheng Z, Guo S, Copps K, Dong X, Kollipara R, Rodgers JT, et al. Foxo1 integrates insulin signaling with mitochondrial function in the liver. Nat Med [Internet]. 2009;15(11):1307–11. Available from: http://www.pubmedcentral.nih.gov/articlerender.fcgi?artid=3994712&tool=pmcentrez&rendertype=abstract

345. Kendrick AA, Choudhury M, Rahman SM, McCurdy CE, Friederich M, Van Hove JLK, et al. Fatty liver is associated with reduced SIRT3 activity and mitochondrial protein hyperacetylation. Biochem J. 2011;433(3):505–14.

346. Zhou C-C, Yang X, Hua X, Liu J, Fan M-B, Li G-Q, et al. Hepatic NAD + deficiency as a therapeutic target for non-alcoholic fatty liver disease in ageing. Br J Pharmacol. 2016;173(15):2352–68.

347. Min HK, Kapoor A, Fuchs M, Mirshahi F, Zhou H, Maher J, et al. Increased hepatic synthesis and dysregulation of cholesterol metabolism is associated with the severity of nonalcoholic fatty liver disease. Cell Metab [Internet]. 2012;15(5):665–74. Available from: http://dx.doi.org/10.1016/j.cmet.2012.04.004

348. Xu F, Gao Z, Zhang J, Rivera CA, Yin J, Weng J, et al. Lack of SIRT1 (mammalian sirtuin 1) activity leads to liver steatosis in the SIRT1+/- mice: A role of lipid mobilization and inflammation. Endocrinology. 2010;151(6):2504–14.

349. Purushotham A, Schug TT, Xu Q, Surapureddi S, Guo X, Li X. Hepatocyte-Specific Deletion of SIRT1 Alters Fatty Acid Metabolism and Results in Hepatic Steatosis and Inflammation. Cell Metab [Internet]. 2009;9(4):327–38. Available from: http://dx.doi.org/10.1016/j.cmet.2009.02.006

350. Li Y, Wong K, Giles A, Jiang J, Lee JW, Adams AC, et al. Hepatic SIRT1 attenuates hepatic steatosis and controls energy balance in mice by inducing fibroblast growth factor 21. Gastroenterology. 2014;146(2):539–49.

351. Pfluger PT, Herranz D, Velasco-Miguel S, Serrano M, Tschöp M. Sirt1 protects against high-fat diet-induced metabolic damage. Proc Natl Acad Sci U S A [Internet]. 2008;105(28):9793–8. Available from: http://www.ncbi.nlm.nih.gov/pubmed/18599449%5Cnhttp://www.ncbi.nlm.nih.gov/pmc/articles/PMC2474520/pdf/zpq9793.pdf

352. Marmier S, Dentin R, Daujat-Chavanieu M, Guillou H, Bertrand-Michel J, Gerbal-Chaloin S, et al. Novel role for carbohydrate responsive element binding protein in the control of

ethanol metabolism and susceptibility to binge drinking. Hepatology. 2015;62(4):1086–100.

353. Yin H, Hu M, Liang X, Ajmo JM, Li X, Bataller R, et al. Deletion of SIRT1 from hepatocytes in mice disrupts lipin-1 signaling and aggravates alcoholic fatty liver. Gastroenterology [Internet]. 2014;146(3):801–11. Available from: http://dx.doi.org/10.1053/j.gastro.2013.11.008

354. Tummala KS, Gomes AL, Yilmaz M, Graña O, Bakiri L, Ruppen I, et al. Inhibition of De Novo NAD+ Synthesis by Oncogenic URI Causes Liver Tumorigenesis through DNA Damage. Cancer Cell [Internet]. 2014;26(6):826–39. Available from: http://linkinghub.elsevier.com/retrieve/pii/S1535610814003924

355. Jung TW, Lee KT, Lee MW, Ka KH. SIRT1 attenuates palmitate-induced endoplasmic reticulum stress and insulin resistance in HepG2 cells via induction of oxygen-regulated protein 150. Biochem Biophys Res Commun [Internet]. 2012;422(2):229–32. Available from: http://dx.doi.org/10.1016/j.bbrc.2012.04.129

356. Gariani K, Menzies KJ, Ryu D, Wegner CJ, Wang X, Ropelle ER, et al. Eliciting the mitochondrial unfolded protein response by nicotinamide adenine dinucleotide repletion reverses fatty liver disease in mice. Hepatology. 2016;63(4):1190–204.

357. Tilg H, Moschen AR. Evolution of inflammation in nonalcoholic fatty liver disease: The multiple parallel hits hypothesis. Hepatology. 2010;52(5):1836–46.

358. Gariani K, Ryu D, Menzies K, Yi H-S, Stein S, Zhang H, et al. Inhibiting poly-ADP ribosylation increases fatty acid oxidation and protects against fatty liver disease. J Hepatol [Internet]. 2016; Available from: http://www.ncbi.nlm.nih.gov/pubmed/27663419

359. Cambronne XA, Kraus WL. Location, Location, Location: Compartmentalization of NAD+

Synthesis and Functions in Mammalian Cells. Trends Biochem Sci. 2020;45(10):858–73.

360. Nikiforov A, Kulikova V, Ziegler M. The human NAD metabolome: Functions, metabolism and compartmentalization. Crit Rev Biochem Mol Biol. 2015;00(00):1–14.

361. Satrustegui J, Pardo B, Del Arco A. Mitochondrial transporters as novel targets for intracellular calcium signaling. Physiol Rev. 2007;87(1):29–67.

362. Luongo TS, Eller JM, Lu MJ, Niere M, Raith F, Perry C, et al. SLC25A51 is a mammalian mitochondrial NAD+ transporter. Nature. 2020;588(7836):174–9.

363. Lomax RB, Camello C, Van Coppenolle F, Petersen OH, Tepikin A V. Basal and Physiological Ca2+ Leak from the Endoplasmic Reticulum of Pancreatic Acinar Cells. J Biol Chem. 2002;277(29):26479–85.

364. Heritage D, Wonderlin WF. Translocon Pores in the Endoplasmic Reticulum Are Permeable to a Neutral, Polar Molecule. J Biol Chem. 2001;276(25):22655–62.

365. Csala MS, Bánhegyi G, Benedetti A. Endoplasmic reticulum: A metabolic compartment. 2006;

366. Csala M, Bánhegyi G, Benedetti A. Endoplasmic reticulum: A metabolic compartment. FEBS Lett. 2006;580(9):2160–5.

367. Chou J, Matern D, Mansfield B, Chen Y-T. Type I Glycogen Storage Diseases: Disorders of the Glucose-6- Phosphatase Complex. Curr Mol Med [Internet]. 2002 Mar 1 [cited 2016 Nov 24];2(2):121–43. Available from: http://www.eurekaselect.com/openurl/content.php?genre=article&issn=1566-5240&volume=2&issue=2&spage=121

368. Gerin I, Veiga-da-Cunha M, Achouri Y, Collet J-F, Van Schaftingen E. Sequence of a putative glucose 6-phosphate translocase, mutated in glycogen storage disease type Ib [1].

FEBS Lett [Internet]. 1997 Dec 15 [cited 2016 Nov 24];419(2–3):235–8. Available from: http://doi.wiley.com/10.1016/S0014-5793%2897%2901463-4

369. Nicole Draper1,9, Elizabeth A Walker1,9, Iwona J Bujalska1, Jeremy W Tomlinson1 SMC, Wiebke Arlt1, Gareth G Lavery1, Oliver Bedendo1, David W Ray2, Ian Laing3, Ewa Malunowicz4 PCW, Martin Hewison1, Philip J Mason6, John M Connell7 CHLS& PMS. Mutations in the genes encoding 11β-hydroxysteroid dehydrogenase type 1 and hexose-6-phosphate dehydrogenase interact to cause cortisone reductase deficiency. Nat Genet. 2003;

370. Lavery GG, Walker EA, Tiganescu A, Ride JP, Shackleton CHL, Tomlinson JW, et al. Steroid Biomarkers and Genetic Studies Reveal Inactivating Mutations in Hexose-6-Phosphate Dehydrogenase in Patients with Cortisone Reductase Deficiency.

371. Piccirella S, Czegle I, Lizák B, Margittai E, Senesi S, Papp E, et al. Uncoupled redox systems in the lumen of the endoplasmic reticulum. Pyridine nucleotides stay reduced in an oxidative environment. J Biol Chem [Internet]. 2006 Feb 24 [cited 2016 Nov 24];281(8):4671–7. Available from: http://www.ncbi.nlm.nih.gov/pubmed/16373343

372. Bublitz C, Lawler CA. The levels of nicotinamide nucleotides in liver microsomes and their possible significance to the function of hexose phosphate dehydrogenase. Biochem J. 1987;245:263–7.

373. McCormick KL, Wang X, Mick GJ. Evidence that the 11 ??-hydroxysteroid dehydrogenase (11 ??-HSD1) is regulated by pentose pathway flux: Studies in rat adipocytes and microsomes. J Biol Chem. 2006;281(1):341–7.

374. Lavery GG, Walker EA, Turan N, Rogoff D, Ryder JW, Shelton JM, et al. Deletion of hexose-6-phosphate dehydrogenase activates the unfolded protein response pathway and induces skeletal myopathy. J Biol Chem. 2008;283(13):8453–61.

375. Arlt W, Stewart PM. Adrenal Corticosteroid Biosynthesis, Metabolism, and Action. Endocrinol Metab Clin North Am. 2005;34(2):293–313.

376. Beato M, Sánchez-Pacheco A. Interaction of Steroid Hormone Receptors with the Transcription Initiation Complex. Endocr Rev. 1996;17(6):587–609.

377. Tomlinson JW, Walker EA, Bujalska IJ, Draper N, Lavery GG, Cooper MS, et al. 11??-Hydroxysteroid dehydrogenase type 1: A tissue-specific regulator of glucocorticoid response. Endocr Rev. 2004;25(5):831–66.

378. Morgan SA, McCabe EL, Gathercole LL, Hassan-Smith ZK, Larner DP, Bujalska IJ, et al. 11 -HSD1 is the major regulator of the tissue-specific effects of circulating glucocorticoid excess. Proc Natl Acad Sci [Internet]. 2014;111(24):E2482–91. Available from: http://www.pubmedcentral.nih.gov/articlerender.fcgi?artid=4066483&tool=pmcentrez&rendertype=abstract

379. Tomlinson JW, Stewart PM. Cortisol metabolism and the role of 11β-hydroxysteroid dehydrogenase. Best Pract Res Clin Endocrinol Metab. 2001;15(1):61–78.

380. Hewitt KN, Walker EA, Stewart PM. Minireview: Hexose-6-Phosphate Dehydrogenase and Redox Control of 11ℕ-Hydroxysteroid Dehydrogenase Type 1 Activity.

381. Morgan SA, Hassan-Smith ZK, Lavery GG. MECHANISMS IN ENDOCRINOLOGY: Tissue-specific activation of cortisol in Cushing's syndrome. Eur J Endocrinol [Internet]. 2016 Aug [cited 2016 Nov 25];175(2):R83-9. Available from: http://www.ncbi.nlm.nih.gov/pubmed/26957494

382. Lavery GG, Walker EA, Draper N, Jeyasuria P, Marcos J, Shackleton CHL, et al. Hexose-6-phosphate dehydrogenase knock-out mice lack 11??- hydroxysteroid dehydrogenase type 1-mediated glucocorticoid generation. J Biol Chem. 2006;281(10):6546–51.

383. Bergstrom J. Percutaneous Needle Biopsy of Skeletal Muscle in Physiological and Clinical Research . Scand J Clin Lab Investig. 1975;35(7):609–16.

384. Wythe S, Davies T, Martin D, Feelisch M, Gilbert-Kawai E. Getting the most from venous occlusion plethysmography: Proposed methods for the analysis of data with a rest/exercise protocol. Extrem Physiol Med. 2015;4(1):4–8.

385. Greenfield ADM, Whitney RJ, Mowbray JF. Methods for the investigation of peripheral blood flow. Brit Med Bull. 1963;19(2):101–9.

386. Matthews DR, Hosker JP, Rudenski AS, Naylor BA, Treacher DF, Turner RC. Homeostasis model assessment: insulin resistance and β-cell function from fasting plasma glucose and insulin concentrations in man. Diabetologia. 1985;28(7):412–9.

387. Pesta D, Gnaiger E. High-Resolution Respirometry: OXPHOS Protocols for Human Cells and Permeabilized Fibers from Small Biopsies of Human Muscle. In: Methods in Molecular Biology. 2012. p. 25–58.

388. Horscroft JA, Burgess SL, Hu Y, Murray AJ. Altered Oxygen Utilisation in Rat Left Ventricle and Soleus after 14 Days, but Not 2 Days, of Environmental Hypoxia. PLoS One. 2015 Sep;10(9):e0138564.

389. Huang DW, Sherman BT, Lempicki RA. Systematic and integrative analysis of large gene lists using DAVID bioinformatics resources. Nat Protoc. 2009;4(1):44–57.

390. Huang DW, Sherman BT, Lempicki RA. Bioinformatics enrichment tools: paths toward the comprehensive functional analysis of large gene lists. Nucleic Acids Res. 2009;37(1):1–13.

391. Subramanian A, Tamayo P, Mootha VK, Mukherjee S, Ebert BL, Gillette MA, et al. Gene set enrichment analysis: A knowledge-based approach for interpreting genome-wide

expression profiles. Proc Natl Acad Sci. 2005;102(43):15545–50.

392. Liberzon A, Birger C, Thorvaldsdóttir H, Ghandi M, Mesirov JP, Tamayo P. The Molecular Signatures Database Hallmark Gene Set Collection. Cell Syst [Internet]. 2015;1(6):417–25. Available from: https://www.sciencedirect.com/science/article/pii/S2405471215002185

393. Yaffe D, Saxel O. Serial passaging and differentiation of myogenic cells isolated from dystrophic mouse muscle. Nature. 1977;270(5639):725–7.

394. Blau HM, Pavlath GK, Hardeman EC, Chiu CP, Silberstein L, Webster SG, et al. Plasticity of the Differentiated State. Science (80-). 1985;230(4727):758–66.

395. Wong CY, Al-Salami H, Dass CR. C2C12 cell model: its role in understanding of insulin resistance at the molecular level and pharmaceutical development at the preclinical stage. J Pharm Pharmacol. 2020;72(12):1667–93.

396. Tan B, Dong S, Shepard RL, Kays L, Roth KD, Geeganage S, et al. Inhibition of nicotinamide phosphoribosyltransferase (NAMPT), an enzyme essential for NAD+ biosynthesis, leads to altered carbohydrate metabolism in cancer cells. J Biol Chem. 2015;290(25):15812–24.

397. Kim JO, Ma R, Akagami R, McKenzie M, Johnson M, Gete E, et al. Long-term outcomes of fractionated stereotactic radiation therapy for pituitary adenomas at the BC cancer agency. Int J Radiat Oncol Biol Phys [Internet]. 2013;87(3):528–33. Available from: http://dx.doi.org/10.1016/j.ijrobp.2013.06.2057

398. Costford SR, Bajpeyi S, Pasarica M, Albarado DC, Thomas SC, Xie H, et al. Skeletal muscle NAMPT is induced by exercise in humans. AJP Endocrinol Metab. 2010;298(1):E117–26.

399. Zhang H, Ryu D, Wu Y, Gariani K, Wang X, Luan P, et al. NAD+ repletion improves mitochondrial and stem cell function and enhances life span in mice. Science (80-). 2016;352(6292):1436–43.

400. Mills KF, Yoshida S, Stein LR, Grozio A, Kubota S, Sasaki Y, et al. Long-Term Administration of Nicotinamide Mononucleotide Mitigates Age-Associated Physiological Decline in Mice. Cell Metab. 2016;24(6):795–806.

401. Brown KD, Maqsood S, Huang JY, Pan Y, Harkcom W, Li W, et al. Activation of SIRT3 by the NAD+ precursor nicotinamide riboside protects from noise-induced hearing loss. Cell Metab. 2014;20(6):1059–68.

402. Diguet N, Trammell SAJ, Tannous C, Deloux R, Piquereau J, Mougenot N, et al. Nicotinamide Riboside Preserves Cardiac Function in a Mouse Model of Dilated Cardiomyopathy. Circulation. 2018;137(21):2256–73.

403. Vaur P, Brugg B, Mericskay M, Li Z, Schmidt MS, Vivien D, et al. Nicotinamide riboside, a form of Vitamin B3, protects against excitotoxicity-induced axonal degeneration. FASEB J. 2017;31(12):5440–52.

404. Liu L, Su X, Iii WJQ, Mitchison TJ, Baur JA, Rabinowitz JD, et al. Quantitative Analysis of NAD Synthesis-Breakdown Fluxes. Cell Metab. 2018;27(5):1067-1080.e5.

405. Martens CR, Denman BA, Mazzo MR, Armstrong ML, Reisdorph N, McQueen MB, et al. Chronic nicotinamide riboside supplementation is well-tolerated and elevates NAD+ in healthy middle-aged and older adults. Nat Commun. 2018;9(1):1286.

406. Dollerup OL, Christensen B, Svart M, Schmidt MS, Sulek K, Ringgaard S, et al. A randomized placebo-controlled clinical trial of nicotinamide riboside in obese men: safety, insulin-sensitivity, and lipid-mobilizing effects. Am J Clin Nutr. 2018 Jul 10;108(2):343–53.

407. Conze DB, Kruger CL. Safety assessment of nicotinamide riboside , a form of vitamin B 3. 2016;

408. Trammell SA, Brenner C. TARGETED, LCMS-BASED METABOLOMICS FOR QUANTITATIVE MEASUREMENT OF NAD+ METABOLITES. Comput Struct Biotechnol J. 2013 Jan;4(5).

409. Airhart SE, Shireman LM, Risler LJ, Anderson GD, Nagana Gowda GA, Raftery D, et al. An open-label, non-randomized study of the pharmacokinetics of the nutritional supplement nicotinamide riboside (NR) and its effects on blood NAD+ levels in healthy volunteers. PLoS One. 2017;12(12):e0186459.

410. Larsen S, Nielsen J, Hansen CN, Nielsen LB, Wibrand F, Stride N, et al. Biomarkers of mitochondrial content in skeletal muscle of healthy young human subjects. J Physiol. 2012;590(14):3349–60.

411. Mootha VK, Lindgren CM, Eriksson K-F, Subramanian A, Sihag S, Lehar J, et al. PGC-1α-responsive genes involved in oxidative phosphorylation are coordinately downregulated in human diabetes. Nat Genet. 2003;34(3):267–73.

412. Bickerton AST, Roberts R, Fielding BA, Hodson L, Blaak EE, Wagenmakers AJM, et al. Preferential uptake of dietary fatty acids in adipose tissue and muscle in the postprandial period. Diabetes. 2007;56(1):168–76.

413. Hill BG, Benavides GA, Lancaster JJR, Ballinger S, Dell'Italia L, Zhang J, et al. Integration of cellular bioenergetics with mitochondrial quality control and autophagy. Biol Chem. 2012;393(12):1485–512.

414. Vannini N, Campos V, Girotra M, Trachsel V, Rojas-Sutterlin S, Tratwal J, et al. The NAD-Booster Nicotinamide Riboside Potently Stimulates Hematopoiesis through

Increased Mitochondrial Clearance. Cell Stem Cell. 2019;24(3):405-418.e7.

415. Goody MF, Kelly MW, Lessard KN, Khalil A, Henry CA. Nrk2b-mediated NAD+ production regulates cell adhesion and is required for muscle morphogenesis in vivo. Nrk2b and NAD+ in muscle morphogenesis. Dev Biol. 2010;344(2):809–26.

416. Lauretani F, Russo CR, Bandinelli S, Bartali B, Cavazzini C, Di Iorio A, et al. Age-associated changes in skeletal muscles and their effect on mobility: an operational diagnosis of sarcopenia. J Appl Physiol. 2003;95(5):1851–60.

417. Dodds RM, Syddall HE, Cooper R, Benzeval M, Deary IJ, Dennison EM, et al. Grip Strength across the Life Course: Normative Data from Twelve British Studies. PLoS One. 2014;9(12):e113637.

418. Cruz-Jentoft AJ, Baeyens JP, Bauer JM, Boirie Y, Cederholm T, Landi F, et al. Sarcopenia: European consensus on definition and diagnosis: Report of the European Working Group on Sarcopenia in Older People. Age Ageing. 2010;39(4):412–23.

419. Das A, Huang GX, Bonkowski MS, Longchamp A, Li C, Schultz MB, et al. Impairment of an Endothelial NAD+-H2S Signaling Network Is a Reversible Cause of Vascular Aging. Cell. 2018 Mar;173(1):74-89.e20.

420. Yoshino J, Baur JA, Imai S ichiro. NAD+Intermediates: The Biology and Therapeutic Potential of NMN and NR. Cell Metab. 2017;27(3):513–28.

421. Steensberg A, Keller C, Starkie RL, Osada T, Febbraio MA, Pedersen BK. IL-6 and TNF-α expression in, and release from, contracting human skeletal muscle. Am J Physiol - Endocrinol Metab. 2002;283(6 46-6).

422. Ryu D, Zhang H, Ropelle ER, Sorrentino V, Mázala DAG, Mouchiroud L, et al. NAD+ repletion improves muscle function in muscular dystrophy and counters global

PARylation. Sci Transl Med. 2016;8(361):1–15.

423. Amici SA, Young NA, Narvaez-Miranda J, Jablonski KA, Arcos J, Rosas L, et al. CD38 Is Robustly Induced in Human Macrophages and Monocytes in Inflammatory Conditions. Front Immunol. 2018;9:1593.

424. Polzonetti V, Carpi FM, Micozzi D, Pucciarelli S, Vincenzetti S, Napolioni V. Population variability in CD38 activity: Correlation with age and significant effect of TNF-α-308G > A and CD38 184C > G SNPs. Mol Genet Metab. 2012;105:502–7.

425. Lavery GG, Hauton D, Hewitt KN, Brice SM, Sherlock M, Walker EA, et al. Hypoglycemia with Enhanced Hepatic Glycogen Synthesis in Recombinant Mice Lacking Hexose-6-Phosphate Dehydrogenase.

426. Rechsteiner M. The distribution of pyridine nucleotides between nucleus and cytoplasm. J Cell Physiol [Internet]. 1974;84(3):481–6. Available from: http://www.ncbi.nlm.nih.gov/pubmed/4154947

427. Cambronne XA, Stewart ML, Kim D, Jones-brunette AM, Morgan RK, Farrens DL, et al. Biosensor reveals multiple sources for mitochondrial NAD +. 2016;352(6292).

428. Lavery GG, Walker EA, Draper N, Jeyasuria P, Marcos J, Shackleton CHL, et al. Hexose-6-phosphate dehydrogenase knock-out mice lack 11??- hydroxysteroid dehydrogenase type 1-mediated glucocorticoid generation. J Biol Chem. 2006;281(10):6546–51.

429. Fang EF, Lautrup S, Hou Y, Demarest TG, Croteau DL, Mattson MP, et al. NAD + in Aging: Molecular Mechanisms and Translational Implications. Trends Mol Med. 2017;23(10):899–916.

430. Dolopikou CF, Kourtzidis IA, Margaritelis N V., Vrabas IS, Koidou I, Kyparos A, et al. Acute nicotinamide riboside supplementation improves redox homeostasis and exercise

performance in old individuals: a double-blind cross-over study. Eur J Nutr. 2019;0(0):0.

431. Liu M, Li L, Chu J, Zhu B, Zhang Q, Yin X, et al. Serum N 1 -Methylnicotinamide Is Associated With Obesity and Diabetes in Chinese. J Clin Endocrinol Metab. 2015;100(8):3112–7.

432. Kannt A, Pfenninger A, Teichert L, Tönjes A, Dietrich A, Schön MR, et al. Association of nicotinamide-N-methyltransferase mRNA expression in human adipose tissue and the plasma concentration of its product, 1-methylnicotinamide, with insulin resistance. Diabetologia. 2015;58(4):799–808.

433. Clement J, Wong M, Poljak A, Sachdev P, Braidy N. The Plasma NAD+ Metabolome is Dysregulated in 'normal' Ageing. Rejuvenation Res. 2018;rej.2018.2077.

434. Chaleckis R, Murakami I, Takada J, Kondoh H, Yanagida M. Individual variability in human blood metabolites identifies age-related differences. Proc Natl Acad Sci. 2016;113(16):4252–9.

435. Covarrubias AJ, Lopez-Dominguez JA, Perrone R, Kale A, Newman J, Iyer SS, et al. Aging-related inflammation driven by cellular senescence enhances NAD consumption via activation of CD38 + macrophages. bioRxiv [Internet]. 2019 [cited 2019 May 23]; Available from: http://dx.doi.org/10.1101/609438

436. Lin AL, Zhang W, Gao X, Watts L. Caloric restriction increases ketone bodies metabolism and preserves blood flow in aging brain. Neurobiol Aging. 2015;36(7):2296–303.

437. Ingram DK, Roth GS. Glycolytic inhibition as a strategy for developing calorie restriction mimetics. Exp Gerontol. 2011;46(2–3):148–54.

438. Hagopian K, Ramsey JJ, Weindruch R. Influence of age and caloric restriction on liver glycolytic enzyme activities and metabolite concentrations in mice. Exp Gerontol.

2003;38(3):253–66.

439. Goody MF, Henry CA. A need for NAD+ in muscle development, homeostasis, and aging. Skelet Muscle. 2018;8(1):1–14.